A QUANTITATIVE EVALUATION OF THE MODAL DISTRIBUTION OF MINERALS IN COAL DEPOSITS IN THE HIGHVELD AREA AND THE ASSOCIATED IMPACT ON THE GENERATION OF ACID AND NEUTRAL MINE DRAINAGE

KL Pinetown • RH Boer

WRC Report No. 1264/1/06

Water Research Commission

A QUANTITATIVE EVALUATION OF THE MODAL DISTRIBUTION OF MINERALS IN COAL DEPOSITS IN THE HIGHVELD AREA AND THE ASSOCIATED IMPACT ON THE GENERATION OF ACID AND NEUTRAL MINE DRAINAGE

Report to the

Water Research Commission

by

KL PINETOWN AND RH BOER

on behalf of the
Department of Geology
University of the Free State

WRC Report No. 1264/1/06
ISBN No. 1-77005-440-5

MAY 2006

Disclaimer

This report emanates from a project financed by the Water Research Commission (WRC) and is approved for publication. Approval does not signify that the contents necessarily reflect the views and policies of the WRC or the members of the project steering committee, nor does mention of trade names or commercial products constitute endorsement or recommendation for use.

Printed by Silowa Printers: 012 804 1164

EXECUTIVE SUMMARY

The objective of this investigation was to gain a qualitative understanding of the mineralogy of the coal measures occurring in the Highveld coalfield of South Africa. The project focused on the identification of minerals occurring in coal and the understanding of the distribution of these minerals among the various coal seams. Furthermore, the lateral distribution patterns of minerals in coal were researched. In addition, an effort was made to establish the relationship between the mineralogy of the coal and the associated water quality.

The different depositional environments that have been recognized by other workers in the coal-bearing strata of the Ecca Group are associated with characteristic physicochemical conditions. Such characteristic physicochemical conditions dictate the precipitation of typical mineral assemblages. Thus, based on theoretically considerations, there should be a direct link between the depositional environment and the modal proportion of minerals and mineral assemblages.

Samples were collected from the No. 1, No. 2, No. 4 and No. 5 coal seams, as well as their roof and floor lithologies in both the Witbank and Highveld coalfields.

Low-temperature ashing (LTA) and X-ray diffraction (XRD) carried out on selected samples accentuated the need and practicality of integrating other analytical techniques with XRD. XRD on LTA coal proved to be more accurate in identifying minerals that occur as rare constituents, i.e. < 5 modal percent, especially since the organic material in coal tends to obscure interpretations from raw coal XRD;

There are numerous variables influencing the results from X-ray fluorescence (XRF) analyses on coal. Differences were observed, firstly, between whole coal and fusion disk XRF, and secondly, between whole coal results of mixed proportions of two samples. The calcination and fusion of coal samples introduces some difficulties concerning the loss of important constituents in coal, such as sulphur and possibly phosphorus. The conditions during preparation of XRF disks, such as temperature, need to be kept constant if similar results are to be obtained each time. A disadvantage of using whole coal briquettes refers to the "infinite thickness" issue. X-rays are often absorbed into coal briquettes resulting in lower count rates, while mass absorption is accounted for in fusion disks by the addition of La_2O_3 during preparation. The differences between whole coal results of mixed proportions of two samples could also be attributed mass absorption effects. Elements such as iron have a higher mass absorption resulting in lower count rates than is to be expected. The possibility of segregation of heavy minerals in samples during mixing and storage has been considered, and was minimized by correct sample handling and thorough mixing. The standard XRF technique is recognized as precise and reliable, but in this case whole coal analysis was more suitable.

The mineral components in coal were expressed as a percentage of the inorganic constituents. Minerals detected in the XRD patterns were semi-quantitatively evaluated in terms of dominant (>40% of the mineral fraction), major (10-40%), minor (2-10%), accessory (1-2%) and rare (<1%) constituents. The inorganic fraction consisted primarily of dominant quartz and kaolinite, and sometimes even dominant

pyrite, calcite and dolomite. The latter three were almost ubiquitous in the coal. The Ca-phosphate mineral, crandallite was detected in the western region of the Witbank and Highveld coalfields. Although only present in low concentrations, fluorapatite was detected throughout in the Witbank coal except in the extreme northeastern region. Fluorapatite was not detected in samples from the Highveld coal.

Chemical analyses confirmed the mineralogical interpretations. The inorganic components make up approximately 8 to 35 wt% of a coal sample. SiO_2 concentrations varied between and 35 wt% of a sample, Al_2O_3 between 0.5 and 16 wt%, Fe_2O_3 between 0.03 and 10 wt%, and S between 0.15 and 8 wt%. Minor concentrations of CaO (0 to 8 wt%) and MgO (0 to 1 wt%) were present. P_2O_5 occurred in concentrations of 0 to 3.5 wt% and K_2O was in the order of 0 to 1.3 wt%. Na_2O values were the lowest varying between 0 and 0.45 wt%. The only difference in chemistry between Witbank and Highveld coal was a slight increase in Na_2O (0 to 0.51 wt%) in the Highveld coal.

Acid-base accounting (ABA) results for the collected samples show that the lithological units in the coalfields have the ability to contribute to deterioration in ground and surface water quality. A positive correlation was recognized between the types of minerals, i.e. modal proportion of sulphide, carbonate and clay minerals, present in the coal and the associated water quality, i.e. the severity of the AMD problem.

Two types of screening criteria was used to determine whether acid or alkaline conditions will prevail once all acid consuming and acid producing minerals has been oxidized. From the NNP, or net neutralizing potential, it can be predicted that the No. 5 coal Seam, the No. 4 coal Seam and the unit between No. 2 and No. 4 coal seams will be predominantly acidic. The NNP of the other units vary between -20 kg/t and 20 kg/t, therefore these stratigraphic units could become either acidic or alkaline. The unit between No. 1 and No. 2 coal seams is the only unit possessing enough neutralizing potential to buffer the acid produced, but could still become acid since the NNP is less than 20 kg/t.

The NPR or NP: AP ratios, for all stratigraphic units (except between No. 1 and No. 2 coal seams) are less than 1:1 suggesting that acid conditions will dominate. The NPR ratio between No. 1 and No. 2 coal seams is at least 3:1 implying that enough buffering capacity is available to counteract the acid. The AP and NP are largely dependant on the presence of pyrite and calcite, respectively. Good correlations were obtained between the NP and CaO% and the AP and S%. Therefore it is possible to use the mineralogy to predict these factors. It should also be remembered that these predictions do not take time and weathering rates into consideration, thus such conditions will only be obtained once ideal situations are reached.

Finally, the study has contributed by recognizing regional distribution patterns of mineral matter in the No. 2 seam coal in the Witbank and Highveld coalfields.

A significant amount of useful mineralogical information has been compiled during the course of this study. However, the interpretation of the available data has not yet been optimized. We recommend that the

interpretation of available information should be completed and that additional information should be gathered where required.

ACKNOWLEDGEMENTS

The research in this report emanated from a project funded by the Water Research Commission entitled:

"The quantitative evaluation of the modal distribution of minerals in coal deposits in the Highveld area and the associated impact on the generation of acid and neutral mine drainage".

The Steering Committee responsible for this project consisted of the following persons:

Mr HM du Plessis	Water Research Commission (Chairman)
Mr KC Pietersen	Water Research Commission
Prof FDI Hodgson	University of the Free State
Dr RH Boer	Ferret Mining & Environmental Services (Pty) Ltd
Mr W Pulles	Pulles Howard & de Lange Inc
Prof WA van der Westhuizen	University of the Free State
Ms M Eksteen	Khutala Colliery
Prof MV Fey	University of Stellenbosch
Prof JS Ogola	University of Venda
Mr HD Naudé	Department of Minerals and Energy
Dr ME Ligthelm	DWAF, Mpumalanga region
Prof JF Botha	University of the Free State
Dr AS Parsons	Chamber of Mines of South Africa
Mr DA Salmon	Anglo Coal
Dr VE Cogho	Ingwe Coal
Mr NJ Benson	University of the Free State

The financing of the project by the Water Research Commission and the contribution of the members is gratefully acknowledged.

We appreciatively acknowledge the analytical contribution and technical assistance of Dr Colin R Ward from the School of Biological, Earth and Environmental Sciences, University of New South Wales, Australia.

In particular, we thank Professor Frank Hodgson and Dr Brent Usher, from the Institute for Groundwater Studies at the University of the Free State for their advice and support.

TABLE OF CONTENTS

APPENDICES ARE CONTAINED ON THE ATTACHED CD ROM

List of Figures

LIST OF TABLES

1 INTRODUCTION

1.1 Overview

Research into the mineralogical composition of the South African coal measures has been sorely neglected. A definite need exists to understand the mineralogical composition in order to assess the contribution towards pollution emanating from coal in a qualitative manner. The most significant form of pollution associated with the coal mining industry is the phenomena of Acid Mine Drainage (AMD).

The mining of coal exposes this resource to ideal conditions for adverse reactions to take place. AMD is primarily caused by the oxidation of the sulphide minerals. In coalmines, the minerals pyrite (FeS_2) and marcasite (FeS_2) are largely responsible for AMD problems. The use of water during coal mining provides a suitable medium and supplies sufficient oxygen for pyrite oxidation to occur. The rate of oxidation is dependant on temperature, pH, oxygen concentration, chemical composition of the pore water and microbial population. Waters affected by these reactions could be neutral or strongly acidic and are invariably loaded with toxic heavy metals and sulphate salts.

Attaining ideal conditions for AMD formation is more complex than just the oxidation of sulphide minerals. Various reactions between many other mineral phases give rise to a complex combination of constituents with numerous adverse and positive effects on the surrounding environment. It is this interaction between minerals and the immediate environment, especially the surrounding groundwater, which creates the real problem associated with coal mining.

In order to specify the cause and find a solution to this problem it is necessary to discover, firstly, exactly what is being dealt with in terms of the nature of coal (i.e. minerals, macerals, fixed carbon, moisture, etc.) and secondly, attempt to quantify the extent to which interaction has taken place or could take place between the coal and the environment. Thus it is clear that water-rock interactions form the basis of the pollution generating reactions. In order to understand these water-rock interactions it is imperative to have a good understanding and knowledge of the building blocks of the rock, i.e. the minerals and macerals.

The primary aims of the project were:

- To perform a selection survey of the coal mines and coal residue deposits in the Highveld area that would be suited to contribute in a meaningful manner towards the evaluation of the environmental impact associated with acid mine drainage (AMD) generation;
- Evaluate, through on-site investigations, as well as laboratory-based studies, the modal proportions of primary and secondary minerals in in situ coal seams and in residue deposits

- Prepare a guideline on the significance of the modal distribution of primary and secondary mineral phases associated with coal, specifically for South African conditions, in terms of the potential impact on the generation of acid mine drainage.
- The occurrence and modal distribution of primary and secondary minerals associated with in situ coal seams and residue deposits would primary be performed on a regional scale, however, a selected number of sites would be studied in detail in order to obtain an understanding of the mineralogical variation over mine-scale areas.

The phased approach that was followed during this project, have been described in more detail below:

Phase 1: Data collection

Firstly, available sources of relevant mineralogical information that deals with coal seams and surface residue deposits in the Highveld area have been scrutinized. These sources would include published literature, available company reports and unpublished information. Based on the knowledge gaps in the availability of mineralogical information, a detailed sampling programme was developed that included the physical sampling of coal seams in underground, as well as open pit exposures. The sampling programme also included surface residue deposits. On-site sampling was performed in collaboration with the mine geologist. A concerted effort was made to establish a representative collection of coal samples from the Highveld area in terms of the primary and secondary mineral assemblages.

Phase 2: Mineralogical analyses

For the mineralogical analyses of coal samples, the standard procedure followed in this study was to obtain optical petrographic information, both transmitted and reflected light microscopy, as well as semi-quantitative XRD data for each sample. The primary focus of the microscopy was the correlation with minerals identified or ambiguous in the accompanying X-ray diffractogram. In addition, the microscopic description focussed on textural features that relates to the susceptibility to weathering of the various mineral phases. The optical and XRD mineralogical information was supplemented by XRF data on selected samples. SEM and EPMA was applied to selected samples for which it was essential to obtain compositional data for solid-solution minerals, and to obtain fine-scale features such as alteration rims. The latter techniques were also used to verify the identification of grains too fine-grained to be unambiguously identified by optical microscopy. Small volume samples of unknown mineral phases were identified with the X-ray film method using the Debye-Scherrer camera.

Phase 3: Visualization of mineralogical data

Use was made of a GIS software package for interactive visualization of the data. The mineralogical database was constructed so that programs such as the Windows Interpretation System for the Hydrogeologist (WISH) could use it. Maps showing the regional trends for different minerals were generated and an overall interpretive map in terms of acid generating potential, based solely on the mineralogy, was included as part of the research product.

Phase 4: Mineralogical assessments

A range of mineralogical assessment techniques were applied. This task comprises an important part of the project and the mineralogical software package, MINPET 2.02, was used for graphical depiction of mineralogical features, as well as structural formulae calculations. The results of the mineralogical assessments were evaluated and the practical implication in terms of the four environmental facets of prediction, prevention, control, and remediation of acid and neutral mine drainage was discussed.

1.2 Study area

Coalmines situated in both the Witbank and Highveld coalfields were included in this study. The Witbank coalfield is situated east of Johannesburg. The southern boundary of the coalfield is considered to run from approximately 5 km south of Delmas Colliery in an east-northeast direction to about 5 km south of South Witbank Colliery. From this point eastwards, for about 60 km, a natural boundary is formed by a series of inliers of Rooiberg Felsite, known as the Smithfield Ridge.

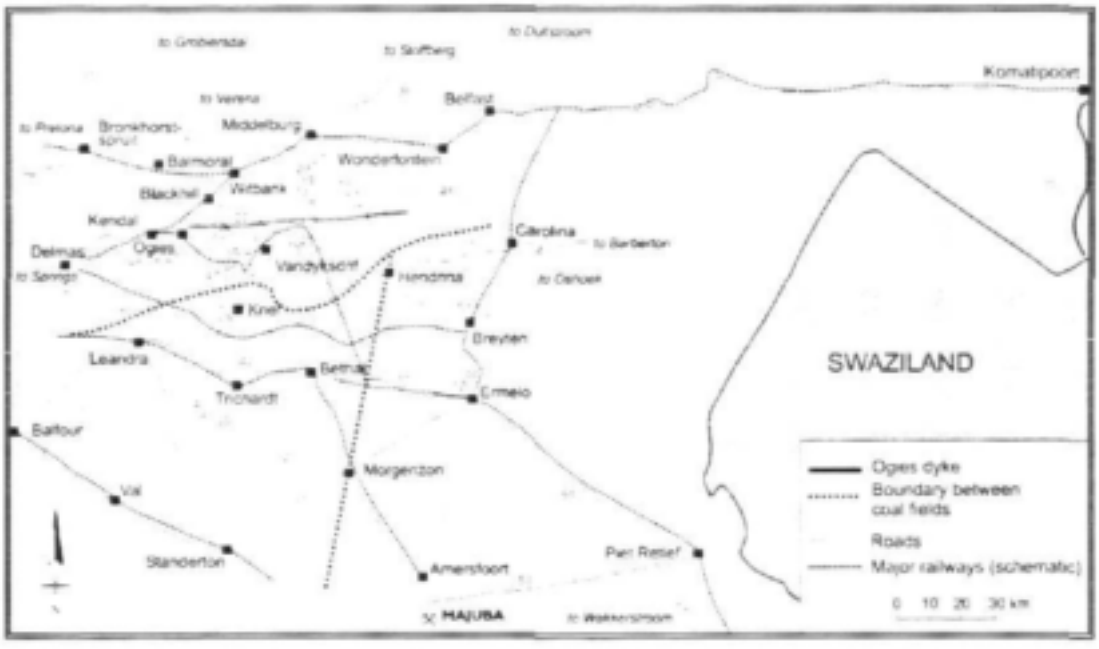

Figure 1. Collieries in Mpumalanga as well as southern boundary between Witbank and Highveld coalfields, and eastern boundary of Highveld coalfield (after Snyman, 1998). 1 – Arnot; 2 – Kriel; 3 - Arthur Taylor; 4 – ATCOM; 5- Bank 2; 6 - Bank 5; 7 – Blackwattle; 8 – Boschmans; 9 – Bothasrust; 10 – Delmas; 11 – Dover; 12 - Driehoek (Wessselton); 13 – Duvha; 14 – Eastside; 15 – Eikeboom; 16 – Elandsfontein; 17 – Ermelo; 18 – Glisa; 19 – Goedehoop; 20 – Greenside; 21 – Khutala; 22 – Kleinkopje; 23 – Koornfontein; 24 – Lakeside; 25 - Landau (Kromdraai); 26 – Leeuwfontein; 27 – Leeuwpan; 28 – Matla; 29 – Mavela; 30 – Middelburg; 31 - New Clydesdale; 32 - New Denmark; 33 – Northfield; 34 – Olifantslaagte; 35 – Optimum; 36 – Phoenix; 37 – Polmaise; 38 – Rietspruit; 39 - Secunda: Bosjesspruit; 40 - Secunda: Brandspruit; 41 - Secunda: Middelbult; 42 - Secunda: Syferfontein; 43 - South Witbank; 44 – Spitzkop; 45 – Strathrae; 46 – Tavistock; 47 - Van Dyks Drift; 48 – Waterpan; 49 - Witbank Consolidated; 50 - Woestalleen (Noodhulp section); 51 - Consbrey Dump; 52 – Protea; 53 – Mpisi; 54 – TBS; 55 - Nkomati Anthracite (after Smith and Whittaker 1986; Jordaan 1986; Schoeman and Boshoff 1996)

The Highveld coalfield is situated south of the Witbank field. Its eastern boundary is formed by a straight line through Hendrina, Davel and Morgenzon (Snyman, 1998) (Figure 1).

1.3 Geology and tectonic setting

Folloing the Pan-African tectonothermal event, which brought about the assembly of Gondwana, the southern edge of this super-continent experienced a prolonged period of sedimentation. The Cape Supergroup was deposited from the Ordovician to the upper Devonian as beach, deltaic and shallow marine clastic sediments on a broad, relatively stable platform. The Cape Fold Belt was part of the more extensive Pan Gondwanian Mobile Belt generated through compression, collision and terrain accretion along the southern margin of Gondwana. The associated foreland basin fragmented as a result of Gondwana break-up, and is preserved today in South America (Parana Basin), southern Africa (Karoo Basin), Antarctica (Beacon Basin) and Australia (Bowen Basin) (Catuneanu *et al., 1998*).

The Karoo Basin is a retroarc foreland basin developed in the front of the Cape Fold Belt, in relationship to the Late Palaeozoic-Early Mesozoic subduction episode of the palaeo-Pacific plate underneath the Gondwana plate. The maximum megasequence of the Karoo sedimentary succession exceeds 6 km and reflects changing environments from glacial to deep marine, deltaic, fluvial and aeolian (Catuneanu *et al.,* 1998).

A period of glacial sedimentation during the Permian-Carboniferous marks the beginning of numerous phases giving rise to the formation of the Karoo Supergroup in which most of the coal deposits of southern Africa are deposited (Thomas *et al.,* 1993). Diamictites and associated fluvio-glacial sediments of the Dwyka Group were deposited by both grounded and floating ice (Catuneanu *et al.,* 1998). After glaciation a shallow sea remained, fed by large volumes of meltwater (Smith *et al.,* 1993). Black clays and muds accumulated on the submerged platform under cold climatic conditions to form the Lower Ecca, while deltas prograded into the Ecca and eventually combined to form broad alluvial plains constituting the Upper Ecca. The distribution and the thickness of the lower seams are controlled mainly by glacial, pre-Karoo valleys and pre-Karoo topographic highs, while the upper seams were controlled by the basinward extent of delta progradation and by pre-Karoo highs around the basin margin (Smith and Whittaker, 1986a).

Towards the end of the Triassic the deposits of the Beaufort Group formed on semi-arid alluvial plains mainly as a result of floodplain aggradation. With increased aridification coarse-grained debris fans prograded into the central parts of the basin (Molteno Formation) and these fans were later drained by fine-grained meandering belts (Elliot Formation). The periodic floods provided a few coarser-grained deposits and together with aeolian sand dune deposits were preserved as the Clarens Formation, which marks the end of Karoo sedimentation. The wide range of structural and sedimentary settings, together with various ages, climates, and plant communities are the reasons for the difference in organic and inorganic material and the degree of maturity or rank of the coal of the region (Falcon, 1986).

SUPERGROUP	AGE (Ma)		GROUP	FORMATION
KAROO	140	Jurassic	Drakensberg	Drakensberg
	195			Clarens
	225	Triassic		Elliot
	230	Upper Permian	Beaufort	Adelaide Subgroup
	260	Middle Permian	Ecca	Volksrust
				Vryheid
				Pietermaritzburg
	300	Lower Permian	Dwyka	

Figure 2. Lithostratigraphic nomenclature for the Karoo Supergroup (after Azzie, 2002)

The regional geology of the study area is characterized by numerous post-Karoo age dolerite sills and dykes which outcrop on the surface, while rocks of the Vryheid Formation of the Ecca Group covers most of the surface area. The five separate bituminous coal seams are preserved in the Vryheid Formation (Cairncross, 2001), and were deposited under cool, wet climatic conditions. To the north outcrops of the Transvaal Supergroup and the Ventersdorp Supergroup can be observed, as well as several tillite and diamictite outcrops of the Dwyka Group.

1.3.1 The Witbank coalfield

The Witbank coalfield, also previously known as the Springs-Witbank coalfield, is currently the most important in the country, and extends over a distance of some 180 km from the Brakpan and Springs areas in the west, to Belfast in the east and about 40 km in a north-south direction. The mines of this coalfield are situated primarily within the Olifants River Catchment as seen in Figure 1 (Smith and Whittaker, 1986b).

1.3.1.1 Origin and stratigraphy

The strata of the Karoo basin consist primarily of sandstone, carbonaceous shale, siltstone, minor conglomerate and several coal seams (Cairncross, 2001). Stratigraphic columns for different parts of the coalfield are illustrated in Figure 3. This wide range of sedimentary and structural settings within which the coal seams were deposited, combined with the range of ages, climates and plant communities give rise to the numerous differences in terms of organic and inorganic matter and the degree of maturity of the coal seams (Falcon, 1986).

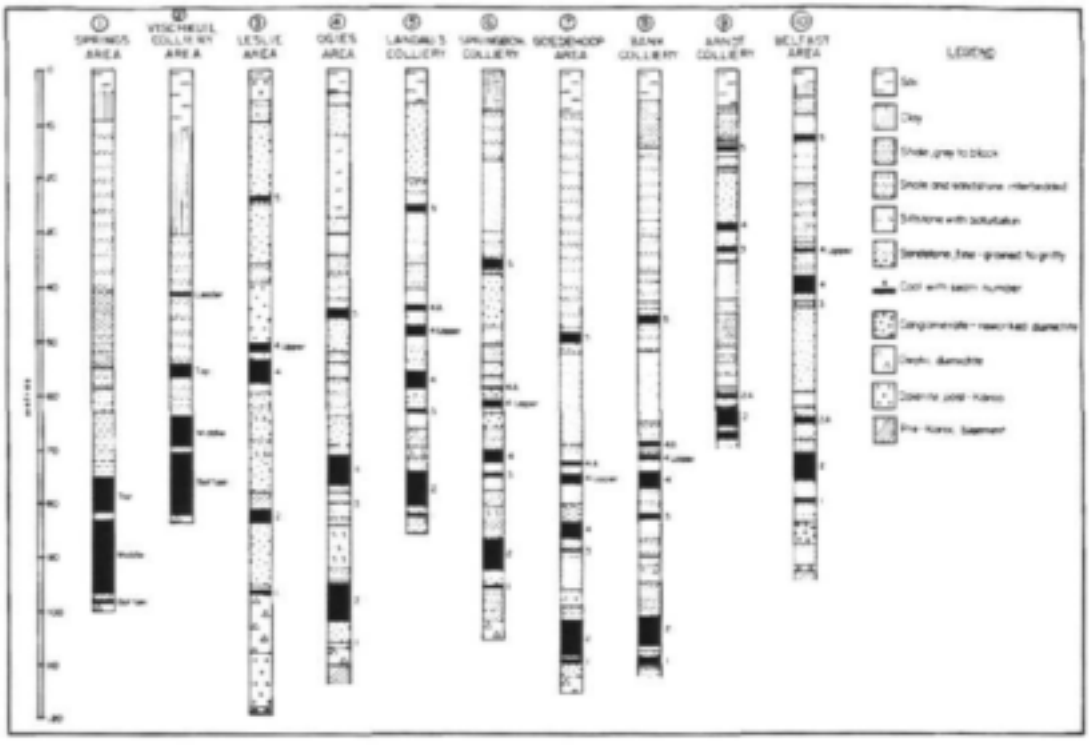

Figure 3. Stratigraphic columns for different parts of the Witbank coalfield (Smith and Whittaker, 1986b)

The sediments of the Ecca Group of the Karoo Supergroup were deposited on an undulating Karoo floor, which influenced the distribution and thickness of the sedimentary formations as well as the coal seams. Although post-Karoo erosion has removed substantial volumes of coal a maximum of 180 m of Karoo strata has been preserved. Several major glacial valleys are recognized in the area in which Dwyka sediments are the thickest in the deepest palaeo valley. Numerous ridges, mainly of igneous rocks are observed of which the Smithfield Ridge felsite forms the southern boundary of the coalfield. The five seams are contained within a 70 m succession and parting thickness between the seams is reasonably constant across the field (Smith and Whittaker, 1986b).

1.3.1.2 Description of coal seams

Four of the five seams in the coalfield are consistently developed over strike length of approximately 180 km. The No. 2 Seam is economically the most important, but No's. 5, 4 and 1 seams are mined in areas where the local quality is high and the thickness is suitable for mining purposes. The least economically important Seam, No. 1 Seam, is better developed in the northern and eastern part of the field where it is approximately 1.5 to 2 m thick. It consists mainly of lustrous to dull coal with local shale and sandstone parting and a competent sandstone or grit roof, especially in the Arnot area (Snyman, 1998).

The No. 2 Seam constitutes approximately 69% of the resources of the Highveld coalfield. An average natural thickness of 6.5 m is found in the central part and increases to about 8.5 m in the south-west

where the upper part is shaly and not economic. In the east it is about 3 m thick. A consistent sandstone parting divides the seams into a No. 2 and No.2 Upper Seam. Mining conditions are generally favourable where sandstone provides a competent roof. There are areas where shale is present in the roof (Smith and Whittaker, 1986b). The No. 3 coal Seam is discontinuous throughout the coalfield and not of economic importance.

In addition to the No. 4 Seam (or 4 Lower), this coal zone generally contains a No. 4 Upper and No. 4A seams as observed in Figure 1.6, both of which are too thin to be economically important. The main No. 4 Seam consists of dull to dull lustrous coal with a natural thickness varying between 2.5 m in the central part of the field to 6.5 m elsewhere. The roof shale presents poor stability conditions. The No. 5 Seam, which is approximately 1.8 m thick in most areas, consists mainly of bright coal with thin shale and mudstone partings and a weak laminated sandstone roof. The Seam has been eroded extensively and its distribution is controlled mainly by present-day topography (Snyman, 1998).

1.3.1.3 Structure

The distribution of the seams is controlled by the pre-Karoo topography, but the seams are mainly flat and dip only slightly in a southerly direction. Steeper dips are observed in the lower seams while seams Nos. 4 and 5 have a rather regular disposition. The No. 4 Seam is also greatly influenced by the erosional effects of the overlying sandstone. The strata of the Karoo are generally unfolded with abundant small faults (Smith and Whittaker, 1986b).

Dolerite dykes and sills affected most of the areas of the coalfield. Large sections of the coal seams have been devolatilised and are rendered useless for mining purposes. General north, north-east and east trends are noticed in the case of the dykes while the most prominent dyke, named Ogies Dyke strikes west-east for approximately 100 km. To the north of Ogies Dyke smaller dykes are less common than in the south and vary considerably in thickness from 0.5 m to 1 m in the north to 5 m thick in the south (Smith and Whittaker, 1986b).

The extent to which areas of coal seams in the immediate vicinity of such intrusions are burnt or devolatilised depends not only on the thickness of the intrusion, but the temperature, period of molten flow and attitude of the intrusion, and the intrusions are classified into a porphyritic and non-porphyritic groups. The amount of displacement caused by dolerite sills is equivalent to the thickness of the sill. However, the associated devolatilisation presents a more serious problem to mining and coal resources estimation (Smith and Whittaker, 1986b).

1.3.2 The Highveld coalfield

The Highveld coalfield covers an area of approximately 7000 km^2 and extends over a distance of some 95 km from Nigel and Greylingstad in the west to Davel in the east, and 90 km in a north-south direction

(Jordaan, 1986). As seen from the distribution of mines the coalfield is situated in Vaal River Catchment area.

1.3.2.1 Origin and stratigraphy

Similar to the sedimentation in the Witbank coalfield, the rocks of the Karoo Supergroup in the Highveld coalfield were deposited on undulating pre-Karoo surfaces. However, post-Karoo erosion removed large volumes of coal along the northern margin of the field. Glacial diamictite, siltstone and mudstone deposits are overlain by clastic sediments and coal successions. The sediments were deposited in shallow marine fluvio-deltaic environments while the coal accumulated as peat in swamps and marshes associated with the sedimentary rocks (Jordaan, 1986).

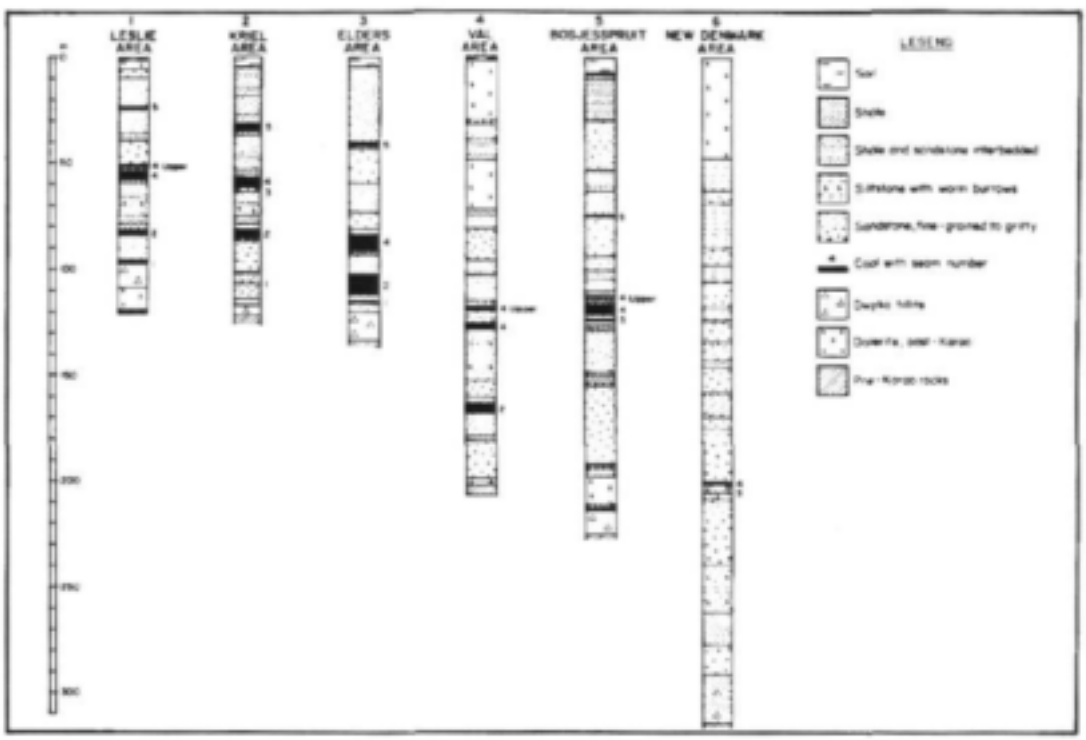

Figure 4. Stratigraphic columns for different parts of the Highveld coalfield (Jordaan, 1986)

Three phases of sedimentation took place, the first delta-dominated phase giving rise to upward coarsening cycles of dark grey, micaceous siltstone, fine-grained sandstone with abundant carbonaceous material, and coarse-grained sandstone, while widespread bioturbation is found in these rocks. The fluvially dominated coal-bearing horizon is about 75 m thick in which five coal seams have been recognized in the northern and western parts, but the lower two seams are absent in the southern and eastern parts. Above Nos. 4 and 5 coal seams glauconitic sandstones are indicative of marine transgression periods. Micaceous shale, siltstone and white sandstone of the upper deltaic succession overlie the coal zone (Jordaan, 1986).

1.3.2.2 Description of coal seams

As seen from Figure 4, there are five seams recognized in the coalfield, namely, Nos. 1, 2, 3, 4 and 5. The No. 4 Seam is further subdivided into Nos. 4 Upper, 4A and 4 coal seams. Nos. 2, 4, 4 Upper and 5 seams are economically important. The Nos. 1, 3 and 4A coal seams are thin and discontinuous. The thickness of No. 2 coal Seam varies from 1.5 to 4 m, but can reach 8 m in the west and north-east. Irregularly distributed shale partings are present in the Seam, and due to the variability of the coal, only the upper 2 to 3 m, or the basal 2 to 3 m forms the mineable horizon. It consists of bituminous coal with roof rocks ranging from fine-grained sandstone, intercalated sandstone, siltstone and mudstone (Jordaan, 1986).

The No. 4 Seam consists mainly of dull coal with shale intercalations in the upper part of the Seam. It's thickness varies from 1 to 12 m but averages at 4 m (Snyman, 1998). The roof is variable and consists of grit, coarse- to fine-grained sandstone, intercalated sandstone and siltstone, shale or coal, while the generally competent floor consists of sandstone and siltstone. The No.4 Upper Seam comprises low grade bituminous coal and can only be mined where the in-Seam parting is thick enough. It is characterized by a strong, coarse-grained sandstone floor and a weak interlaminated sandstone and siltstone roof (Jordaan, 1986).

The No. 5 coal Seam consists mainly of bright coal. It is present across the majority of the coalfield but only reaches a mineable thickness in the northern and western parts (Snyman, 1998). The natural thickness varies between 1 and 2 m. The roof comprises a fine-grained sandstone and siltstone (Jordaan, 1986).

1.3.2.3 Structure

The seams are generally flat, but the intrusion of dolerite sills caused significant displacement in the strata. Dolerite dykes and sills, which might be of the same age as the Drakensberg Formation, are present mainly along north-south, north-east and north-west trends covering large areas. The dykes especially had a destructive effect on the coal seams in most areas of the coalfield and devolatilised zones range from 1 to 30 m. The sills are present over large parts of the coalfield, but considerable material has been removed to due post-Karoo erosion. These sills are porphyritic and non-porphyritic in character (Jordaan, 1986).

1.4 Palaeo-climate and vegetation

The most important factors influencing the formation of coal in the early stages of plant accumulation and degradation are (i) tectonic control and sedimentary environments, (ii) plant communities, (iii) prevailing climatic conditions, and, (vi) conditions such as water level, Eh and pH, and salinity. This

section will therefore briefly discuss the vegetation and climatic conditions present during the formation of the above-mentioned coal seams.

Cold to cool temperate conditions where present during the existence of the Permian swamps of the basins of Gondwana. The coal-bearing successions accumulated on relatively stable continental depressions in the form of different types of basins, the Karoo retro arc foreland basin being one of them. Different plant species contribute different forms of decaying humic matter, which will therefore influence the product of accumulation and degradation. So too does changes in climate provide different temperatures, humidity, and rainfall, which affects the rate and type of decay of the plant, matter (Falcon, 1986).

Major floral and climatic changes brought about by continental drift may have effected the migration of vegetational belts, which is especially evident during Karoo sedimentation. The most significant feature with regard to climate during Karoo times is the early Dwyka glaciation. With this phase drawing to a close, rapid glacial advances and retreats from local ice cap centres took place, and the continent passed through numerous distinct vegetational phases starting during Late Carboniferous and Early Permian times. Climatic changes vary from Permian-Carboniferous arctic to subarctic, cold temperate to temperate, and finally into hot, arid desert conditions ending in volcanism.

The earliest pre-Karoo floras have been described to occur during the Lower-Carboniferous age, which was followed by Dwyka glaciation. At the end of the Dwyka new plant assemblages began to flourish, and mixed *Glossopteris-Gangamopteris* flora was resident in the Mid-Ecca swamps. The Upper Ecca and Beaufort were characterized by Glossopteris with swampy flats and abundant reed-like horsetails. The Molteno sediments of the Upper Triassic yielded fern-like flora called Dicroidium, which died out during the deposition of the semi-arid Clarens Formation towards the Late Triassic-Early Jurassic (Falcon, 1986; Smith, *et al.*, 1993).

1.5 Topography

The topography of the study area is characterized by gently undulating surfaces with several local streams, larger rivers and pans shaping the landscape. Average surface elevations are around 1540 mamsl, but sandstone plateaus such as those in the north reaches 1600 mamsl (Azzie, 1999).

1.6 Groundwater and drainage systems

Three catchment areas, namely the Komati Catchment, the Olifants Catchment, and the Vaal Catchment situated in the northeastern, central and southwestern parts of the coalfields serves as the main drainage systems. Surface water quality of the Loskop Dam, Witbank Dam, Middelburg Dam, Nooitgedacht Dam, the Grootdraai Dam and other smaller rivers and streams can be obtained in Grobbelaar (2001). The

Olifants River and Steenkoolspruit are the major drainage valleys in the Witbank Dam catchment, while the Klein Olifants River is the primary drainage valley in the Middelburg Dam catchment (Chelin, 2000).

According to Azzie (1999) and Grobbelaar (2001) two groundwater systems are present, namely, the weathered and unweathered Ecca Group\Vryheid Formation aquifers. The first lies between depths of 5 and 12 m below surface and occurs at the interface of soil and bedrock. Rainfall infiltrating into the weathered rock reaches impermeable layers of sediments below the weathered zone. Groundwater flow patterns usually follow the topography. The aquifer within the weathered zone is usually generally low-yielded (range 100 – 2000 L/hour) because of its insignificant thickness (Hodgson and Krantz, 1998).

The lower system occurring in the unweathered Vryheid Formation consists of sandstones, siltstones, shales and coal. Groundwater within these sediments will be contained within fractures, joints and bedding planes. The Ogies Dyke is impermeable over much of its length and thus compartmentalizes the groundwater. Of all the unweathered sediments in the Ecca the coal seams have the highest hydraulic conductivity (Grobbelaar, 2001).

The depth of the water table is between 1 and 8 m below surface, and water levels have been recorded to be within 5 to 15 m of the ground surface. Pre-Karoo aquifers are not tapped often due to their great depths and low-yielding character (Grobbelaar, 2001).

2 PREVIOUS RESEARCH

2.1 Geochemistry and mineralogy of the Ecca Group

Various factors affect the major and trace element distributions in sedimentary rocks. These would include variables such as source rock compositions, intensity of weathering, sedimentation rates, depositional environments, and diagenesis. Depending on the depositional history and the above-mentioned factors, different mineral assemblages are observed in different lithologies.

The Ecca Group becomes shalier in a southerly direction and is composed almost entirely of shale south of a line through Bloemfontein and Harding. The Vryheid Formation can be divided into several cycles of sedimentation in which a succession of depositional environments can be recognized (Van Vuuren and Cole, 1979). Coarse, fluviodeltaic sandstones makes up the proximal facies of this gently subsiding shelf platform, and wedges out into siltstone and mudstone facies (Pietermaritzburg and Volksrust Formations) in the south (Snyman, 1998). The formation is composed mainly of coarse-grained arkose, conglomerate, micaceous siltstone, carbonaceous shale, coal seams and thin layers of limestone (Stratten, 1986).

Although numerous references are available with regard to the structural, environmental and depositional conditions of the Karoo Basin, limited literature is available on the mineralogy and geochemistry of these sediments. Previous work in this regard would involve a brief petrological study on the coal-bearing strata of the Ecca sediments by Bühmann and Bühmann (1988) as part of a research project. Coal and rock samples were collected from core drilled in the Witbank coalfield, Mpumalanga coalfield and Vryheid coalfield and analyzed by means of X-ray diffraction in order to evaluate mineralogical variables as indicators of fluctuating palaeo-environments during the formation of the coal deposits.

Clay assemblages dominate the mineralogical components of samples amongst the coal, and are even more abundant amongst the sediments in most cases. These assemblages display variations from kaolinite-free to kaolinite-dominated with subordinate mica and chlorite as well as minor traces of illite\smectite interstratification in the Witbank coalfield. A similar distribution pattern is displayed in the Mpumalanga coalfield, however, chlorite dominance in certain sections of the sequence is commonly associated with the carbonate minerals, and the illite\smectite interstratification contains up to 80% illite in some cases. The clay fraction in the Vryheid coalfield is dominated by chlorite and mica with a low amount of illite\smectite interstratification (Bühmann and Bühmann, 1988).

The relationship between clay and non-clay fractions was examined in terms of the presence and absence of kaolinite. K-feldspar is more abundant in kaolinite dominant samples while plagioclase proportions are higher in kaolinite-free samples. Siderite is more prevalent in kaolinitic samples. Apatite is associated with 2:1 layer silicates, which are indicative of marine environments while crandallite is restricted to kaolinite dominant samples.

There is no direct association between pyrite and any clay minerals; however the presence of pyrite does suggest marine influence or a reducing environment. Mica and chlorite are both regarded as detrital components, which were formed under conditions of low chemical weathering resulting in the absence of kaolinite where a marine water environment was present. The presence of freshwater aids the transformation of illite, chlorite and smectite to kaolinite (Bühmann and Bühmann, 1988). As shown by Bühmann and Bühmann the use of prevailing mineral assemblages could serve as a dependable indicator as to what depositional conditions were.

Another study that provides valuable information on the mineralogy and geochemistry of the Karoo sediments was conducted by Azzie (2002) using both X-ray fluorescence (XRF) and X-ray diffraction (XRD) techniques. It was found that the sediments consist predominantly of the two oxides SiO_2 and Al_2O_3. The sandstones (including the glauconitic layers) have between 41 and 87 wt% SiO_2, while the shales and siltstones have between 27 and 61 wt% SiO_2. Al_2O_3 was highest in the siltstones and shales (9 – 23 wt%) followed by the sandstones (5 – 24 wt%). Fe_2O_3, CaO, MgO, Na_2O and K_2O are present in smaller concentrations than SiO_2 and Al_2O_3, while P_2O_5, MnO and Cl were barely present in any of the rocks. From XRD interpretations Azzie (2002) deduced that kaolinite and quartz are the main mineral constituents in all rock samples, while feldspars occur in major to minor proportions. Illite and siderite were present in major to minor amounts while pyrite, calcite and dolomite were present in minor to trace proportions in the shales and siltstones.

A comparison of available data on the Karoo coal-bearing successions with other coal-bearing successions in Australia and USA show that the sandstones, shales and siltstones in the Karoo Supergroup are reasonably similar in composition to those in other countries, despite differences in age, depositional environment and source compositions. Documented information on the geochemistry of coal-bearing strata is published by Nicholls (1968), and Styan and Bustin (1984), and includes a range of varying conditions under which coal-bearing strata have been deposited. However, extensive mineralogical information on the Karoo strata is still necessary and substantial information could be provided in this study.

2.2 Review of mineral matter in coal

Extensive research studies and projects have been conducted on coal universally, and even more so, on the complexity of its constituents. Such detailed studies on the mineralogy and geochemistry of coal have been carried out in abundance in countries such as Australia, Canada, India, Pakistan and USA, amongst others. However, similar mineralogical and geochemical studies have not been performed on South African coal. Characterizing coal minerals in other deposits of different age, depositional environment and source areas has relevance to understanding minerals in South African coal deposits. Although much is gained from petrographical or chemical studies of the organic constituents, the mineral matter in coal also provides information on the depositional conditions and geological history of the coal-bearing sequences and individual coal beds (Ward, 2002).

The composition of coal could be divided into organic constituents, inorganic constituents, and fluid constituents in the organic and inorganic matter. Non-crystalline organic matter consists of lithotypes and macerals, and amorphous phases, while crystalline organic matter such as the hartite-evenkite group is also present. Crystalline or mineral inorganic matter comprises of crystals, grains and aggregates of different minerals, and, metamict and gel minerals. Volcanic and cosmic materials would form part of the amorphous or non-crystalline inorganic matter. Liquid and gas phases occur in minerals together with fluid inclusions to form the fluid constituents of coal (Vassilev and Vassileva, 1996).

The crystalline inorganic matter occurring in coal may form as a result of a range of different processes. These include input of fragmental sediment into the original peat-forming environment by epiclastic and pyroclastic processes, accumulation of skeletal particles and other biogenic components within the peat deposit, and precipitation of material in the peat swamp or in the pores of the peat bed. The minerals are often visible in hand specimen, and can frequently be observed in examination of drill-cores, outcrops or mine exposures.

Such megascopic occurrence include thick bands or lenticles of clay-rich or pyritic material, rounded pellets or nodules of mineral matter and dispersed crystals of mineral matter within the coal, as well as mineral that forms coatings on, or infillings in, cleats and other fractures. Microscopic data reveal that many of the minerals in coal occur in a very intimate association with organic constituents. Minerals may therefore also occur as isolated euhedral crystals, as broken, presumably detrital fragments, as microscopic nodules, or in some cases as sub-microscopic crystalline aggregates or framboids. Many minerals, however, occur as petrifactions, representing infillings of cell cavities in the individual coal macerals (Ward, 1986).

Various coal samples contain similar assemblages of major and minor minerals. There is, however, comprehensible distinctions concerning modes of occurrence and the genesis of these minerals. So too is the understanding of certain terms such as epigenetic and syngenetic of the utmost importance. Syngenetic minerals in this case would refer to minerals that have formed contemporaneously with, and by essentially the same processes as the enclosing sediment. Epigenetic minerals occur after the deposition of the sediment. In understanding the genesis of mineral in coal the terms detrital and authigenic are also significant. Detrital minerals results from the mechanical disintegration of the parent rock and commonly occurs as a result of syngenetic processes forming sedimentary rocks, while authigenic minerals are formed or generated in place and have not been transported. These minerals therefore commonly occur due to epigenetic processes that may take place after deposition (Bates and Jackson, 1980).

Although the amount of inorganic matter varies considerably, the major minerals in the crystalline matter of coal are normally quartz, kaolinite, illite, calcite, pyrite, plagioclase, K-feldspar, and occasionally gypsum, Fe-oxyhydroxides, sulphates, dolomite, ankerite and siderite. These minerals will be discussed

in general with regard to their abundance and mode of occurrence in coalfields across the world and in South Africa.

2.2.1 Quartz

Quartz is the most common mineral in coal and is both detrital and authigenic in origin. It is found as pore infillings in the organic matter in coal, a mode of occurrence that clearly indicates its authigenic origin. Epigenetic quartz is massive or is present as bipyramidal crystals (Vassilev and Vassileva, 1996). Such crystals might have a volcanic origin or could have been precipitated authigenically. Occurrences where quartz has filled the cells of plant tissues at the early stage of development have been observed; however, according to Ward (2002) the origin of this silica is uncertain. However, a large proportion of silica in modern-day peats is of biogenic origin (Ward, 1986).

The introduction of silica by hydrothermal solutions results in the quartz filling cracks, forming lenses and encrusting coal fragments. It may constitute up to half of the mineral matter in Australian coal (Ward, 1986), but makes up only 10% of the oxidation residues. This percentage may vary considerably depending on the depositional setting. Coals from the Gunnedah Basin in New South Wales, Australia contain relatively low amounts of quartz of detrital origin as observed by Ward *et al.* (1999). Similarly, Ward *et al.* (2001b) also noticed that quartz formed a major part of the mineral matter of coal seams in the Gloucester Basin with significantly elevated amounts (>40%) of this mineral in the lower seams of the basin, which in this case may represent contamination of the original peat by quartz-rich tuffaceous sediment.

Electronic low-temperature (oxygen-plasma) ashing of some reference materials from the North American Argonne Premium coal series showed that quartz made up approximately 7 to 20% of the LTA residues. However, the mineral was more abundant in ash prepared at 370°C (Ward *et al.*, 2001a). Thus, the significance of this detrital and/or authigenic mineral is apparent, despite the difference in age and depositional environment between northern hemisphere and southern hemisphere coal. Furthermore, numerous authors such as (Mackowsky, 1968; Bouška, 1981; Ward, 1984) have observed and confirmed the presence and modes of occurrence of quartz in coal.

2.2.2 Clay minerals, feldspars and micas

Clay minerals present are mainly kaolinite, subordinate illite and minor amounts of montmorillonite. In most cases, kaolinite makes up almost all the mineral matter along with quartz. It may occur in the pores and cell cavities of the coal macerals or as layers, lenses and lenticles. Authigenic kaolinite is a result of diagenetic alteration of illite, montmorillonite, feldspars, muscovite, other alumino-silicates, and pyroclastic glasses. Some clay minerals, which occur as veinlets or crusts and fine films on slickenside surfaces in coal, may have epigenetic origin. There are various theories concerning the origin of kaolinite as suggested by Ward (1986).

Occurrences where kaolinite has been sourced from volcanic material input to the original peat deposit has been observed (Ward, 2002), however, Al is soluble under low pH conditions and can thus be leached from any detrital mineral material and transported to areas with higher pH where it is authigenically precipitated (Vassilev and Vassileva, 1996). This precipitation leads to the formation of various minerals such as bauxite-group minerals, depending on the precipitation conditions. The occurrence of quartz and kaolinite as the dominant mineral matter in coal is not uncommon. In some high rank coal the concentrations of illite, mica and chlorite can be higher than kaolinite probably as a result of decomposition of some pre-existing minerals (Vassilev and Vassileva, 1996).

Although more commonly associated with the non-coal strata, illite is often completely absent as a discrete mineral constituent in coal samples (Ward, 1986). Not only the partings in coal, but also the overlying and underlying shales, contain more illite than kaolinite (Mackowsky, 1968). It occurs frequently in the form of mixed-layer or interstratified clay minerals. Its low concentration may simply reflect a low proportion of detrital input to the peat swamp, or indicate that the mineral in its pure form is susceptible to alteration (Ward, 1986). It also occurs in reasonable proportions in ash residues of North American coal as studied by Ward (2001a) and its mainly detrital presence in coal from Bulgaria, the United States, Australia, Japan, Canada, China and South Africa has been observed by Vassilev and Vassileva (1996).

Although occurring is lesser percentages, montmorillonite and chlorite are also found in coal throughout the world, and represent one of the principle clay minerals in Australian bituminous coal, other than kaolinite. They are most likely to be of detrital origin (Ward, 1984, 1986; Vassilev and Vassileva, 1996).

Feldspars are represented by K-feldspars and plagioclases as semi-rounded grains and prismatic crystals of detrital, or even pyroclastic origin (Ward, 1986). These minerals are common in non-coal strata, or at least in the coal-bearing sequences. Mica is represented by muscovite and subordinate biotite. Muscovite and biotite may both be of detrital origin while muscovite may also be as a result of diagenetic weathering of feldspars (Vassilev and Vassileva, 1996).

2.2.3 Sulphide minerals

One of the major contributors to air and water pollution originating from coal mining operations is the group of sulphide minerals, which commonly occur in coal and occasionally in coal-bearing sequences. It is therefore important to understand the mode of occurrence of sulphur in coal. The total sulphur in coal can be used as an environmental indicator of the original peat. High sulphur content is often associated with marine influence at the time of/or immediately after deposition. Higher concentrations of sulphur are usually found at interfaces that indicate a change of environment (i.e. fresh to brackish water).

There are three major forms of sulphur identified in coal, namely organic, pyritic and sulphate sulphur (Mackowsky, 1968; Bouška, 1981; Ward and Gurba, 1998). Organic sulphur is part of the plant tissue and forms as the plant grows. It is chemically bound to the carbon molecules, but it is not as well established

as inorganic sulphur. Syngenetic organic sulphur is derived primarily from original plant sulphur. Reduced hydrogen sulphide can also react to form organic sulphur compounds if iron is not readily available to form pyrite. The organic sulphur in coal is mainly attached to the side chains of the organic molecules in the form of (-SH) groups. With the increase in coalification and rank, the (-SH) content of the macerals decreases due to condensation. Low-sulphur coal contains mostly syngenetic organic sulphur (Ward and Gurba, 1998).

Pyritic and sulphate sulphur forms are often referred to as inorganic sulphur. Sulphate sulphur is often formed by oxidation of the pyritic sulphur. Inorganic sulphur is introduced to the coal during and/or after peat accumulation and during coalification. Pyritic sulphur mainly occurs as pyrite and marcasite. Sulphur forms including galena, sphalerite and millerite have also been reported in some coal samples (Ward and Gurba, 1998). This type of sulphur can form syngenetically during peat formation as a result of microbial reduction of aqueous sulphate during early diagenesis. Bacterial reduction of sulphate takes place in a variety of sedimentary environments; both marine and freshwater, wherever organic matter and sulphate coexist in the absence of oxygen. Syngenetic pyrite is usually characterized by small, isolated crystallites and framboids (Vassilev and Vassileva, 1996).

Epigenetic pyrite is usually observed as large crystals, massive forms with various overgrowths encompassing the previous overgrowths or as cleat- and fracture-filling pyrite. This secondary incorporation of sulphur is determined by the availability of sulphate, the reactivity of the organic matter, the extent of sulphate reduction and the availability of iron and other metals to form mineral sulphides. Some epigenetic occurrences may represent remobilisation of organic sulphur or syngenetic sulphides within the coal, while other may be the result of factors outside the original depositional system, such as nearby igneous intrusions, or caused by post-depositional fluid movement through the coal-bearing succession. Unlike most syngenetic pyrite, post-depositional sulphides are not necessarily an indication of marine influence on the formation of the coal Seam (Spiker *et al.*, 1994; Ward, 2002).

Primary sulphate is formed by equilibration of sulphate molecules with water molecules and catalyzed by sulphate reducing bacteria early in diagenesis. Secondary sulphate is formed by late stage oxidation of sulphide (i.e. during weathering) by one of the following mechanisms:

a) Utilizing O_2 as an oxidizing agent

$$S^{2-} + 2O_2 \Rightarrow SO_4^{2-} \qquad (1)$$

b) Utilizing Fe^{3+} or some other oxidizing agent in the absence of oxygen

$$S^{2-} + 8Fe^{3+} + 4H_2O \Rightarrow SO_4^{2-} + 8Fe^{2+} + 8H^{+} \qquad (2)$$

The sulphide oxidation via reaction (2) is generally faster than via reaction (1), and is predominant under natural conditions. Generally coal show a wide variation of primary and secondary sulphate and very few coal are dominated by one source (McCarthy *et al.* 1998).

2.2.4 Carbonate minerals

The carbonates of calcium, iron magnesium and manganese are some of the most obvious of the incombustible constituents since they occur as the common cleat infillings of coal seams (Williamson, 1967) and are mostly authigenic minerals in coal (Vassilev and Vassileva, 1996). These minerals are of both syngenetic and epigenetic origin. Syngenetic calcite, dolomite, and ankerite occur as individual grains, lenses or infilling cell pores, or as veinlets filling cavities of cementing of fractures coal fragments, suggesting an epigenetic origin. Larger, spheroidal to regular masses of syngenetic minerals, mainly calcite but also including siderite, dolomite, pyrite and quartz, occur in some seams as coal concretions. These minerals accumulations are regarded as representing concretions formed in the peat bed, either during plant deposition or after early diagenesis. Siderite occurrences include nodules with a typically radiating crystal structure and replacements of the maceral components. An abundance of syngenetic siderite is usually thought to indicate deposition of the coal mainly under non-marine conditions (Vassilev and Vassileva, 1996).

Epigenetic carbonates, such as calcite, dolomite, ankerite, and siderite, are common cleat infilling materials in coal seams. In some cases the cleat fillings may show chemical variations such as those observed in some North American coal (Ward, 2002). Vassilev and Vassileva (1996), along with various authors, have observed the presence of other carbonates such as smithsonite, magnesite, rhodochrosite, and witherite, amongst others.

2.2.5 Phosphate minerals

Phosphate minerals in coal exist as minor to rare constituents of the mineral matter, but are still associated with coal deposits. They are detrital and authigenic in origin. Phosphorus in coal occurs mainly as inorganic phosphates and lesser amounts of organically bound phosphorus complexes. Sources of phosphorus may be in enriched volcanic material introduced during peat accumulation or the organic matter in the peat bed (Ward, 2002).

A range of phosphate minerals can occur in coal, including apatite and the aluminophosphates of the crandallite group, which occur mainly as syngenetic cell and pore infillings, or as epigenetic cleat and fracture fillings due to the remobilisation of phosphate formed earlier within the coal Seam. Crandallite-group minerals are composed of four principal elements, namely phosphorus, calcium, barium/strontium and aluminium. Crandallite occurs as 3μm size colloidal precipitates, as concretions and as porous aggregates as large as 100 μm (Rao and Walsh, 1999). Apatite occurs as prismatic crystals and occasionally in clusters. Occurrences of uranium phosphate, goyazite and vivianite, as well as the association between phosphorus and some rare earth elements have been observed (Vassilev and Vassileva, 1996).

2.2.6 Other minerals

Although the spectrum of minerals occurring in coal has been reviewed in considerable detail, subsidiary amounts of less common minerals also occur in coal. Chlorite, which in some cases would be regarded as a significant constituent, occurs as an authigenic mineral together with other chlorides such as halite. Alumino-silicate volcanic glass has also been observed as spheres, spheroids and angular particles. The accessory minerals in coal show great variety, but their low concentrations create difficulty in determining some of them (Vassilev and Vassileva, 1996).

2.3 Mineral matter in South African coal

Meaningful observations can be made by investigating at the information on the distribution, occurrence and abundance of minerals in the coal deposits of the Karoo Supergroup, which has been gathered up to date. A study by Gaigher (1980) deduced that the inorganic matter in some South African coal is dominated by clay minerals, mainly kaolinite and illite, followed by quartz and then the carbonates calcite, dolomite and siderite. Mineral matter is seen to vary over a range of 11 to 36% of a total sample. Gaigher (1980) observed that quartz contents are extremely variable. Samples taken in the centre of the Witbank No. 2 Seam had the lowest quartz contents, while the Witbank No. 5 Seam samples contained higher proportions of quartz (17 to 35% of mineral matter). Nearly all No. 2 Seam samples contained dolomite and siderite in addition to calcite, while pyrite was present in all samples from the respective coalfields sampled in this study.

The most important constituents of mineral matter in coal, which consists of the clay mineral fraction, are analyzed in more detail. Samples from the Witbank coalfield No. 2 and 4 Seam contained abundant kaolinite with only traces of illite and expandable clays such as illite-smectite and montmorillonite. Regular interstratified illite-montmorillonite dominates the clay fraction of the No. 5 Seam samples (Gaigher, 1980). On average, the clay mineral composition of Witbank coal falls close to the composition field for Australian coal, but with somewhat less expandable clays. In the Witbank No. 2 Seam, coal from the extremities of the coalfield are of slightly lower rank, containing kaolinite values as high as 88% compared to the 61% kaolinite from the central part of the coalfield.

Similarly, Azzie (2002) found that the principle clay mineral present in coal samples from the Highveld area was kaolinite. It was not established whether mixtures of discrete montmorillonite and illite were present. Quartz was absent, or present in trace quantities in the coal units. Calcite and magnesite were dominant carbonate phases while pyrite was generally a minor constituent. Concentration of the phosphate apatite was highest in the coal samples and very rare or absent in the sediments. Ankerite, microcline and anatase were also identified using XRD analysis.

The occurrence of aragonite in carbonate lenses in coal from the Witbank area has been noted by Van der Spuy and Willis (1991). Although, aragonite has been observed in coal from other countries (Vassilev and Vassileva, 1996), the lack of this carbonate was emphasized by Van der Spuy and Willis (1991), and

its occurrence confirmed by Azzie (2002). However, the XRD analyses of carbonate lenses from coalmines in the Witbank area indicated that aragonite is a major mineral phase in some of these assemblages. Seeing that the individual mineral concentration in coal is less than 5%, it is difficult to identify minerals in lower concentrations. Thus, after an examination of a diffraction scan Van der Spuy and Willis (1991) concluded that most of the strongest peaks of aragonite are obscured by, and appear as "shoulders" on either side of peaks of minerals such as quartz, kaolinite and pyrite, therefore the presence of aragonite in South African coal could be possible.

According to Gaigher (1980) the chemical analyses of coal ash from South African coal show the residue to have features of hydrolysate sediment, modified by the element collecting activities of the plants and the low Eh – pH conditions. SiO_2, MgO, Na_2O and K_2O percentages were significantly low when compared to crustal averages, probably due to their solubility under humid conditions. The enrichment in Al_2O_3 and TiO_2, with median values between 26% and 1.2% respectively, might also have been as a result of leaching and accumulation by plants. P_2O_5 has a varying concentration in coal from 0.05 to 4%.

Similar average concentrations for Al_2O_3 and TiO_2 where obtained by Azzie (2002), with significant correlation between TiO_2 and quartz (r_s=0.81) suggesting that to some degree they are complexed with the organic matter. Unlike in the Gaigher study, available analyses of sulphur and iron showed good agreement with each other (r_s=0.76) and pyrite from Azzie's mineralogical interpretations. From analyses for calcium, magnesium and the carbonate minerals it was deduced that calcite was more abundant in the coal samples than dolomite; yet both do occur in the coal, and sometimes in substantial amounts that are well within the order of 10 to 40 wt% total the mineral composition. Insufficient data was available to indicate a correlation between Na_2O, K_2O and CaO, and the feldspars in the coal.

With regard to trace elements, Gaigher (1980) was unable to establish whether there are any major variations in certain trace element concentrations between the different coalfields. However, it was noted that the coal ash seemed to be enriched in tungsten, gallium, and sometimes strontium, with respect to the earth's crust. Azzie (2002) has, thus, contributed considerably to knowledge on the association between major and trace elements, and various mineral constituents in coal. Good correlation between Nb and quartz (r_s=0.75), and between TiO_2 and Nb, Zr, Th, Sc, Y and Cu was observed, however, no explanation could be presented for this association. Although no phosphate minerals were identified, a significant correlation exists between Sr and Ca, but not for Sr and calcite and dolomite. A similar scenario exists for Ba, which showed weak correlations with the oxides and the minerals. Rb has a strong correlation with K_2O in coal (r_s=0.93), suggesting that Rb is related to K itself and not any particular mineral component. The only significant correlation regarding Zr was with quartz. Zr concentrations are usually higher in felsic rocks and so too in granite. It may be indicative of the influence of igneous material. Concentrations of this element do not exceed 300 ppm in coal.

The very brief background regarding mineralogical research on South African coal suggests that more could be done to increase our knowledge of our coal deposits. Therefore, information gained by the objectives of this study will be exceptionally valuable.

3 THE GEOCHEMISTRY AND MINERALOGY OF COAL MEASURES

3.1 Sampling

The reliability and value of this investigation is primarily dependable on the quality of the database. A number of parameters defined the integrity of the database. These characteristics include the following;

- The sample localities had to be representative of the entire study area, i.e. the Witbank and Highveld coalfields;
- It was important to obtain representative samples from the various coal seams;
- The samples that were included into the database had to show typical maceralogical characteristics.
- The exact coordinates of the sampling position had to be recorded. Furthermore, a complete sample description had to be completed.

A total of four-hundred-and-forty-four (444) samples were eventually included into the database. These samples were collected from nineteen (19) different collieries and provide an adequate representation of the various collieries and types of coal encountered in the Witbank and Highveld coalfields (Fig. 5 and Table 1). It is clear that a larger number of samples from a larger array of collieries would refine the findings. However, we are confident that the current dataset adequately describes the main mineralogical features of the Witbank and Highveld coalfields. The samples characteristics and localities are described in detail in Appendix 1.

Table 1. List of sampling localities and number of samples

Locality	Number of samples
Arnot Colliery	42
Arnot-North Colliery	24
Bank Colliery	21
Bankfontein Colliery	3
Bankfontein Borehole 1	7
Bankfontein Borehole Wedge 1	12
Bankfonten Borehole Wedge 2	9
Bankfontein Borehole Wedge 3	14
Bankfontein Borehole Wedge 4	11
Bankfontein Borehole Wedge 5	15
Delmas Colliery	16
Douglas Colliery	41
Forzando Colliery	13
Greenside Colliery	30
Kleinkopje Colliery	16
Khutala Colliery	16
Koornfontein Colliery	19
Kromdraai Colliery	11
Lakeside Colliery	7
Leeufontein Colliery	33
Middelburg Colliery	22
Optimum Colliery	13
Rietspruit Colliery	13
Witbank Colliery	10
Tavistock Colliery	20
Union Colliery	6
Total	444

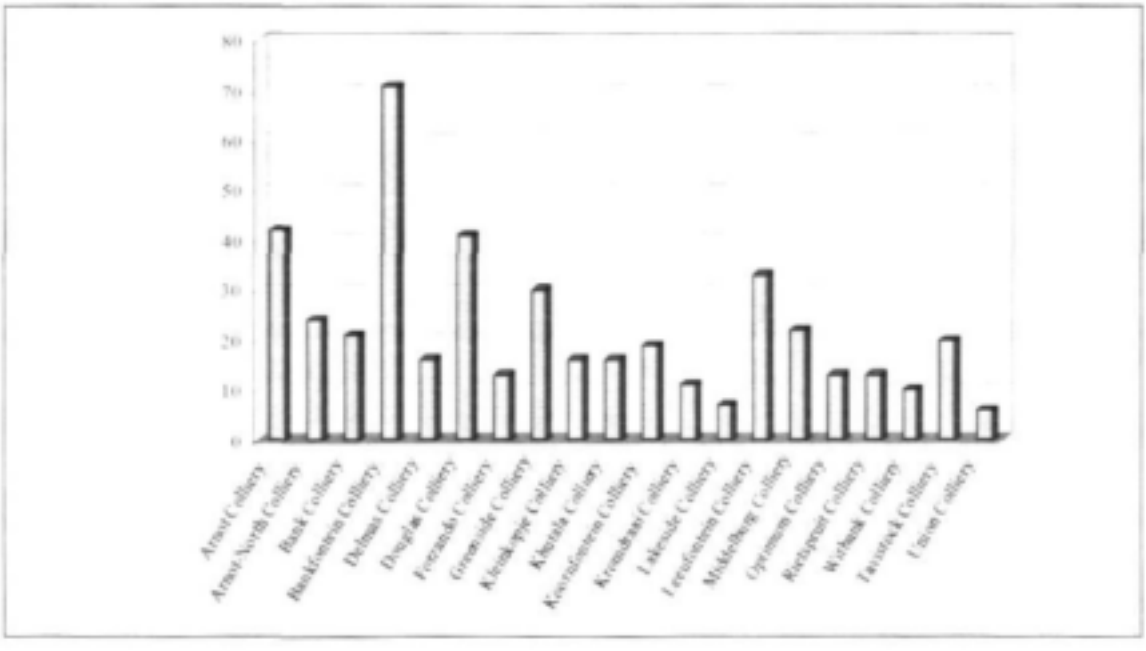

Figure 5. Sample distribution among the various collieries

3.2 Experimental and analytical methods used in coal mineralogy

Researchers in coal mineralogy and geochemistry have encountered continuous difficulties with analytical procedures. In order to improve the accuracy with which analytical techniques are performed, and the correctness of results, various experimental methods have come to pass. The need for such improvements in coal analyses has its origin in the fact that mineral matter in coal constitutes only about 10-30 wt% of a sample. The excessive amounts of organic matter tend to obscure results in various ways, and the low concentrations of inorganic matter contribute to difficulties in analyses. However, not all experimental methods prove to be precise, and an expected degree of error accompanies most results. A look at such techniques would emphasize the importance of accuracy and care during analytical procedures.

The main objectives of some experiments are to separate mineral matter from organic matter in coal, and there are a few ways through which this can be done. Many researchers make use of chemical treatment in order to isolate the mineral matter. This method is more cost efficient compared to acquiring analytical instruments such as oxygen-plasma ashers which will be discussed later.

Ward (1974) addressed the problem by suggesting a chemical treatment of small amounts of coal with hot (85°C), concentrated hydrogen peroxide. Approximately 100 ml of hydrogen peroxide is added to 1 g of pulverised coal and the mixture is left to oxidize for a few days. The coal changes to a grey-brown or white residue when the reaction is complete. Once the process was complete, the residue was then separated in a centrifuge and dried. In this case drying was carried out in the laboratory to avoid dehydration and structural changes in the clay minerals. X-ray diffraction of this residue was able to identify quartz and kaolinite in most cases. Phosphate minerals and calcium oxalate minerals were also observed. The technique proved to be a low-cost technique for isolating insoluble mineral matter, but it has limitations. The reactions that take place with the hydrogen peroxide, depending on the constituents of the coal, could be spontaneous and are dangerous to handle. Even though chlorides are not abundant in coal, the organic acids may attack both chlorides and carbonate where present. Kunze and Dixon (1986) proposed an almost identical technique for the removal organic matter, and once again the same limitation concerning the susceptibility of carbonates is emphasized.

O'Shay *et al.* (1990) used hydrogen peroxide to determine the potential acidity in the pyritic overburden developed in mining areas. The oxidation of iron disulphides, such a pyrite and marcasite from mine spoils produces this acidity problem. To prevent excessive acidity problems from occurring on the spoil surface, or to correct acidity problems that may have occurred after leveling the spoil, a rapid, accurate, and reproducible potential acidity technique was required. The original and modified acidity potential methods were applied to samples from a mine spoil. Samples were pre-treated with $CaCl_2$ to remove residual acid, then oxidized with H_2O_2. Potential acidity values obtained from samples using the modified method were compared with potential acidity values from the original method. The modified method proved to be accurate and less variable in comparison to original potential acidity method.

Chemical treatment prior to mineral matter identification in some Pakistani coal was carried out by Khan *et al.* (2002). Extractions were made separately with ammonium acetate, HCl, HNO_3 and HCl+HF+HCl solutions, as well as an acid mixture consisting of H_2O, HNO_3, HCl and HF. The extraction residues and virgin coal were ashed at 750°C. Cu, Mn, Zn, Fe, Ca, Mg, Na and K were determined using various methods. According to Khan *et al.* (2002) complete demineralization of coal requires successive treatments with various acids. Prolonged soaking followed by extraction is recommended to compensate for complex porosity and vesicular channels. Lithophillic elements like Fe, Ca, Mg and K can be effectively extracted compared to chalcophillic elements like Cu, Mn and Zn with all the aforementioned extracts.

In most instances the amount of material, which can be accommodated during one analysis, is minute, making it difficult to accommodate larger samples. Furthermore, working with chemicals requires extreme cautiousness and procedures might take up to weeks, thus rather time consuming when working with many samples. Therefore, techniques such as normative interpretation of ash analysis data and low-temperature ashing may be a commendable alternative.

Normative interpretations are based on the chemical composition of the coal's high-temperature ash. Such techniques would assume that the various elements in the ash were originally partitioned between particular minerals, and hence represent an attempt to derive a "theoretical" mineralogy from the chemical analysis data. They are most effective if the actual minerals present are known from independent evidence, such as X-ray diffraction (Ward, 1999).

One of the most established methods of isolating mineral matter in coal without major alteration is through low-temperature oxygen-plasma ashing. This technique is described thoroughly by Gluskoter (1965). Oxygen is passed through a high-energy electromagnetic field produced by a radio-frequency oscillator. An electrodeless ring discharge takes place in the gas, and activated oxygen is produced. The activated gas is a mixture of atomic and ionic species as well as vibrationally excited states. The activated oxygen passes over the sample, which is placed in a Pyrex boat 5 cm below the radio-frequency field until the organic matter is decomposed. The actual ashing temperature appears to lie between 150° and 200°C. A light-coloured dry mineral residue remains when the oxidation process is complete (Gluskoter, 1965; Ward, 1986). This technique probably represents the most reliable method for determining the percentage of total mineral matter in coal (Ward, 1999).

3.2.1 Experimental procedures followed during this study

An attempt was made to isolate the mineral matter of the coal used in this study for XRD analyses thereafter. Although chemical treatment before analysis was considered, the technique presented numerous difficulties and limitations with regard to the facilities available and the enormous amount of samples which where to be analyzed.

Thus, it was therefore decided to make use of a muffle furnace to oxidize a few samples. Small amounts of material were placed in porcelain holders, and left in a muffle furnace first for 50 hours at 350°C, then for 60 hours at 250°C, and lastly for 70 hours at 150°C. According to Kruger (1981) an ashing temperature of 350°C is optimum as ashing at temperatures higher than this might give rise to changes in the mineralogical composition, while the process will take place exceptionally slower at lower temperatures.

As seen from Tables 2 to 4 below, the percentage weight loss decreases tremendously as the temperature is lowered, even though the heating period is increased. However, to draw a reasonable conclusion from this experiment the behaviour of the minerals in coal during ignition must be understood. As mentioned before, the assemblage encountered in the coal consists primarily of quartz, kaolinite, montmorillonite, illite and mixed-layer clays, pyrite, calcite, dolomite and siderite, and possibly feldspars, micas, phosphates and chlorides. From literature it is rather apparent that most of the mineral groups mentioned should not undergo transformation due to a temperature increase up to 350°C (Ribbe, 1974; Vaughan and Craig, 1978; Kruger, 1981; Reeder, 1983; Nriagu and Moore, 1984). However, results obtained in this experiment prove that normal ashing in a muffle furnace can bring about phase changes, depending on the circumstances during the procedure and the mineral assemblage involved.

Weight loss in the initial stages would be accredited primarily to the loss of H_2O. Due to the combustion of organic matter at higher temperatures oxidation would commence. The X-ray diffraction patterns of each sample after it was heated and the virgin coal are illustrated in Appendix 2.

The XRD patterns of sample LU1 are illustrated in Appendix 2. The pattern remains similar despite an increase in temperature, with background interference peaks more subtle and the appearance of the strongest peaks of calcite and dolomite, which are especially noticeable in the sample that has been heated to 350°C. From the percentage weight loss at 350°C it is clear that there is a reasonable amount of inorganic matter present in this sample as minor phases become detectable even though more than half of the material has disappeared. However, as noted by Kruger (1981), it is also clear that combustion at lower temperature has almost no effect on the sample even though the duration of combustion was lengthened, as observed in Table 3-3.

Table 2. Results after heating for 50 hours at 350°C (units in grams)

*Sample	**Crucible	C&S(before)	S(before)	C&S(after)	S(after)	S wt loss	% wt loss
LU1	20.10	30.10	10.00	23.80	3.70	6.30	63.00
LU24	18.60	28.50	9.90	19.40	0.80	9.10	91.92

Sample LU 24 was rich in organic material as observed in the percentage weight loss both at 350°C and 250°C as seen in Tables 3-1 and 3-2, respectively. The XRD patterns for this sample are illustrated in Figure A2-8. Problems with the ashing technique emerged especially with the combustion of this sample. Although a large volume of the organic material could be removed successfully, mineral phases remaining in the ash had undergone alteration at 350°C. As seen from XRD patterns, in the small amount of ash remaining, a reasonable amount of phases are present. X-ray diffraction of the virgin coal produced an inadequate pattern in terms of the manual interpretation method applied.

The visibility of the peaks on the diffraction patterns improve as the temperature is raised, and only at 250°C are some peaks slightly detectable. At 350°C the major mineral phases are prominent; however, the occurrence of these specific minerals in coal is not necessarily as a result of reactions that has taken place in natural systems, but could be due to reactions taking place in the furnace. Calcite is dominant throughout the experiments at all temperatures, while kaolinite, anhydrite, dolomite, and hematite only appears at 350°C. Kaolinite is also the dominant clay mineral in most coal and is therefore expected to be present; so too has dolomite been observed together with calcite in South African coal. The phases, which pose a problem, are anhydrite and hematite. Anhydrite is a calcium-sulphate and hematite is an iron-oxide mineral.

These phases were not observed in studies by Gaigher (1980), Azzie (2002) or Bühmann and Bühmann (1988), thus their occurrence could have an alternative origin. Pyrite and calcite, which often co-exist in the same assemblage, are both thought to be stable under temperatures as those used in the experiments. However, it appears that these minerals were altered during the combustion process. The oxidation of pyrite results in the formation of hematite and a loss in sulphur as SO_2. Calcite decomposes to CaO and CO_2 during combustion. Therefore, it is possible for the SO_3 from pyrite and the CaO from calcite to react to form $CaSO_4$, anhydrite. Ward *et al.* (2001a) noted similar occurrences in a study involving the low-temperature ashing and ashing in a muffle furnace. Minerals such as kaolinite and pyrite were significantly lower in the ash prepared in a muffle furnace at 370°C. The same minerals were more abundant in the low-temperature ash, confirming the alteration of constituents, which could possibly take place in a muffle furnace. The oxidation of pyrite is not uncommon in the presence of oxygen, thus the formation of hematite is explained. Furthermore, this sulphur was available to combine with the calcium from the calcite to form anhydrite.

Table 3. Results after heating for 60 hours at 250°C (units in grams)

Sample	Crucible	C&S(before)	S(before)	C&S(after)	S(after)	S wt loss	% wt loss
LU1	20.40	30.50	10.10	29.80	9.40	0.70	6.93
LU24	32.00	40.20	8.20	36.40	4.40	3.80	46.34

Table 4. Results after heating for 70 hours at 150°C (units in grams)

Sample	Crucible	C&S(before)	S(before)	C&S(after)	S(after)	S wt loss	% wt loss
LU1	20.00	30.20	10.20	29.70	9.70	0.50	4.90
LU24	22.70	26.20	3.50	26.10	3.40	0.10	2.86

*S – Sample; **C – Crucible

After ashing a few more samples it was decided that the process has an adverse effect on the original mineralogy, which is of utmost importance. Researchers in the field such as Dr. James Willis (personal communication) from the University of Cape Town, South Africa believes that unwanted transformations may take place in a furnace involving sulphur and even phosphorus. Although the formation of anhydrite and hematite could form due to natural processes as well, the experimentally induced transformation of mineral phases seems more likely and should be avoided at all costs.

Ashing at lower temperatures was just too time-consuming for the amount of samples involved and produced poor results as seen from the experiments, while ashing at higher temperatures brought about unnecessary changes in the samples. Prof. Colin Ward from the University of New South Wales, Sydney, Australia kindly agreed to ash ten coal samples and analyse them using X-ray diffraction together with Siroquant™ interactive interpretation software, as well as X-ray fluorescence. Oxidizing the organic matter and isolating the minerals without major alteration can be achieved successfully with low-temperature oxygen-plasma ashing (Ward, 1999).

Figures A2-9 to A2-12 in Appendix 2 illustrates the difference in peak visibility before and after the samples were subjected to low-temperature ashing. Figure A2-9 depicts the unashed XRD pattern of sample M-20. The dominant minerals, namely, quartz, kaolinite and pyrite are visible, however, the pattern is slightly obscure due to background peaks, which in this case are caused by the organic material in the coal. A similar pattern is obtained from the X-ray diffraction of the unashed KOR-10 sample as illustrated in Figure A2-11. Kaolinite along with minor calcite and dolomite made up the mineralogy.

The Siroquant™ software allows the proportions of up to 25 different minerals in a mixture to be quantified from a conventional X-ray powder diffractometry pattern using Rietveld techniques. Rietveld (1969) developed a formula to give the intensity at any point in the scan of a single mineral, with information on how to refine relevant crystal structure and instrumental parameters by least-squares analysis of the profile. Siroquant™ calculates a theoretical XRD profile and fits it to the measured pattern by full-matrix least-squares refinement of the following Rietveld parameters: phase scales, line asymmetry, phase preferred orientation, phase linewidths, instrument zero, the lineshape parameter for each phase, and the phase unit cell dimensions. A calculated XRD pattern of each mineral could be generated from its known crystal structure, and the sum of all calculated patterns can be fitted to the observed XRD pattern of a multi-mineral sample by least squares analysis to find the optimum individual phase scales. These are then used to determine the mineral percentages.

The parameters can be adjusted simply and interactively with the program, to replicate more closely the mineral's contribution to the measured pattern and allow for variation due to atomic substitution, layer disordering, preferred orientation, and other factors in the standard pattern used. Crystallographic and chemical data as well as reference patterns can be developed for use in Siroquant™ directly from measured XRD patterns of a specific mineral, allowing minerals with poorly developed crystal structures to be incorporated in the analysis (Ward *et al.*, 2001a).

Although there was some difficulty in converting raw Siemens and Phillips diffraction files, Figures A2-10 and A2-12 illustrate the X-ray diffraction patterns of samples M- 20 and KOR-10, respectively. The peaks of the patterns are noticeably distinguishable compared to those in the unashed patterns. Results from the Siroquant™ interpretation shows that sample M-20 consists of 21.5% quartz, 51.5% kaolinite, 12.2% illite, 3.9% mixed layer clays and 11.0% pyrite, while sample KOR-10 consists of 0.2% quartz, 78.4% kaolinite, 4.6% illite, 1.6% pyrite, 3.7% calcite, 10.3% dolomite and 1.3% bassanite. In the latter case, the bassanite is thought to represent artifacts of the plasma ashing process, formed when organically associated Ca or Ca from calcite, and in some cases Na, combines with organic sulphur released during the oxidation of organic matter (Ward *et al.*, 2001a).

The use of LTA to isolate mineral matter is effective despite minor occurrences of artifacts such as bassanite. The oxidation of sulphides such as pyrite was also avoided, causing the original mineralogy to remain unaltered. Secondly, the detection of poorly crystalline and rare minerals such as illite and mixed-layer clays is made easier with the help of the Siroquant™ software. The X-ray fluorescence data concerning these ten samples is in good agreement with the Siroquant™ interpretation and the interpretation technique applied at the University of the Free State (UFS).

There are numerous techniques used for determining the whole rock chemical composition, with X-ray fluorescence being among the most reliable. The ten samples ashed at the University of New South Wales (UNSW) were also analyzed by UFS and UNSW using their standard XRF procedures in order to determine the variations in whole coal XRF analysis and fused disk XRF analysis. As proposed by Dr. Willis from the University of Cape Town (UCT), whole coal XRF analyses for major and trace elements regarding coal samples are more accurate, since no unwanted changes are brought about, as is the case when heating and fusing samples. A brief explanation of the sample preparation procedures will highlight distinct differences in total chemical composition and mineral disintegration temperatures.

The preparation procedure used at UNSW involves heating the material initially to 400°C, and then increasing the temperature gradually with 100°C until 815°C is reached. This temperature is held until a constant mass is obtained. The ash percentage is then determined as a percentage of the unashed/ air-dried coal. The sample is heated to 1020°C after which the loss on ignition (LOI) is determined and fusion is affected according to the Norrish and Hutton (1969) technique. The results are presented in Table 3-4. The loss in weight after 815°C, which includes loss in organic carbon, sulphur, water and other volatile

constituents, is disregarded. Therefore, carbonate phases still containing CO_2 would lose this at 1020°C (Reeder, 1983). This procedure was also applied by UFS and results are observed in Tables 3-5 and 3-6.

Table 5. UNSW XRF data – 1020°C ash – normalised LOI and SO_3 free

Sample	SiO_2	TiO_2	Al_2O_3	Fe_2O_3	MgO	CaO	Na_2O	K_2O	P_2O_5	TOTAL
BH1-5	42.43	1.34	32.39	2.95	4.54	12.92	1.47	1.20	0.77	100.00
DOU37	64.00	1.54	31.16	0.37	0.53	1.56	0.38	0.37	0.08	100.00
KHU10	41.38	2.00	36.93	3.80	3.85	11.12	0.19	0.38	0.36	100.00
KOR10	45.34	1.94	39.65	2.99	2.21	6.96	0.29	0.41	0.21	100.00
LK1	29.42	0.76	17.07	34.46	4.24	13.25	0.52	0.20	0.07	100.00
LU13	59.17	1.21	31.52	0.92	1.43	4.80	0.38	0.53	0.04	100.00
M20	59.03	1.15	27.80	9.86	0.39	0.28	0.20	1.22	0.08	100.00
OPT12	61.11	2.79	33.24	0.83	0.37	0.36	0.48	0.58	0.24	100.00
R2M	49.24	1.44	32.52	1.53	1.21	8.70	0.25	0.47	4.64	100.00

Table 6. UFS XRF data – 1020°C ash (UNSW method)

Sample	SiO_2	TiO_2	Al_2O_3	Fe_2O_3	MnO	MgO	CaO	Na_2O	K_2O	P_2O_5	LOI	Total
BH1-5	40.76	1.25	32.33	3.25	0.06	4.56	13.23	0.31	1.19	1.12	1.94	100.00
DOU37	60.00	1.76	33.20	1.60	0.04	0.49	1.39	0.00	0.37	0.04	1.11	100.00
KHU10	35.66	1.71	31.99	5.63	0.06	6.30	16.64	0.00	0.31	0.31	1.41	100.00
KOR10	44.89	1.92	40.47	1.30	0.07	2.03	6.30	0.04	0.33	0.22	2.43	100.00
LK1	24.33	0.52	13.38	43.79	0.09	1.56	6.08	0.00	0.26	0.00	9.99	100.00
LU13	41.67	1.19	23.21	10.42	0.00	1.79	10.12	0.00	0.30	0.00	11.31	100.00
M20	55.90	1.10	24.77	16.15	0.00	0.14	0.14	0.00	1.20	0.07	0.53	100.00
OPT12	60.39	2.91	34.45	0.67	0.00	0.11	0.28	0.00	0.45	0.22	0.50	100.00
R2M	45.39	1.30	34.32	1.79	0.04	0.99	8.65	0.00	0.36	5.38	1.79	100.00

Table 7. UFS XRF data – 1020°C ash (UNSW method) – normalised LOI and SO_3 free

Sample	SiO_2	TiO_2	Al_2O_3	Fe_2O_3	MnO	MgO	CaO	Na_2O	K_2O	P_2O_5	TOTAL
BH1-5	41.57	1.27	32.97	3.31	0.06	4.65	13.49	0.32	1.21	1.15	100.00
DOU37	60.67	1.78	33.57	1.62	0.04	0.50	1.41	0.00	0.37	0.04	100.00
KHU10	36.17	1.74	32.44	5.71	0.06	6.39	16.87	0.00	0.31	0.31	100.00
KOR10	46.01	1.97	41.48	1.34	0.07	2.08	6.46	0.04	0.33	0.22	100.00
LK1	27.03	0.58	14.86	48.65	0.10	1.74	6.76	0.00	0.29	0.00	100.00
LU13	46.98	1.34	26.17	11.74	0.00	2.01	11.41	0.00	0.34	0.00	100.00
M20	56.20	1.10	24.90	16.23	0.00	0.14	0.14	0.00	1.21	0.07	100.00
OPT12	60.70	2.93	34.63	0.68	0.00	0.11	0.28	0.00	0.45	0.23	100.00
R2M	46.21	1.32	34.95	1.82	0.05	1.00	8.80	0.00	0.36	5.47	100.00

The standard procedure followed at UFS involves drying the samples at 110°C for 24 hours to determine the H_2O content, then heating them to 980°C to obtain the LOI. The problem with applying this method was that a percentage of carbonate minerals were not completely disintegrated. Thus, during the preparation of the fusion disk any CO_2 still left will be lost, leaving less of the ash originally weighed off to prepare the disk and resulting in lower totals. Samples were subsequently heated to 1050°C and 1080°C to ensure complete decomposition of all phases. Results for the 1050°C and 1080°C ash are found in Tables 3-7 to 3-10. This rise in temperature resulted in an increase in the LOI. Results obtained for the 1050°C and 1080°C ash are very similar, since each sample was individually for 5 hours.

Table 8. UFS XRF data – 1050°C ash

Sample	SiO_2	TiO_2	Al_2O_3	Fe_2O_3	MnO	MgO	CaO	Na_2O	K_2O	P_2O_5	H_2O-	LOI	Total
BH1-5	11.11	0.36	8.47	0.34	0.02	1.28	2.85	0.06	0.31	0.29	3.06	73.66	101.81
DOU37	12.65	0.28	6.71	0.14	0.01	0.37	1.49	0.00	0.08	0.01	1.25	79.67	102.66
KHU10	7.71	0.36	7.00	1.27	0.02	1.34	3.54	0.00	0.06	0.06	3.29	74.36	99.01
KOR10	13.19	0.56	12.03	0.40	0.02	0.77	2.18	0.01	0.11	0.06	2.49	70.43	102.25
LK1	4.90	0.13	2.88	7.86	0.07	0.98	3.27	0.01	0.02	0.01	3.30	78.76	102.19
LU13	9.44	0.19	5.17	0.12	0.01	0.22	0.82	0.00	0.08	0.00	3.64	81.31	101.00
M20	13.00	0.28	5.30	6.11	0.00	0.03	0.05	0.00	0.26	0.01	0.95	77.30	103.29
OPT12	16.06	0.70	7.92	0.17	0.00	0.03	0.06	0.00	0.10	0.04	3.11	74.61	102.80
R2M	14.53	0.42	11.28	0.60	0.01	0.33	2.72	0.00	0.13	1.69	2.47	69.05	103.23

Table 9. UFS XRF data – 1050°C ash - normalised LOI, H_2O and SO_3 free

Sample	SiO_2	TiO_2	Al_2O_3	Fe_2O_3	MnO	MgO	CaO	Na_2O	K_2O	P_2O_5	Total
BH1-5	44.28	1.43	33.76	1.36	0.08	5.10	11.36	0.24	1.24	1.16	100.00
DOU37	58.19	1.29	30.86	0.64	0.05	1.70	6.85	0.00	0.37	0.05	100.00
KHU10	36.10	1.69	32.77	5.95	0.09	6.27	16.57	0.00	0.28	0.28	100.00
KOR10	44.97	1.91	41.02	1.36	0.07	2.63	7.43	0.03	0.38	0.20	100.00
LK1	24.34	0.65	14.31	39.05	0.35	4.87	16.24	0.05	0.10	0.05	100.00
LU13	58.82	1.18	32.21	0.75	0.06	1.37	5.11	0.00	0.50	0.00	100.00
M20	51.92	1.12	21.17	24.40	0.00	0.12	0.20	0.00	1.04	0.04	100.00
OPT12	64.04	2.79	31.58	0.68	0.00	0.12	0.24	0.00	0.40	0.16	100.00
R2M	45.82	1.32	35.57	1.89	0.03	1.04	8.58	0.00	0.41	5.33	100.00

Table 10. UFS XRF data – 1080°C ash

Sample	SiO_2	TiO_2	Al_2O_3	Fe_2O_3	MnO	MgO	CaO	Na_2O	K_2O	P_2O_5	H_2O-	LOI	Total
BH1-5	10.06	0.32	7.61	0.29	0.01	1.17	2.59	0.06	0.29	0.26	2.75	76.05	101.46
DOU37	12.95	0.29	6.85	0.14	0.01	0.37	1.51	0.00	0.08	0.01	1.10	78.93	102.24
KHU10	8.07	0.39	7.36	1.31	0.02	1.41	3.75	0.00	0.07	0.07	3.32	74.99	100.76
KOR10	13.04	0.55	11.99	0.44	0.02	0.76	2.12	0.01	0.11	0.06	2.48	70.61	102.19
LK1	5.12	0.13	2.97	7.79	0.07	1.02	3.38	0.01	0.01	0.01	3.09	78.82	102.42
LU13	10.87	0.22	6.02	0.12	0.01	0.25	0.95	0.00	0.09	0.00	3.46	80.49	102.48
M20	13.38	0.28	5.46	6.29	0.00	0.03	0.05	0.00	0.27	0.01	0.90	74.66	101.33
OPT12	15.71	0.69	7.79	0.16	0.00	0.02	0.06	0.00	0.10	0.04	2.93	72.87	100.37
R2M	12.22	0.35	9.28	0.52	0.01	0.25	2.29	0.00	0.10	1.40	2.34	72.44	101.20

The procedure followed in preparation for whole coal XRF analysis involves making a pressed powder briquette using Hoechst Wax. The method is described in Appendix 1 and results for the whole coal XRF are found in Tables 3-11 and 3-12. Determination of sulphur presented a problem. It was analyzed using powder briquettes at UFS, and a Leco-sulphur analyser at UNSW. The amount of SO_3 obtained by UNSW did not correspond well with the total sulphur recalculated to SO_3 obtained by UFS. Seeing that all or at least most sulphur is lost after the ashing process, the results are normalised to a S- or SO_3-free basis to ensure consistent comparison of the data.

Table 11. UFS XRF data – 1080°C ash - normalised LOI, H_2O and SO_3 free

Sample	SiO_2	TiO_2	$Al2O_3$	Fe_2O_3	MnO	MgO	CaO	Na_2O	K_2O	P_2O_5	Total
BH1-5	44.40	1.41	33.58	1.28	0.04	5.16	11.43	0.26	1.28	1.15	100.00
DOU37	58.31	1.31	30.84	0.63	0.05	1.67	6.80	0.00	0.36	0.05	100.00
KHU10	35.95	1.74	32.78	5.84	0.09	6.28	16.70	0.00	0.31	0.31	100.00
KOR10	44.81	1.89	41.20	1.51	0.07	2.61	7.29	0.03	0.38	0.21	100.00
LK1	24.96	0.63	14.48	37.98	0.34	4.97	16.48	0.05	0.05	0.05	100.00
LU13	58.66	1.19	32.49	0.65	0.05	1.35	5.13	0.00	0.49	0.00	100.00
M20	51.92	1.09	21.19	24.41	0.00	0.12	0.19	0.00	1.05	0.04	100.00
OPT12	63.94	2.81	31.71	0.65	0.00	0.08	0.24	0.00	0.41	0.16	100.00
R2M	46.25	1.32	35.12	1.97	0.04	0.95	8.67	0.00	0.38	5.30	100.00

Table 12. UFS XRF data – Whole coal analyses

Sample	SiO_2	TiO_2	Al_2O_3	Fe_2O_3	MgO	CaO	Na_2O	K_2O	P_2O_5	S	H_2O-	LOI	Total
BH1-5	6.30	0.31	4.78	0.25	0.39	2.34	0.25	0.35	0.31	0.80	3.06	82.66	101.80
DOU37	7.99	0.27	3.91	0.12	0.09	1.25	0.00	0.07	0.00	0.63	1.25	84.67	100.25
KHU10	4.73	0.44	5.12	0.71	0.63	3.95	0.00	0.07	0.07	0.67	3.29	78.36	98.04
KOR10	7.48	0.55	6.63	0.28	0.34	1.93	0.02	0.11	0.07	0.38	2.49	81.43	101.71
LK1	2.11	0.08	2.17	7.51	0.40	3.25	0.04	0.00	0.00	1.44	3.30	78.76	99.06
LU13	4.32	0.14	2.76	0.08	0.04	0.67	0.01	0.07	0.00	0.55	3.64	87.31	99.59
M20	7.59	0.21	3.19	4.68	0.00	0.00	0.00	0.23	0.01	2.89	0.95	80.30	100.05
OPT12	11.01	0.78	4.51	0.15	0.00	0.00	0.00	0.08	0.04	0.62	3.11	79.61	99.91
R2M	7.35	0.33	5.92	0.36	0.07	1.87	0.00	0.10	1.40	0.40	2.47	78.05	98.32

Table 13. UFS XRF data – Whole coal analyses - normalised LOI, H_2O and SO_3 free

Sample	SiO_2	TiO_2	Al_2O_3	Fe_2O_3	MgO	CaO	Na_2O	K_2O	P_2O_5	Total
BH1-5	41.23	2.03	31.28	1.64	2.55	15.31	1.64	2.29	2.03	100.00
DOU37	58.32	1.97	28.54	0.88	0.66	9.12	0.00	0.51	0.00	100.00
KHU10	30.09	2.80	32.57	4.52	4.01	25.13	0.00	0.45	0.45	100.00
KOR10	42.96	3.16	38.08	1.61	1.95	11.09	0.11	0.63	0.40	100.00
LK1	13.56	0.51	13.95	48.26	2.57	20.89	0.26	0.00	0.00	100.00
LU13	53.43	1.73	34.13	0.99	0.49	8.29	0.07	0.87	0.00	100.00
M20	47.71	1.32	20.05	29.42	0.00	0.00	0.00	1.45	0.06	100.00
OPT12	66.45	4.71	27.22	0.91	0.00	0.00	0.00	0.48	0.24	100.00
R2M	42.24	1.90	34.02	2.07	0.40	10.75	0.00	0.57	8.05	100.00

As for some examples concerning correlations between these analyses, Figures 6 to 16 illustrates oxides correlations for the tabulated data.

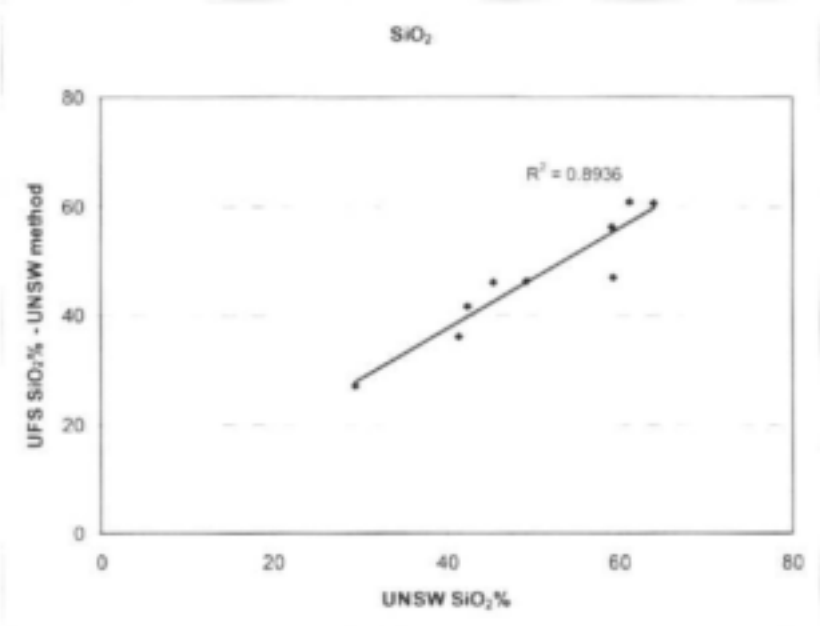

Figure 6. Relationship between UNSW SiO_2% and UFS SiO_2% (UNSW method)

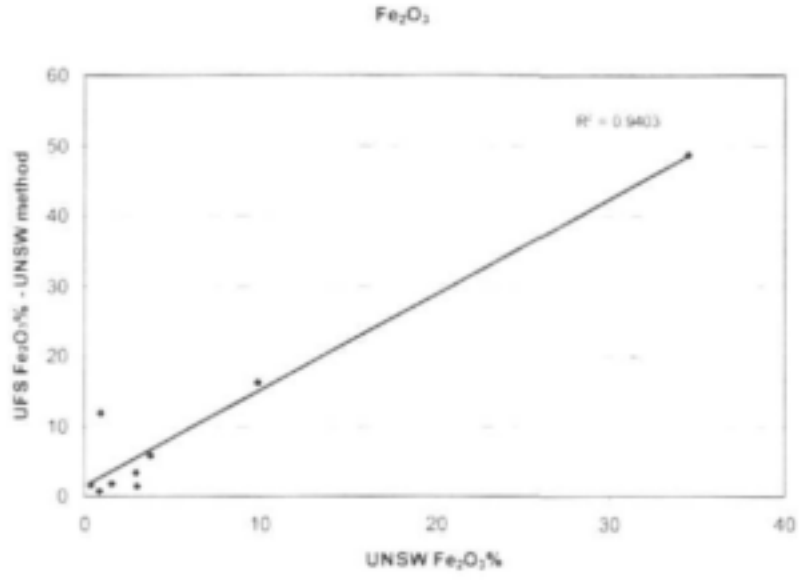

Figure 7. Relationship between UNSW Fe_2O_3% and UFS Fe_2O_3% (UNSW method)

Good correlations were obtained between the UNSW and UFS results based on the UNSW procedure. Figures 6 and 7 illustrate the SiO_2 (r=0.8936) and Fe_2O_3 (r=0.9403) percentages respectively. Figures 8 to 10 illustrate the relationship between UFS SiO_2, Al_2O_3 and Fe_2O_3 at 1050°C and UNSW SiO_2, Al_2O_3 and Fe_2O_3. The correlations observed in these figures confirm the similarity in the ash composition. Correspondingly, Figures 11 and 12 illustrate that the UFS MgO and CaO at 1080°C and the UNSW MgO and CaO are in good agreement regardless of the rise in temperature.

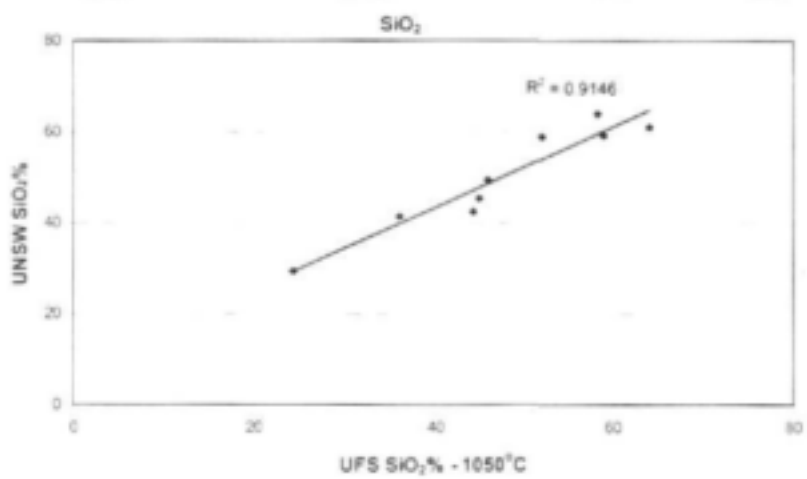

Figure 8. Relationship between UFS SiO_2% at 1050°C and UNSW SiO_2%

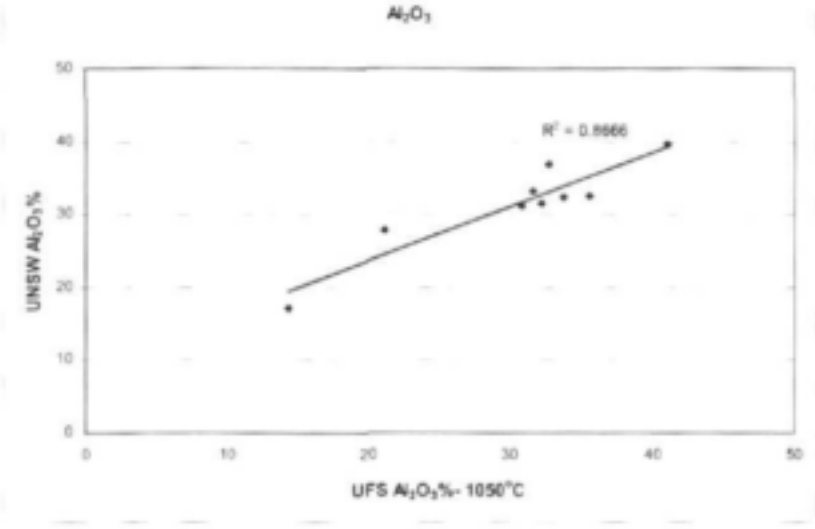

Figure 9. Relationship between UFS Al_2O_3% at 1050°C and UNSW Al_2O_3%

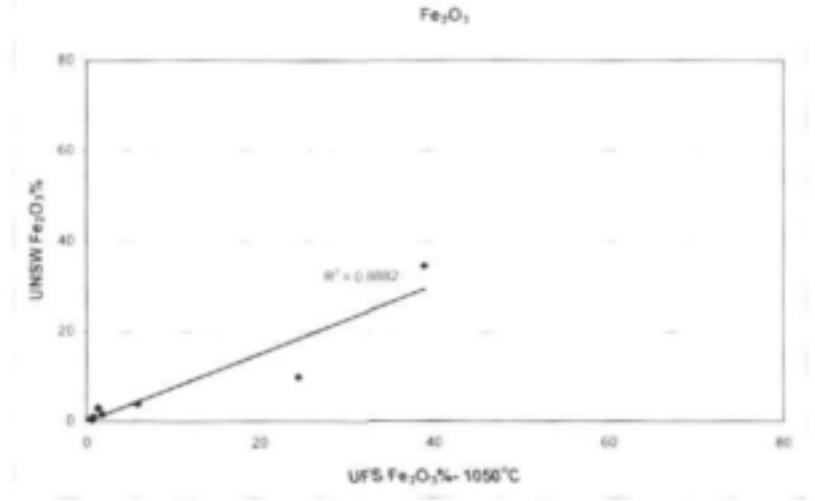

Figure 10. Relationship between UFS Fe_2O_3% at 1050°C and UNSW Fe_2O_3%

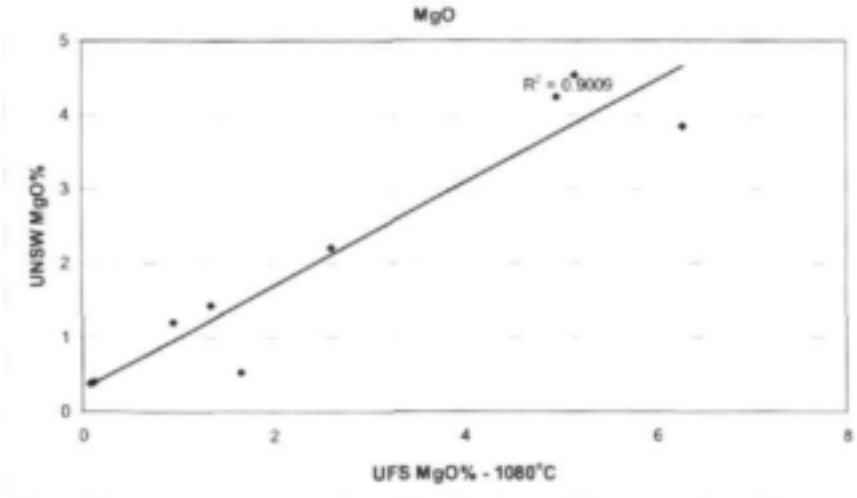

Figure 11. Relationship between UFS MgO% at 1080°C and UNSW MgO%

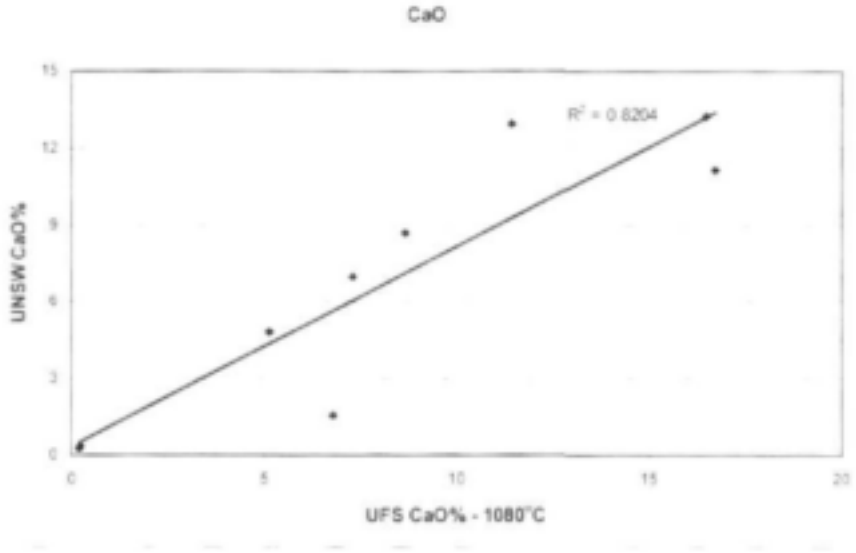

Figure 12. Relationship between UFS CaO% at 1080°C and UNSW CaO%

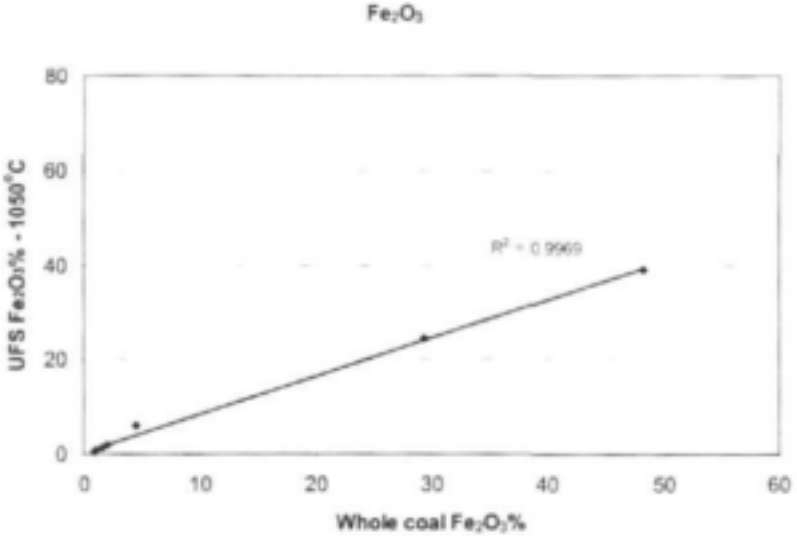

Figure 13. Relationship between Whole coal Fe_2O_3% and UFS Fe_2O_3% at 1050°C

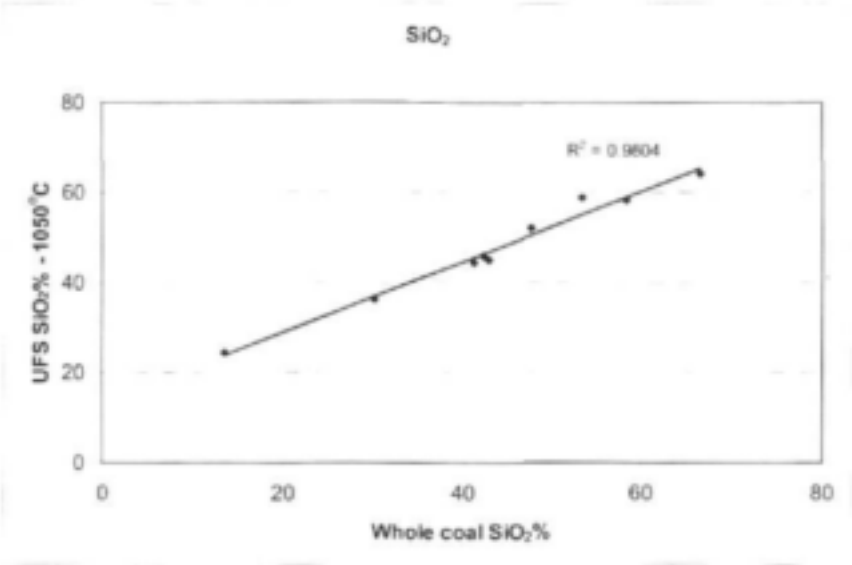

Figure 14. Relationship between Whole coal SiO_2% and UFS SiO_2% at 1050°C

Differences in results were noted mainly in comparisons between the whole coal results and the 1050°C and 1080°C ash analyses as depicted in Figures13 to 16. Compatible correlations are obtained for most of the oxides as seen from the figures; however, there is a range of variables to be considered during the analysis of coal samples. A comparison of the techniques applied here reveals the factors influencing analytical procedures. Differences are noted between whole coal and fusion disk results, as well as between whole coal results of mixed proportions of two samples.

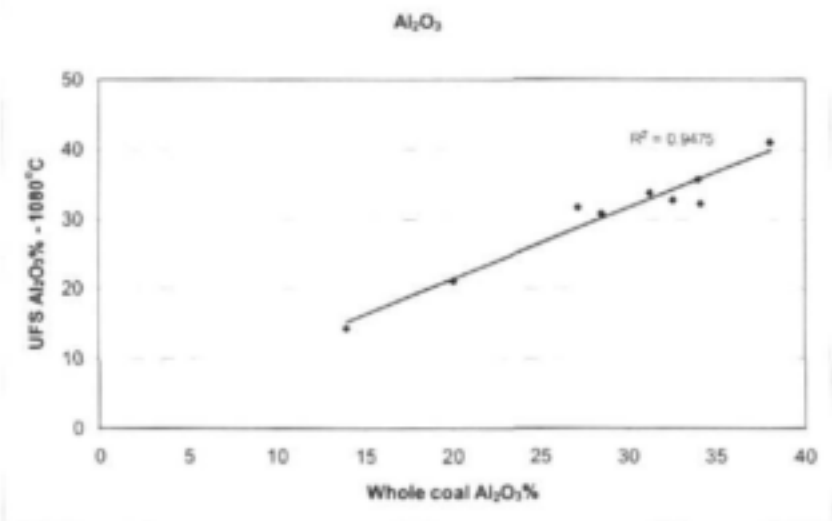

Figure 15. Relationship between Whole coal Al_2O_3% and UFS Al_2O_3% at 1080°C

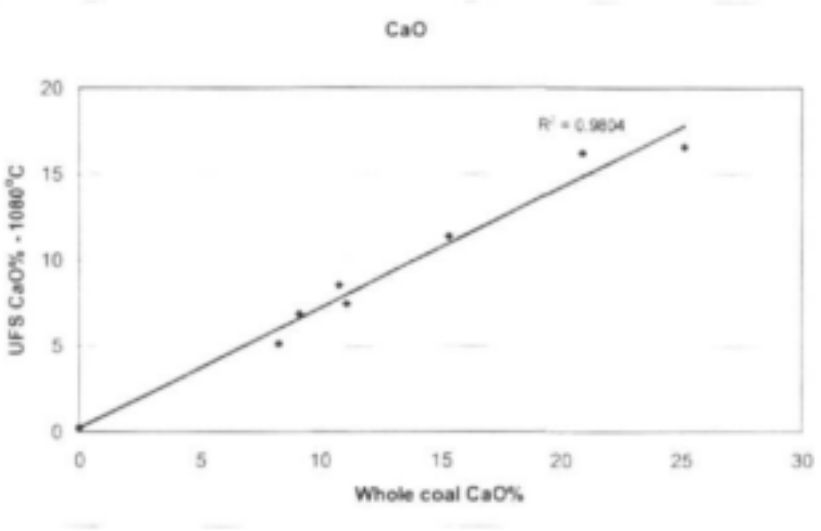

Figure 16. Relationship between Whole coal CaO% and UFS CaO% at 1080°C

If all phases are not completely decomposed at the end of the ashing process, some of the sample will be lost when the disk is fused. This affects the totals of the fusion disk analysis, which should be lower than the powder briquette results. On the other hand, La_2O_3 is added to the fusion disks to account for mass absorption while thicker powder briquettes are prepared to avoid mass absorption. X-rays are still, however, absorbed by the powder briquettes resulting in lower count rates.

Regarding the differences between whole coal mixtures, Table 14 to 16 contains XRF results on whole coal samples for mixtures of samples LK1 and LU13, as well as the pure end members of these samples at the top and bottom of the table. The proportions of these samples were mixed in a Turbula mixer for 30 minutes and analyzed. The "Cal." column represents the values that should be obtained when a proportion of one sample is mixed with a proportion of the other. The oxide name represents the values analyzed for each sample, and the "Diff." column represents the difference between the calculated and the analyzed values for each sample. The sample names are according to the proportion of the sample in the mixture e.g. LK75LU25 represents 75% of sample LK1 and 25% of sample LU13. Calculated values for LOI and H_2O were used since no LOI and H_2O was determined for these mixtures. Results for oxides that occur in low concentrations such as TiO_2, MgO, Na_2O, K_2O, P_2O_5 and S were close to the calculated results. Results for SiO_2, Al_2O_3, Fe_2O_3 and CaO differed from the calculated values.

Table 14. UFS XRF data – Whole coal analyses – Mixtures of samples LK1 and LU13

Sample	SiO_2	Cal.	Diff.	Al_2O_3	Cal.	Diff.	Fe_2O_3	Cal.	Diff.	CaO	Cal.	Diff.
LK1-100	2.11	2.11	0.00	2.17	2.17	0.00	7.51	7.51	0.00	3.25	3.25	0.00
LK75LU25	2.93	2.66	0.27	2.66	2.32	0.35	5.48	5.65	-0.17	2.74	2.61	0.14
LK50LU50	3.74	3.22	0.53	2.92	2.47	0.46	3.21	3.80	-0.59	2.08	1.96	0.12
LK25LU75	3.85	3.77	0.09	2.93	2.61	0.32	1.39	1.94	-0.55	1.37	1.32	0.06
LU13-100	4.32	4.32	0.00	2.76	2.76	0.00	0.08	0.08	0.00	0.67	0.67	0.00

Table 15. UFS XRF data – Whole coal analyses – Mixtures of samples LK1 and LU13 (continued)

Sample	TiO_2	Cal.	MgO	Cal.	Na_2O	Cal.	K_2O	Cal.	P_2O_5
LK1-100	0.08	0.08	0.40	0.40	0.04	0.04	0.00	0.00	0.00
LK75LU25	0.10	0.10	0.33	0.31	0.03	0.03	0.02	0.02	0.00
LK50LU50	0.11	0.11	0.24	0.22	0.02	0.03	0.03	0.04	0.00
LK25LU75	0.13	0.13	0.13	0.13	0.01	0.02	0.05	0.05	0.00
LU13-100	0.14	0.14	0.04	0.04	0.01	0.01	0.07	0.07	0.00

Table 16. UFS XRF data – Whole coal analyses – Mixtures of samples LK1 and LU13 (continued)

Sample	S	Cal.	H_2O-	Cal.	LOI	Cal.	Total	Cal.
LK1-100	1.44	1.44	3.3	3.3	78.76	78.76	99.06	99.06
LK75LU25	1.20	1.22	3.39	3.39	80.65	80.65	99.52	98.94
LK50LU50	0.99	1.00	3.47	3.47	82.54	82.54	99.35	98.83
LK25LU75	0.78	0.77	3.56	3.56	84.42	84.42	98.62	98.71
LU13-100	0.55	0.55	3.64	3.64	86.31	86.31	98.59	98.59

SiO_2, Al_2O_3 and CaO concentrations on the mixtures were slightly higher than those calculated, while Fe_2O_3 was slightly lower. This was because Fe_2O_3 has a higher mass absorption than SiO_2, Al_2O_3 and CaO resulting in lower count rates.

In comparison to the XRD of raw coal and the manual interpretation thereof, the methods used at UNSW prove to be technologically advanced and reliable; however, the process of low-temperature ashing is time-consuming and costly if the apparatus should still be purchased. Although the muffle furnace ashing procedure might not have been an option in this study, it could be applied in studies involving fewer samples successfully. Other alternatives such as chemical pre-treatment should also not be ignored. Regarding the use of the Siroquant™ software for interpretation, this tool could be an incredible advantage for the researcher who has substantial knowledge in the field, but it could be an even greater disadvantage if it is used to avoid attaining important skill and wisdom that can only be achieved the hard way.

Seeing that the most practical, accurate and accessible analytical methods available to conduct a study of this magnitude was raw coal X-ray diffraction and manual interpretation, combined with whole coal X-ray fluorescence, the study was carried out using methods and procedures set out in Appendix 1, and the results are presented and discussed in the following sections with confidence and considerable accuracy.

3.3 Distribution and mode of occurrence of mineral matter in coal

All statistical analyses were performed using the software such as Microsoft Excel and STATISTICA V.5. In some cases outliers were excluded to ensure accurate results. All raw datasets are tabulated in Appendix 2 and are separated according to the mines were samples were collected.

3.3.1 The Witbank coalfield

a. No. 1 coal Seam

Coals from this Seam are characterized by low total ash percentages averaging at 25%, and increasing from west to east across the field. With the exception of sample 3957 from Arnot-North Mine, which was provided by other sources, oxides and trace elements are distributed evenly. The latter sample is located in the vicinity of samples collected at Arnot Mine. However, even though this section of the coalfield is known to have higher ash percentages, the elevated SiO_2 percentage in sample 3957 could be the result of different sampling methods, emphasizing the importance of consistency and accuracy during sampling procedures. This coal sample could have been carbonaceous shale, which was mistaken for coal, or it could have been contaminated. It was therefore excluded from further calculations.

As seen from Table17, oxide concentrations for the coal are in good agreement with brief studies carried out by previous researchers, and no unusual results were obtained. SiO_2, Al_2O_3, K_2O and TiO_2 all decrease from east to west, while Fe_2O_3 and S which are similarly distributed and more abundant in the south-eastern region due to their association with pyrite. In this instance CaO and MgO are abundant in the southern and north-eastern regions respectively, while elevated concentrations of P_2O_5 are located in the extreme western region of the Seam.

Table 17. The minimum, maximum and average concentrations of oxides (wt%) and trace elements (ppm) in No. 1 Coal Seam

Element	Min.	Max.	Ave.	Element	Min.	Max.	Ave.
SiO_2	0.00	17.01	8.58	Rb	0.00	14.7	3.42
TiO_2	0.24	0.91	0.43	Ba	12.46	231.88	109.93
Al_2O_3	2.18	8.41	5.04	Sr	26.37	175.27	92.55
Fe_2O_3	0.04	3.41	1.16	Zr	7.20	177.91	87.65
S	0.27	1.67	0.73	Nb	3.43	16.94	9.40
MnO	0.00	0.00	0.00	Y	12.89	40.94	24.51
MgO	0.00	0.25	0.09	Sc	1.07	13.45	6.39
CaO	0.00	1.57	0.57	Cr	14.37	110.22	42.58
Na_2O	0.00	0.01	0.00	Cu	4.22	46.01	14.23
K_2O	0.00	0.18	0.08	V	13.49	111.2	43.33
P_2O_5	0.00	0.44	0.06	Zn	7.28	48.38	22.58
Mn	0.00	200.01	71.89	Ni	8.30	202.47	54.19

There are no specific visible trends in the distribution of trace elements in the Seam, but certain elements occur in a similar pattern. These concentrations were not significantly elevated, and considerable values could probably be as a result of the nature of the source material. The high-lying northeastern region is characterized by high concentrations of V, Y, Cu, Ba and Mn varying between 0.00 and >200 ppm. Nb, Zr and Ni are highest at the northern and southern centres of the Seam, while reasonable concentrations of Cr, Cu, Rb, Sr and Zn are located in the south-eastern region. High Sc concentrations are found in the eastern centre of the field and in the western centre together with significant Zn. Some significant concentrations of Sr and Y are found in the north-western and south-western regions of the Seam respectively.

There are numerous occurrences of noteworthy correlation coefficients between major and trace elements. This could be because some elements are in close association with the primary environment, or because some elements occur in the same minerals. Similarly, there are many correlations, which are merely coincidence due to the fact that sample numbers were insufficient, and that numerous elements occur in low concentrations in the assemblage. The significant and useful correlations could be explained either in terms of their geochemical characteristics, the source material or the depositional environment.

High correlations for a total of 17 coal samples exists between SiO_2 and, TiO_2 and Al_2O_3, and even more so between TiO_2 and Al_2O_3 (r=0.935). SiO_2 often makes up the bulk of the mineral assemblage and is thus well correlated with the total ash percentage. Aluminium occurs in feldspars, micas, non-kaolinite clay minerals and kaolinite. Feldspars and micas are frequently absent from the mineral assemblage, and this is apparent in the low concentrations of Na and K, suggesting that the relationship between Al_2O_3 and TiO_2 as seen in Figure 17, could be limited to the presence of kaolinite.

TiO_2 in coal is reported to occur in oxides, clays and complexed with organic matter (Azzie, 2002). However, no prominent correlation exists between Ti and kaolinite found in the normative interpretation.

The presence of the Ti phase anatase has not been supported by XRD studies in this study, but this does not exclude the possibility of a separate Ti phase occurring. According to Ward *et al.* (1999) Al and Ti are soluble in highly acid conditions, thus the Ti could be precipitated in conjunction with the kaolinite within the structure or as a separate phase. Anatase is also common as a minor constituent in Australian coal (Ward *et al.*, 1999).

Although there is a clear absence of feldspars and micas in the coal and very low concentrations of K_2O and Na_2O, a good correlation exists between K_2O, Rb and Ba as seen in Figure 18, which could be expected seeing that the source material is broadly accepted to originate from the north (Cadle *et al.*, 1990) where abundant igneous rocks are present. Thus the presence of feldspars and their close relationship with Ba and Rb could be explained. Concentrations of Na_2O are often below the detection limit, therefore, no accurate analyses could be performed with the Na_2O values.

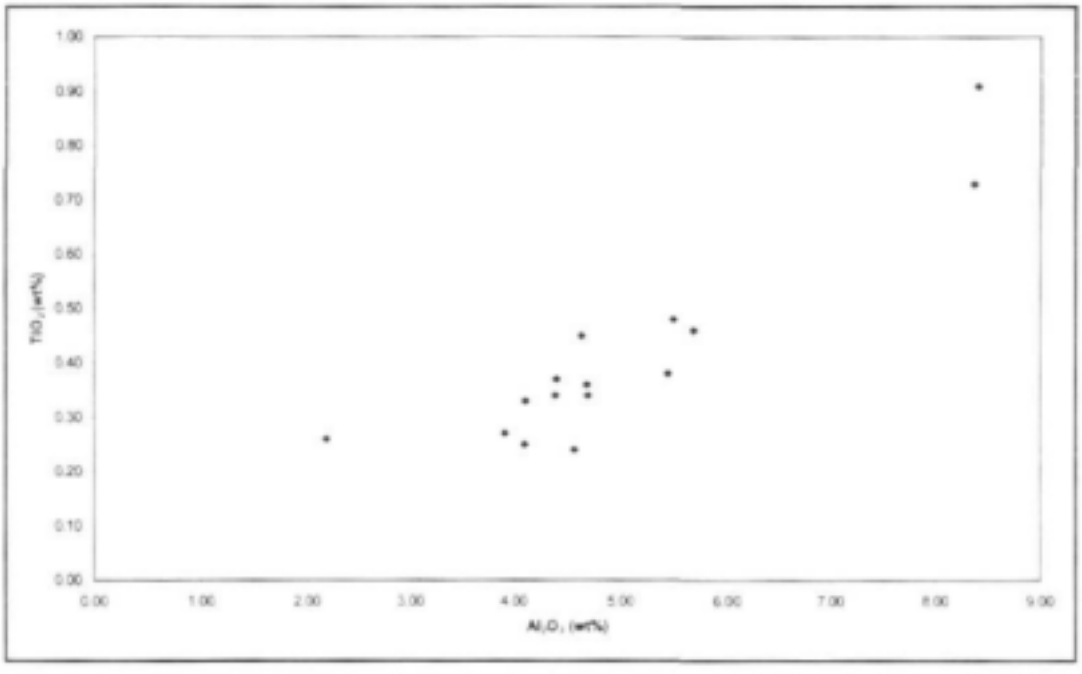

Figure 17. Relationship between TiO_2 and Al_2O_3 concentrations

The expected correlation between Fe_2O_3 and S (r=0.939) is primarily due to the presence of pyrite and can be seen in Figures 19 and 20. The outlier in the north-eastern corner of the graph may force such an exceptional correlation, but correlations between Fe and S are very high in other coal Seam sample sets. Ni also shows a good correlation with Fe_2O_3 and S, and to a lesser extent with pyrite.

This is common in other seams in the field and might be due to some relation between Ni and Fe, but insufficient data was available for this Seam to draw any definite conclusions. Apart from feldspars, carbonate minerals in coal account for almost all MgO and CaO concentrations in the form of dolomite and calcite (Gaigher, 1980). A correlation of r=0.632 was noted between Ca and Mg possibly due to the fact that they are both present in dolomite.

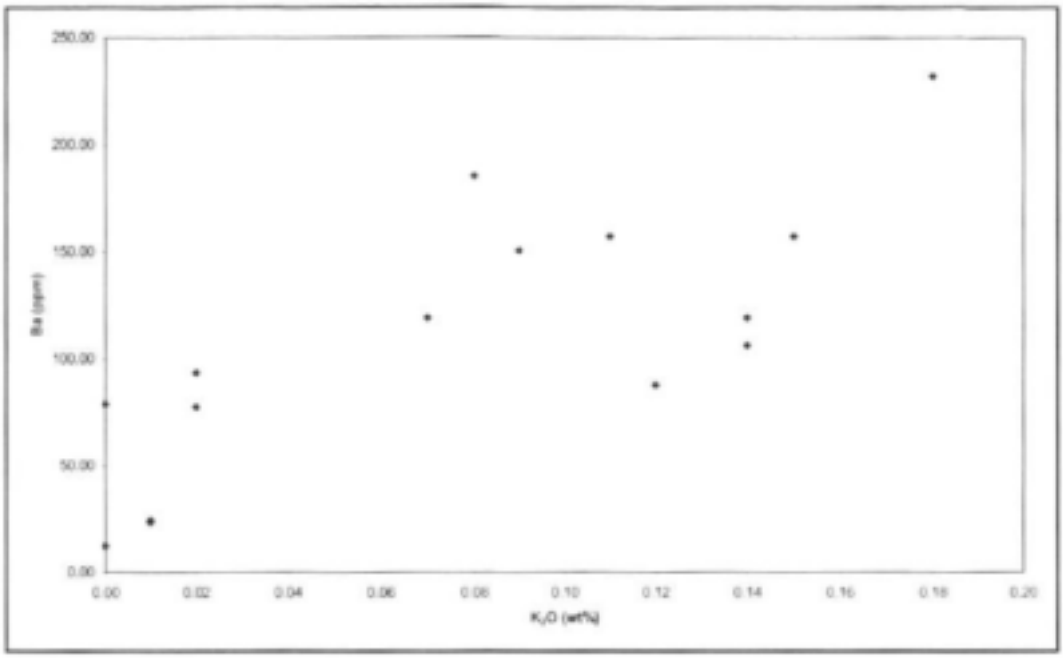

Figure 18. Relationship between K_2O and Ba concentrations

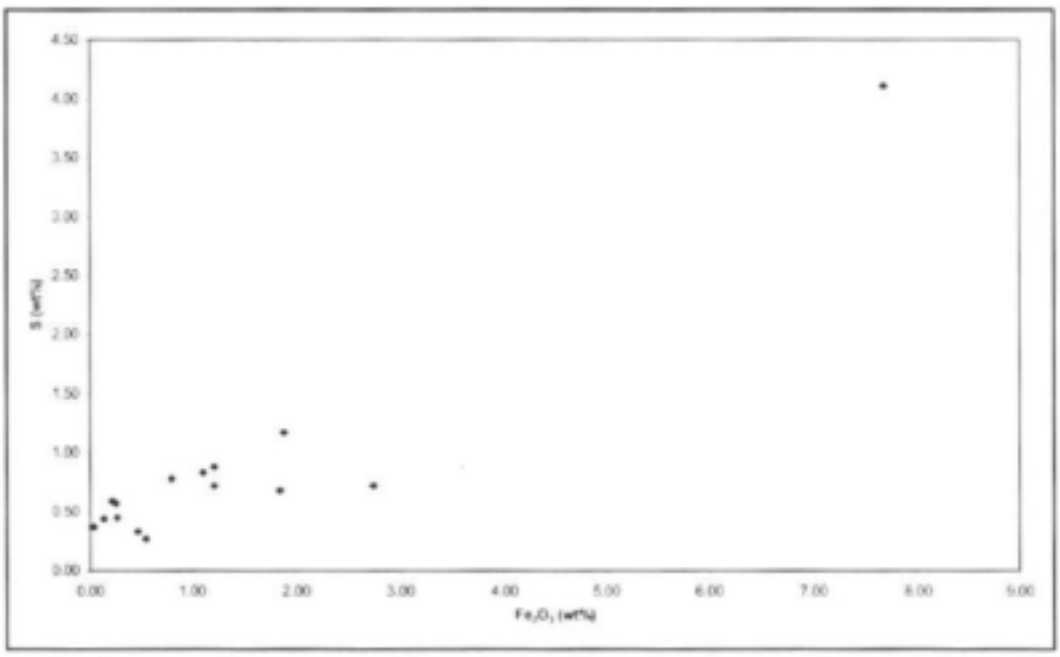

Figure 19. Relationship between Fe_2O_3 and S concentrations

There are a few good correlation yet unusual correlations observed between Cr and SiO_2 (r=0.877), TiO_2 (r=0.899), Al_2O_3 (r=0.805), Na_2O (r=0.885) and K_2O (r=0.924), between V and SiO_2 (r=0.929), TiO_2 (r=0.946), Al_2O_3 (r=0.831), Na_2O (r=0.951) and K_2O (r=0.972), and between Zr and TiO_2 (r=0.927) and Al_2O_3 (r=0.899). As noted by Azzie (2002) the occurrence of Cr, V and Zr could be a reflection of the source material, and similarly, Ward *et al.* (1999) has observed positive correlations between these elements and other oxides. However, this is an isolated incidence occurring mainly in the No. 1 Seam coal. The associations of some rare earth element with phosphate minerals from the goyazite-crandallite

group are also not overlooked as phosphate minerals have been observed in other sample sets used in this study. The correlation between Zr and TiO_2 is probably derived from their geochemical relationship, which is prominent in other rock types as well.

Distributions in the roof and floor lithologies are very different from the coal as is to be expected. These rocks consist of varying proportions of siltstone, sandstone and carbonaceous shale. Although it was difficult to draw up useful correlations due to the limited amount of samples, a brief indication of the chemical composition is provided with these analyses.

Table 18. The minimum, maximum and average concentrations of oxides (wt%) and trace elements (ppm) in siltstone floor rocks of No. 1 coal Seam

Element	Min.	Max.	Ave.	Element	Min.	Max.	Ave.
SiO_2	34.53	61.87	46.78	Ba	115.20	251.50	197.94
TiO_2	0.83	2.15	1.51	Sr	16.30	63.50	46.60
Al_2O_3	7.33	22.32	14.10	Zr	182.60	391.40	273.33
Fe_2O_3	0.38	4.15	1.83	Nb	5.20	17.50	12.09
S	0.18	0.99	0.43	Y	7.50	31.30	20.86
MnO	0.00	0.04	0.02	Sc	12.50	27.30	21.50
MgO	0.00	0.15	0.05	Cr	187.20	341.30	276.91
CaO	0.01	0.18	0.09	Cu	3.20	64.10	29.51
Na_2O	0.02	0.15	0.07	V	194.50	403.10	303.41
K_2O	0.38	1.10	0.73	Zn	31.70	56.70	45.67
P_2O_5	0.02	0.04	0.03	Ni	18.80	382.20	133.31
Rb	0.00	33.70	12.33	Co	6.40	69.10	29.37

As expected the SiO_2 content of the sandstones of the floor rocks were the highest followed by the siltstone as shown in Table 18, and then shale. Abundant Al_2O_3 was observed in the only shale sample available while Fe_2O_3 and S were abundant in the siltstone floor rocks. Low concentrations of Ca and Mg is supported by the absence of carbonate in the XRD patterns of most of these rocks, while the increase in K_2O in comparison to the coal is very prominent and probably due to the presence of illite frequently occurring in the roof and floor lithologies.

Elevated concentrations of Ba, V, Cr and Zr are present in all three rock types, but this time the possibility of phosphate association is ruled out by the low P_2O_5 concentration. This occurrence might once again be due to source rock influence. An exceptionally large concentration of Ni observed in the siltstone samples, in which the Fe_2O_3 and S contents are once again the highest. Seeing that the coal and siltstone samples in which Fe_2O_3, S and Ni are well correlated are not in the same vicinity, and some samples appear to be outliers, no specific reason could be provided for this occurrence. However, the probability of Ni's association with Fe becomes unavoidable.

Table 19. The minimum, maximum and average concentrations of oxides (wt%) and trace elements (ppm) in sandstone roof rocks of No. 1 coal Seam

Element	Min.	Max.	Ave.	Element	Min.	Max.	Ave.
SiO_2	76.66	91.25	85.39	Ba	24.60	223.10	114.31
TiO_2	0.29	1.44	0.93	Sr	20.80	208.80	77.38
Al_2O_3	3.13	7.45	4.90	Zr	181.60	662.00	435.03
Fe_2O_3	0.71	4.01	1.95	Nb	8.70	26.10	16.45
S	0.03	1.44	0.58	Y	3.60	19.50	12.03
MnO	0.00	0.07	0.03	Sc	0.00	8.60	4.04
MgO	0.00	1.63	0.43	Cr	58.40	178.00	108.69
CaO	0.00	4.71	1.26	Cu	0.00	6.30	2.56
Na_2O	0.01	0.11	0.05	V	30.40	69.30	44.15
K_2O	0.09	1.42	0.83	Zn	14.10	91.40	44.31
P_2O_5	0.02	0.03	0.02	Ni	9.20	215.90	75.15
Rb	0.00	35.50	18.61	Co	0.00	164.40	51.14

Roof rocks of the No. 1 coal Seam consisted of some sandstones and one siltstone sample. The bulk mineralogy of sandstones does not always consist strictly of quartz as seen in Table 19. Sandstones in this case show observations of elevated Fe_2O_3 and CaO percentages. Dolomite has been detected in the sandstone and siltstone samples containing reasonable amounts of CaO and MgO. It is possible for this carbonate to exist with calcite in the same assemblage. However, from XRD patterns dolomite or ferroan dolomite for that matter is detected more often in the sediment samples than in the coal, was also noted by Azzie (2002).

K_2O concentrations are supported by the presence of feldspars and illite/smectite clays in the siltstone and sandstones. Although pyrite is mainly associated with the coal, nodules of this mineral have been observed in hand specimen in roof and floor rocks. Good correlation exists between K_2O, Rb and Ba as in the case with the coal. A high concentration of Zr is once again well correlated with TiO_2, as well as with Nb. The occurrence of Zr in coal as discrete particles has been noted by Ward *et al.* (1999). In the latter case a strong correlation between Zr and TiO_2 was observed. Significant correlations exist between Ni, Fe and S along with reasonable correlations between Sr and MgO (r=0.993) and CaO (r=0.995).

Seeing that low P concentrations are present and a negative correlation (r=-0.022) exists between P and Sr, supported by no phosphate phases in the XRD patterns, it is unlikely that Sr-phosphates might be present. Correlation between Cr, V, and Cu, and between Ni and Co are probably as a result of a common magmatic source, although their modes of occurrence are variable.

b. No. 2 coal Seam

A total of 138 coal samples were collected from this Seam on which analyses were done. With this sample set it was possible to make conclusions from some contours graphs drawn using STATISTICA V.5.

SiO_2, TiO_2, Al_2O_3, Na_2O and K_2O concentrations are distributed along a northeast-southwest strike. These components are primarily derived from, and are associated with the mineralogy of the source material. The association of TiO_2 and Al_2O_3 is once again evident in their distribution, as well as their correlation coefficient (r=0.784).

The magnitude of this sample set also makes it possible to avoid unusual correlations based on lower concentrations and insufficient data. A noticeable and expected correlation exists between K_2O and Rb (r=0.785), between Sr and P_2O_5 (r=0.681), and between Ba and Sr (r=0.813). These relationships are due to the association of K_2O and Rb in the primary environment, and the association of Sr, Ba and P_2O_5 with aluminophosphate minerals such as crandallite and goyazite.

The most striking relationship in this Seam is the correlation between Fe_2O_3 and S. With a correlation coefficient of 0.9 it is expected that the Fe_2O_3 and S distribution would be reasonably similar. Despite the two outliers in Figure 20, there is still an exceptional correlation. However, the contour maps present a different situation. Figures 19 and 20 illustrate the Fe_2O_3 and S distribution respectively. There is an overlap of the highest concentrations for both elements in the north-western region of the Seam, but the elevated amounts of Fe_2O_3 in the northern and southern regions are very obvious. After calculating the amount of Fe_2O_3 needed to combine with the total S (all sulphur was thus assumed to have been inorganic/pyritic sulphur), the percentage of Fe_2O_3 left was distributed in a similar pattern to that seen in Figure 19. Only four cases were observed in which S was left after forming pyrite. This distribution for Fe could be as a result of, firstly, the fact that Fe could be present in higher proportions in carbonates such as dolomite and siderite, and clays such as montmorillonite, both of which were present in XRD interpretations. Secondly, because the samples were not heated, the only S that could have been lost was due to oxidation in air during storage or in nature, leaving an excess of Fe. Organic sulphur is rarely present in larger concentrations than 0.6 wt% (Ward *et al.*, 1999). Thus, it is more likely for this excess Fe to be captured in other mineral phases.

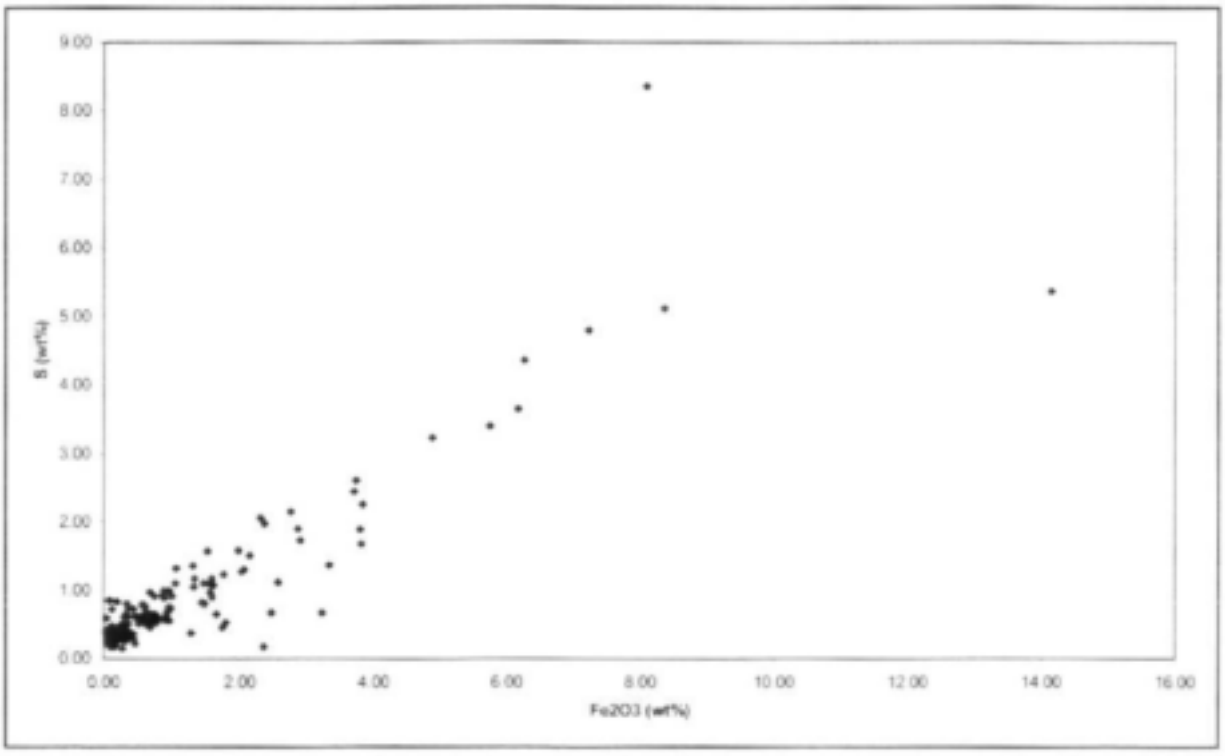

Figure 20. Relationship between Fe_2O_3 and S concentrations

The biggest difficulty in sampling roof and floor lithologies lies in the fact that some mines leave a layer of coal at the top and bottom of the mineable horizons; the coal seams are sometimes just too thick to be able to reach roof rocks, and borehole material in which the whole Seam can be sampled is not always available.

Table 20. The minimum, maximum and average concentrations of oxides (wt%) and trace elements (ppm) in sandstone floor rocks of No. 2 coal Seam

Element	Min.	Max.	Ave.	Element	Min.	Max.	Ave.
SiO_2	43.34	84.73	66.91	Ba	55.70	367.30	195.69
TiO_2	0.38	1.73	1.00	Sr	23.90	498.40	184.42
Al_2O_3	4.42	29.00	13.92	Zr	65.10	448.70	215.93
Fe_2O_3	0.79	5.22	2.13	Nb	6.70	36.10	16.39
S	0.06	0.58	0.24	Y	1.70	57.20	18.97
MnO	0.00	0.16	0.04	Sc	2.40	38.50	13.32
MgO	0.00	6.12	1.47	Cr	40.30	764.30	268.72
CaO	0.02	8.42	2.69	Cu	0.00	96.70	23.25
Na_2O	0.00	0.20	0.07	V	13.80	1018.70	296.49
K_2O	0.30	0.96	0.60	Zn	11.30	94.30	44.00
P_2O_5	0.01	0.12	0.05	Ni	9.10	194.90	54.26
Rb	0.70	108.90	29.50	Co	0.00	83.00	18.66

The floor rocks of the No. 2 coal Seam consisted mainly of sandstone, siltstone and carbonaceous shale of which too few samples were obtained to draw up any useful correlations. SiO_2 concentrations in sandstones shown in Table 20 are slightly lower than in those of the No.1 Seam roof samples; however, Fe_2O_3, CaO, MgO, Na_2O and K_2O concentrations are similar. The elevated Fe_2O_3 would be as a result of the presence of siderite, while K_2O and Na_2O are supported by an increase in illite in the sediments, as observed in the XRD interpretations. The carbonates calcite and dolomite often occur together with siderite. In this case no definite explanation could be given for the increased V concentrations, but the Ni and Fe_2O_3 concentration correspond significantly. Al_2O_3 and K_2O concentrations in the siltstone rocks range from 10 to 24 wt % and 0.64 to 1.48 wt%, respectively. This could be accounted for by the presence of kaolinite, K-feldspars and illite. This situation is the same for the two carbonaceous shale samples, although they contain abundant TiO_2 and Fe_2O_3 in addition to Al_2O_3 and K_2O, which is evident as the XRD patterns show traces of siderite for these samples.

Carbonaceous shale roof rocks of the No.2 coal Seam are similar in chemical composition to the floor shales apart from an average increase in P_2O_5 of 0.30 wt%. The corresponding Ba and Sr values for elevated P_2O_5 are as high as 1000 and 900 ppm, respectively. This elevated P_2O_5, Ba and Sr concentrations are supported by the presence of fluorapatite in XRD interpretations. Siltstone samples collected in the roof of this Seam are almost identical to the floor siltstones in terms of major element oxides and trace elements.

c. No. 4 coal Seam

While the SiO_2, TiO_2, Al_2O_3, Fe_2O_3 and S contents of this Seam are similar to concentrations of the No.1 and No. 2 coal seams, CaO and P_2O_5 show elevations as indicated by Table 18. SiO_2 and Al_2O_3 ($r=0.880$) correlate well and are highest in the north-north eastern region of the Seam, suggesting a possible change in direction of the influx of source material or a change in depositional conditions. Both Fe_2O_3 and

S distributions correspond since their concentrations decrease from west to east. P_2O_5 is highest mainly in the middle of the Seam, while prominent Ca values are found in the south-western area, decreasing towards the east.

Kaolinite is often present as the dominant silicate in some of the mineralogical assemblages. This corresponding distribution of SiO_2 and Al_2O_3 could be as a result of the weathering of feldspars or to the existence of favourable conditions enabling kaolinite precipitation. The presence of kaolinite suggests an acid leaching or freshwater environment, while the chemical breakdown of feldspar occurs mainly in the freshwater environment than in an alkaline or marine environment (Bühmann and Bühmann, 1987). According to Ward (2002), Al is soluble under low pH conditions, and could be leached out from detrital minerals and transported to areas with conditions suitable for kaolinite precipitation.

Thus, interaction of Al_2O_3 with any silica in solution would result in the formation of authigenic kaolinite, depending on the conditions (Ward, 2002). It is also possible that an igneous source with abundant K-feldspar provided this silica and alumina, but most of the feldspar has been weathered giving rise to more kaolinite. Thus, the distribution of SiO_2 and Al_2O_3 could be controlled by the direction of influx of the source material but more likely by the solubility and precipitation conditions of kaolinite.

The sulphide occurring mainly as a secondary or authigenic mineral phase, pyrite is the main reason for the distribution of Fe_2O_3 and S ($r=0.926$) in this manner. It is generally linked to marine influences during peat formation (Bühmann and Bühmann, 1987).

Calcite and dolomite are both abundant in the Seam, while fluorapatite accounts for the majority of P_2O_5 and some of the CaO and Al_2O_3 concentrations. The good correlation between P_2O_5 and Sr ($r=0.886$) implies that phosphates from the crandallite group could be present, even though only fluorapatite has been detected in XRD interpretations.

Table 21. The minimum, maximum and average concentrations of oxides (wt%) and trace elements (ppm) in No. 4 coal Seam

Element	Min.	Max.	Ave.	Element	Min.	Max.	Ave.
SiO_2	0.00	27.63	8.69	Rb	0.00	92.85	11.64
TiO_2	0.06	2.19	0.39	Ba	73.35	2902.38	590.28
Al_2O_3	1.45	12.89	5.11	Sr	58.96	3646.04	703.26
Fe_2O_3	0.06	6.78	2.32	Zr	0.00	657.48	88.60
S	0.31	4.66	1.90	Nb	0.00	22.01	7.42
MnO	0.00	0.00	0.00	Y	3.27	50.98	18.03
MgO	0.03	0.74	0.28	Sc	0.00	37.70	7.36
CaO	0.00	4.86	2.27	Cr	0.00	1049.21	53.21
Na_2O	0.00	0.16	0.04	Cu	5.22	53.77	17.15
K_2O	0.00	0.56	0.16	V	2.66	468.68	45.92
P_2O_5	0.00	1.82	0.48	Zn	0.34	56.77	8.11
Mn	0.00	401.72	98.55	Ni	2.60	102.38	19.97

The sandstones in the roof and floor lithologies of this Seam are characterized by elevated concentrations of Al_2O_3, TiO_2 and K_2O in comparison to the same rocks of the No.1 and No. 2 seams. Fe_2O_3 is also abundant in the roof sandstones; however S values are low averaging at 0.31 wt%. Illite, kaolinite and K-feldspar are well defined in the XRD patterns, but siderite could not be detected easily, suggesting that Fe could be caught up in minor montmorillonite and dolomite. The trace element distributions are very similar to other sandstones with no remarkable correlations except between elements and oxides with specific geochemical relationships; while siltstone and carbonaceous shale roof and floor rocks are also very similar to those of the other seams.

No. 4 coal Seam has a reasonably constant parting consisting of sandstone at Arnot, Douglas, Forzando and Optimum Mines, siltstone in the Rietspruit Mine area and carbonaceous shale at Tavistock Mine. The trace element concentrations are considerably lower and sometimes similar to those in floor and roof lithologies of the same rock type, while major element oxides are compatible as well.

d. No. 5 coal Seam

Table 22 illustrates that the No. 5 coal Seam contains SiO_2, TiO_2, Al_2O_3, Fe_2O_3 and S concentrations which are compatible to the lower seams, along with very low concentrations of CaO, MgO and P_2O_5. At the few locations where samples were available for this coal Seam, the SiO_2, TiO_2, Al_2O_3 and K_2O concentrations decrease from west to east. Fe_2O_3 and S, on the other hand, are distributed evenly amongst the localities. Na_2O is almost negligible throughout all the coal and trace elements are not much different either. The expected correlations are present and so too correlations which arise due to insufficient cases during matrix calculations.

Table 22. The minimum, maximum and average concentrations of oxides (wt%) and trace elements (ppm) in No. 5 coal Seam

Element	Min.	Max.	Ave.	Element	Min.	Max.	Ave.
SiO_2	5.79	29.27	13.05	Rb	0.00	65.71	19.12
TiO_2	0.07	0.47	0.19	Ba	0.00	751.48	145.56
Al_2O_3	2.17	11.15	4.79	Sr	2.85	143.39	52.07
Fe_2O_3	0.22	3.15	1.29	Zr	34.32	340.10	116.80
S	0.34	1.82	0.91	Nb	6.51	41.81	14.26
MnO	0.00	0.00	0.00	Y	0.94	29.60	11.23
MgO	0.00	0.28	0.12	Sc	0.10	11.37	3.85
CaO	0.00	0.13	0.04	Cr	0.00	107.09	15.75
Na_2O	0.00	0.02	0.00	Cu	3.73	15.09	8.51
K_2O	0.15	1.04	0.39	V	5.80	59.18	21.67
P_2O_5	0.00	0.00	0.00	Zn	0.00	9.83	3.89
Mn	0.00	7.50	2.09	Ni	0.00	12.39	2.28

Sandstones, siltstones and carbonaceous shale also make up the roof and floor rocks of the No. 5 coal Seam. The only noticeable difference is that all rock types contain significant elevations in MgO, which could mainly be accounted for by the presence of montmorillonite in the XRD interpretations. CaO and K_2O concentrations were considerable too averaging at 0.28 and 2.72 respectively, and since almost no calcite was present, CaO and K_2O was accounted for by plagioclase feldspar in a few siltstones. Siderite appeared to be a dominant component in some of the XRD interpretations in accordance with the higher Fe_2O_3 and low S values, but some of this Fe_2O_3 also forms part of the montmorillonite phase. Kaolinite, illite and K-feldspar are often found together with siderite in most roof and floor rocks, as is the case for this Seam.

3.3.2 The Highveld coalfield

a. No. 4 coal Seam

Although fewer samples were obtained in this coalfield, Figure 21 illustrates that the concentrations of some major element oxides are similar except for a few samples. However, due to insufficient data, a clear distribution could not be detected, but the data still gives an indication of what major differences are to be expected between the two fields. All except CaO and Na_2O concentrations are very similar to not only the No.4 Seam coal in the Witbank coalfield, but the coal in the other seams as well. The mineral components consist of quartz, major kaolinite, calcite, dolomite, pyrite, siderite and sometimes, major phosphate phases. K-feldspar has also been detected on rare occasions.

Correlations between Fe_2O_3 and S (r=0.887), P_2O_5 and Sr (r=0.933), and K_2O and Rb (0.765) are all due to the presence of pyrite, crandallite and illite, respectively. Ba and Sr are the only trace elements showing any elevation in concentration, while the others are in good agreement with those observed in the seams of the Witbank coalfield.

Roof and floor lithologies for this Seam consist of sandstones and siltstones. Siltstones from the roof and floor rocks are characterized by high Fe_2O_3 and K_2O concentrations, which are evident in the presence of siderite, and K-feldspar in some of the XRD interpretations. Floor sandstones contain less SiO_2 and more Al_2O_3 than roof sandstones in which major illite and feldspars are present. The Fe_2O_3:S ratio is rather high suggesting that most of the Fe is probably accounted for by siderite, since montmorillonite is not a prominent phase in the assemblage. Trace element concentrations for sandstone and siltstones are similar.

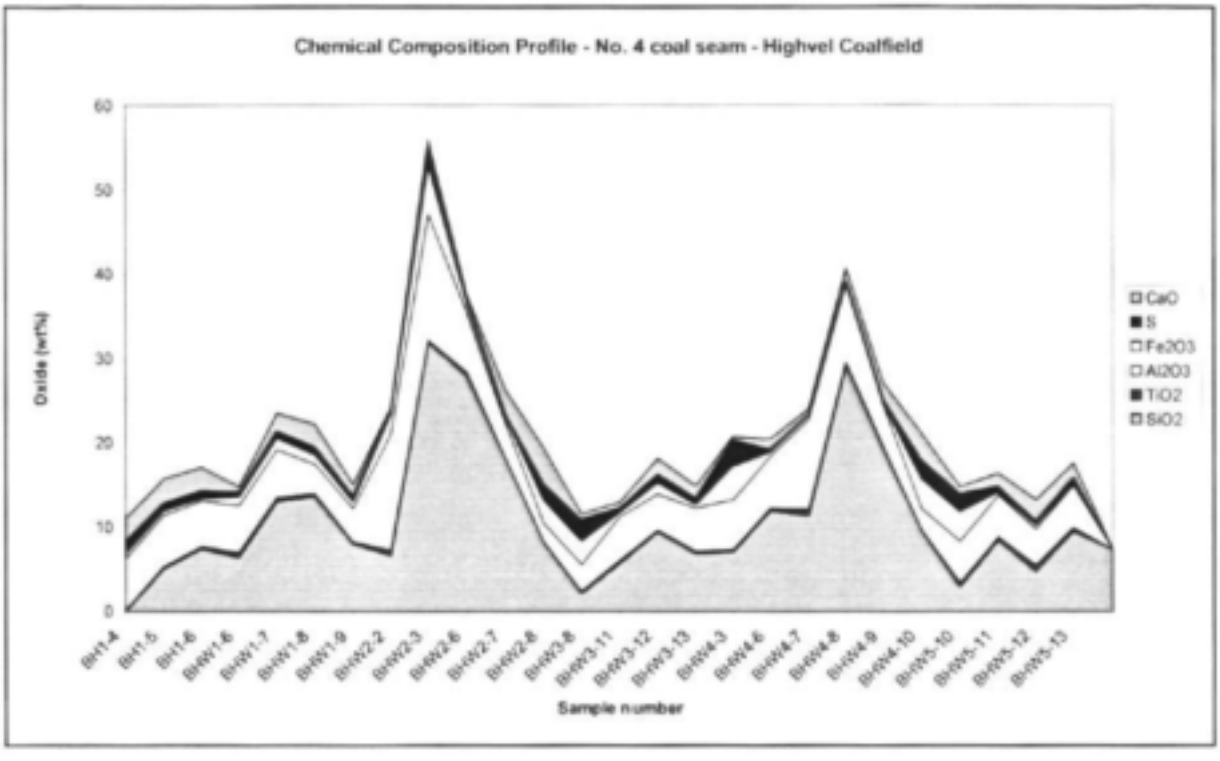

Figure 21. Chemical profile of some element oxides in No. 4 coal Seam

b. No. 5 coal Seam

Unlike the No.5 Seam in the Witbank coalfield, this Seam contains noticeable concentrations of SiO_2, CaO, MgO and Na2O; however illite, feldspars and the carbonates were not detected in the XRD patterns of these samples. Fe_2O_3 and S (r=0.840) have a significant correlation. A few sandstone and shale samples were collected from the roof and floor lithologies, both of which do not contain any significantly elevated concentrations of major or trace elements.

3.3.3 X-ray diffraction results

3.3.3.1 The Witbank coalfield

The X-ray diffraction interpretation method applied at the University of the Free State involves comparing the diffraction scan to separate peak files for minerals included in the software database. All diffraction

peaks may not be completely visible, but, depending on the operator, this method could be applied with great accuracy since the interpretation relies primarily on the researcher's discretion. The occurrence of these minerals in the XRD diffraction patterns is supported by their chemical compositions as explained in the previous sections. One problem that arises in these interpretations concerns chemical components, which are present in low concentrations. Phases such as illite, montmorillonite and feldspar are never abundant or rarely occur as major phases in coal, thus the low concentrations of K_2O and Na_2O are not always represented clearly in the XRD pattern. Similarly, an abundance of a specific element in the XRF results does not necessarily mean that it is indicative of a specific phase. Fe is one such element, which occurs, in various mineral phases. It is easy to make an assumption that most of the Fe would be accounted for by sulphides in this case; however, if gaseous compounds such as SO_3 and CO_2 are unknown, assumptions as to whether the distribution of Fe would be as sulphides or carbonates should be done with great care.

From this XRD interpretation it was possible to identify the main mineral phases and estimate the percentage of each constituent in terms of dominant, major, minor, accessory and rare components. The interpretations will be discussed according to the phases prominent in each Seam. Examples of diffraction scans with identified peaks are illustrated in Figures A2-1 to A2-6 on pages A2-87 to A2-92 in Appendix 2. All samples were analyzed in accordance with specifications set out in Appendix 1. All XRD interpretations are tabulated in Appendix 2 according to sampling localities.

a. No. 1 coal Seam

The mineralogical composition of coal deposits across the world consists of a dominant assemblage of quartz, kaolinite, clay minerals, sulphides, carbonates and phosphates, and some rare minerals characteristic of the depositional environment or the source material. Quartz and kaolinite commonly occur as the dominant phases in this Seam. Calcite, dolomite and pyrite occur mainly as minor phases. It is rather difficult to distinguish between illite and illite/smectite interstratifications using this technique since there are a few peak overlaps occurring at the major illite peak 2θ position, but this phase is not abundant in the Seam. Siderite is rather prominent for a mineral that supposedly occurs mainly in the roof and floor lithologies, even though it was only in minor concentrations. Low concentrations of fluorapatite have been detected in samples from Kleinkopje Mine, while minor montmorillonite is observed in the Arnot Mine area. Roof and floor rocks are dominated by quartz, kaolinite and sometimes minor feldspars and clay minerals.

b. No. 2 coal Seam

Kaolinite, calcite and dolomite are the dominant phases in the No. 2 Seam. Dolomite is more often than not present in larger concentrations than calcite, and sometimes only one of these carbonates appear along with dominant kaolinite proportions. Pyrite and montmorillonite occur as minor phases together with the phosphates fluorapatite and crandallite. Fluorapatite is present mainly in samples in the western

region of the Seam, and decreases towards the east. Crandallite was observed only in one sample coming from the Leeufontein Mine area. Quartz is present in most of the samples and its concentration might vary from dominant to accessory in the coal samples, but it is clearly one of the prevalent phases in the roof and floor lithologies. K-feldspar is prominent in the sandstones, while illite is more common amongst the siltstones and shales. Plagioclase was found infrequently, while siderite constantly appeared in sandstone samples. Calcite and dolomite are present in the sediments, but mainly in lower concentrations. Pyrite rarely makes an appearance in sandstones, but sometimes it can be one of the major phases especially at the roof-coal interface. This precipitation could be due to a change in Eh at the interface.

In order to discover whether there were any differences in the mineralogical or geochemical nature of coal with different roof lithologies, coal underlying sandstones, siltstones and shales were compared. This might have given an indication of the environmental conditions under which the coal were deposited, but the only definite conclusion that could be made was that the general mineralogical and chemical compositions of coal were very similar.

c. No. 4 and No. 5 coal seams

As expected, quartz concentrations seem to decrease towards the west while kaolinite is almost ubiquitous throughout the seams. Calcite, dolomite and montmorillonite still occur in minor concentrations and pyrite sometimes as a major component, while K-feldspar has been observed as an accessory constituent. Once again illite and siderite in the roof and floor rocks contain similar concentrations as in the other seams.

3.3.3.2 The Highveld coalfield

a. No. 4 and No. 5 coal seams

Mineral distributions in the Highveld coalfield are outstandingly similar to the coal and sediment mineralogy of the Witbank coalfield. The main constituents, quartz, kaolinite, calcite, dolomite and minor montmorillonite, occur in the coal in varying proportions, while illite, siderite and K-feldspar are more common in the roof and floor rocks. Only one occurrence of crandallite and plagioclase feldspar was observed in samples BH1-5 and BHW3-5 respectively. In addition, pyrite concentrations are much lower in comparison to the Witbank coalfield.

The XRD interpretation provided a useful indication as to which phases governed the mineralogy and which were enriched or depleted as a result of depositional or source material influences.

3.3.4 Normative Mineralogical Interpretation using SEDNORM

D. R. Cohen and C. R. Ward at the Department of Applied Geology, UNSW, AUSTRALIA, designed the software used to determine the normative mineralogy, called SEDNORM. It calculates the mineralogy especially of sedimentary rocks based on chemical analyses. The sequence of allocating elements or oxides to the various minerals is a function of observed sedimentary mineral assemblages, mineral stabilities in surface environments and the restriction of certain elements to specific minerals e.g. (Phosphorus completely contained in apatite). There is some degree of independent mineralogical data required (XRD, SEM or optical petrology) to control whether minerals such as feldspar, muscovite and montmorillonite are present and the control of compositional parameters for minerals such montmorillonite (within certain restrictions) is optional (SEDNORM – Users Manual, 1990).

The principles, which have to be applied in order to derive the normative mineralogy from the oxide percentages, are set out as follows:

i. Both apatite and crandallite may exist in coal, but phosphorus is assumed to be present in apatite since it is the dominant phosphate in sedimentary rocks.
ii. Any sulphur present is assumed to be consumed in pyrite or gypsum, depending on the degree of oxidation.
iii. Chlorine is allocated to halite.
iv. The distribution of potassium between K-feldspar, illite and muscovite can be fixed and any excess potassium remaining after the clays or muscovite are formed can be assigned to K-feldspar.
v. Options are available to assign calcium and magnesium to the carbonates first and then apatite and gypsum, or in the preferred order. The carbonates permitted are calcite, magnesite and siderite, and calcite is formed in preference to siderite with excess iron being assigned to hematite.
vi. The inclusion of montmorillonite is optional, and a choice is provided regarding the cation ratios in the smectite component, if is appears to be present from sources such as XRD.
vii. To compensate for minor errors in differentiating between structural and absorbed water, the water content could be increased until the Al_2O_3 and SiO_2 are exhausted. Any alumina and silica left will be assigned to gibbsite and quartz, respectively.
viii. In the event of excess chlorine being present sodium is added to the system to form halite, and similarly chlorine is added to form halite if excess sodium is present after feldspar is formed.

The program was applied successfully by Ward *et al.* (1999) in a study concerning the mineralogy of sandstones; however its use in the determination of coal mineralogy has proved to be limited in this study. Nonetheless, correlations between the normative mineralogy and the chemical composition are fairly consistently.

a. Coal

Correlations are obtained between quartz and SiO_2 (r=0.767), pyrite and, Fe_2O_3 (r=0.933) and S (r=0.960), siderite and Fe_2O_3 (0.885), magnesite and CaO (r=0.819) and MgO (r=0.835), calcite and CaO (r=0.812), apatite and P_2O_5 (r=0.919), and slightly between illite-smectite and K_2O (r=0.633) since K_2O is allocated to illite-smectite and K-feldspar. Plots illustrated in Figures 3.24 to 3.32 indicate these relationships.

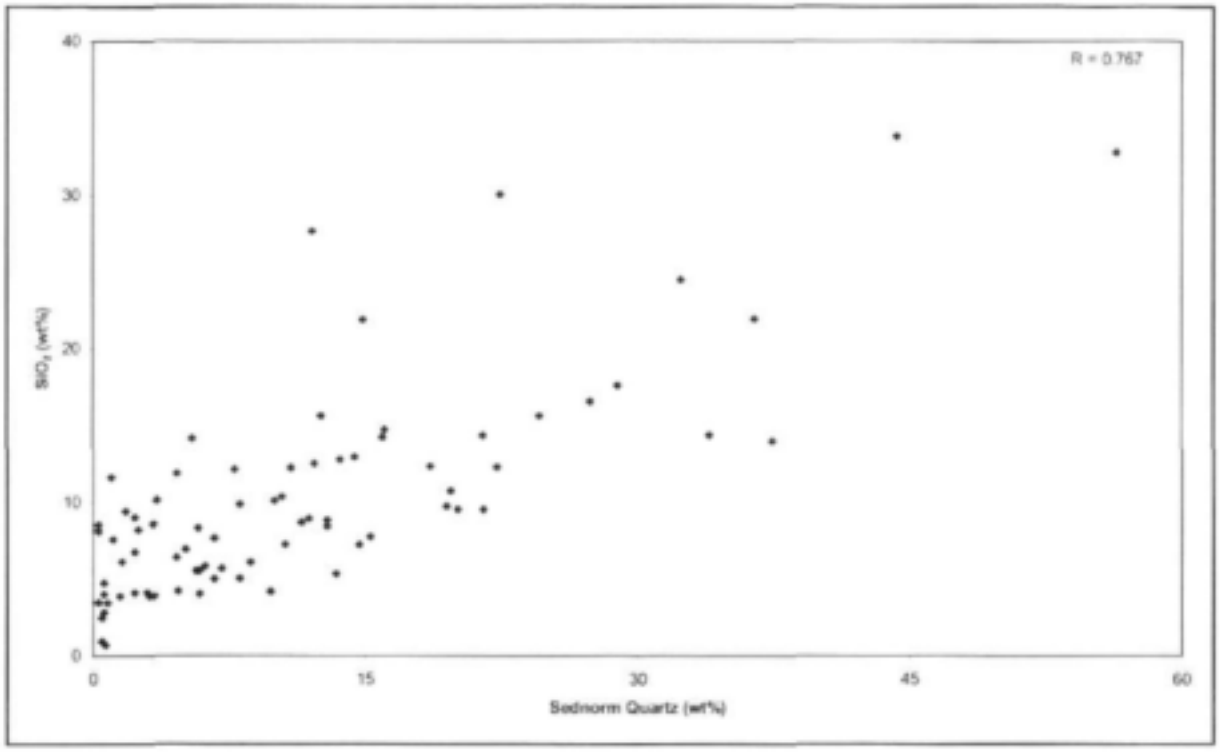

Figure 22. Relationship between normative Quartz and SiO_2 percentages in coal samples

A regression analysis executed in Microsoft Excel proved that the correlation coefficients are almost identical to those obtained from the correlation matrix drawn up in STATISTICA. Since quartz is mainly a minor constituent in the coal, the normative results in Figure 22 corresponds exceptionally well, as SiO_2 is used firstly to form other silicate phases for which there is sufficient amounts of K, Ca, Na, Al, Mg and Fe.

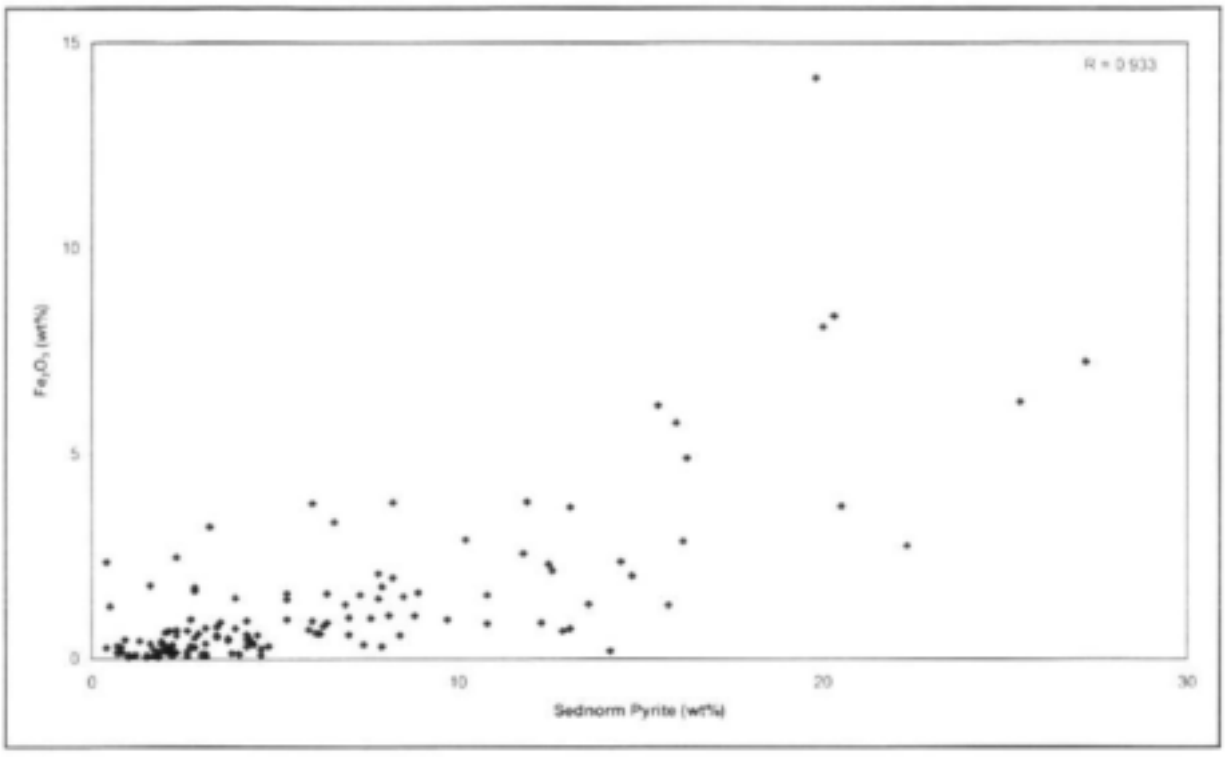

Figure 23. Relationship between normative Pyrite and Fe_2O_3 percentages in coal samples

The correlation coefficient obtained for Fe_2O_3 and siderite in Figure 24 is slightly lower than the correlation coefficient for Fe_2O_3 and pyrite seen in Figure 23. This could be due to the fact that pyrite was more abundant in the coal samples than siderite. Thus, most Fe_2O_3 was available for pyrite formation until all S was used, and the remaining Fe_2O_3 was assigned to siderite.

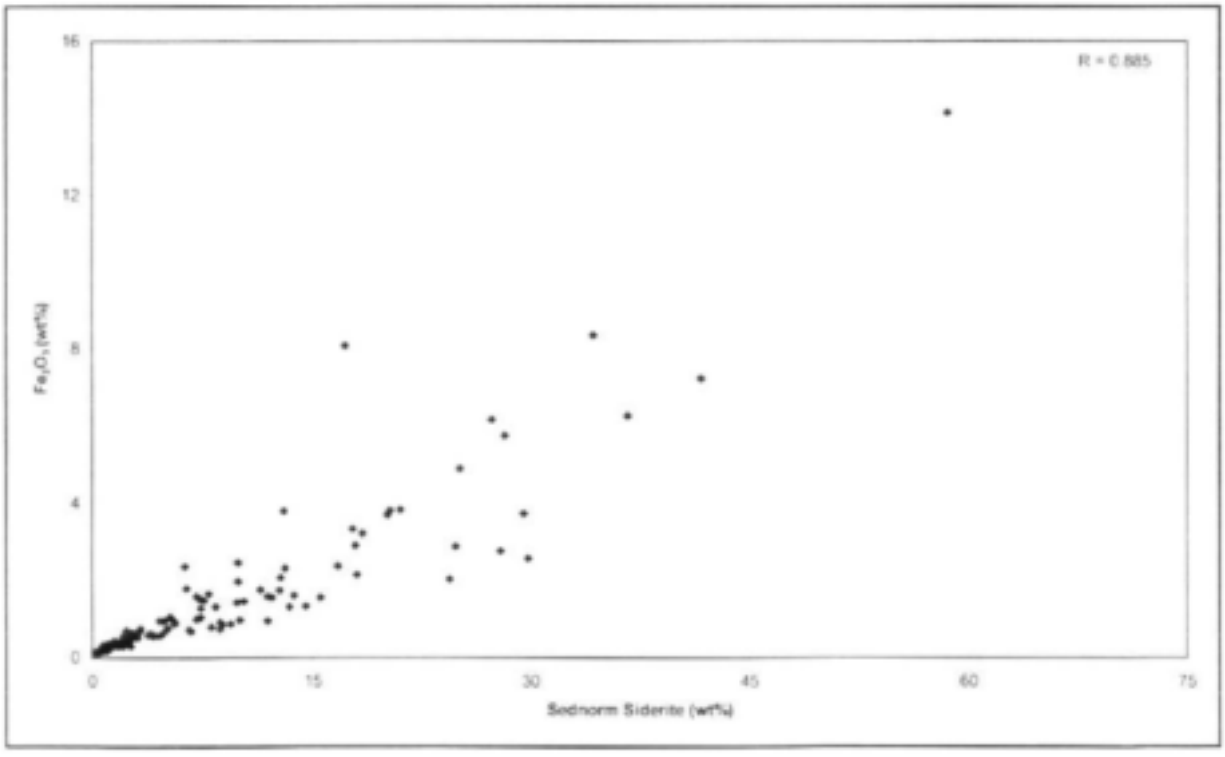

Figure 24. Relationship between normative Siderite and Fe_2O_3 percentages in coal samples

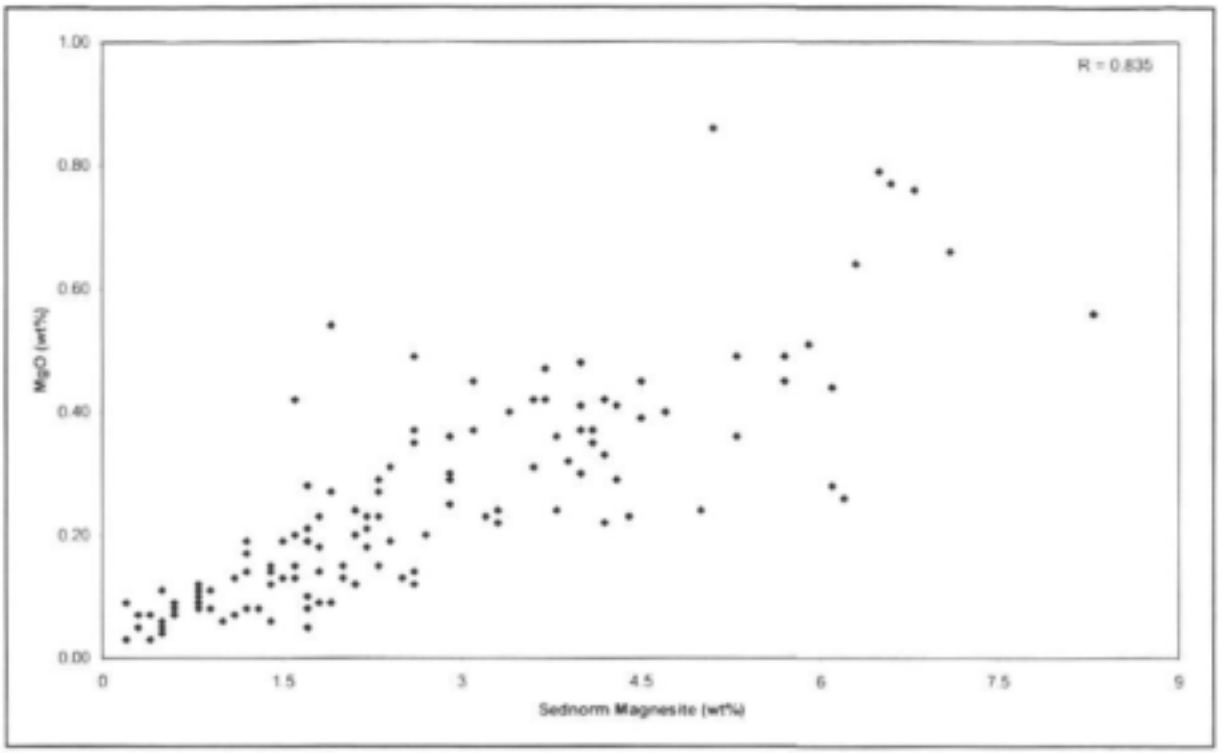

Figure 25. Relationship between normative Magnesite and MgO percentages in coal samples

Remembering that the normative program was designed mainly for Australian sedimentary rocks, it accommodates magnesite as the dominant Mg-carbonate instead of dolomite which is more prominent in South African coal. Yet, the magnesite percentage in Figure 25 is in good agreement with the MgO of which most is supposed to be in the form of dolomite.

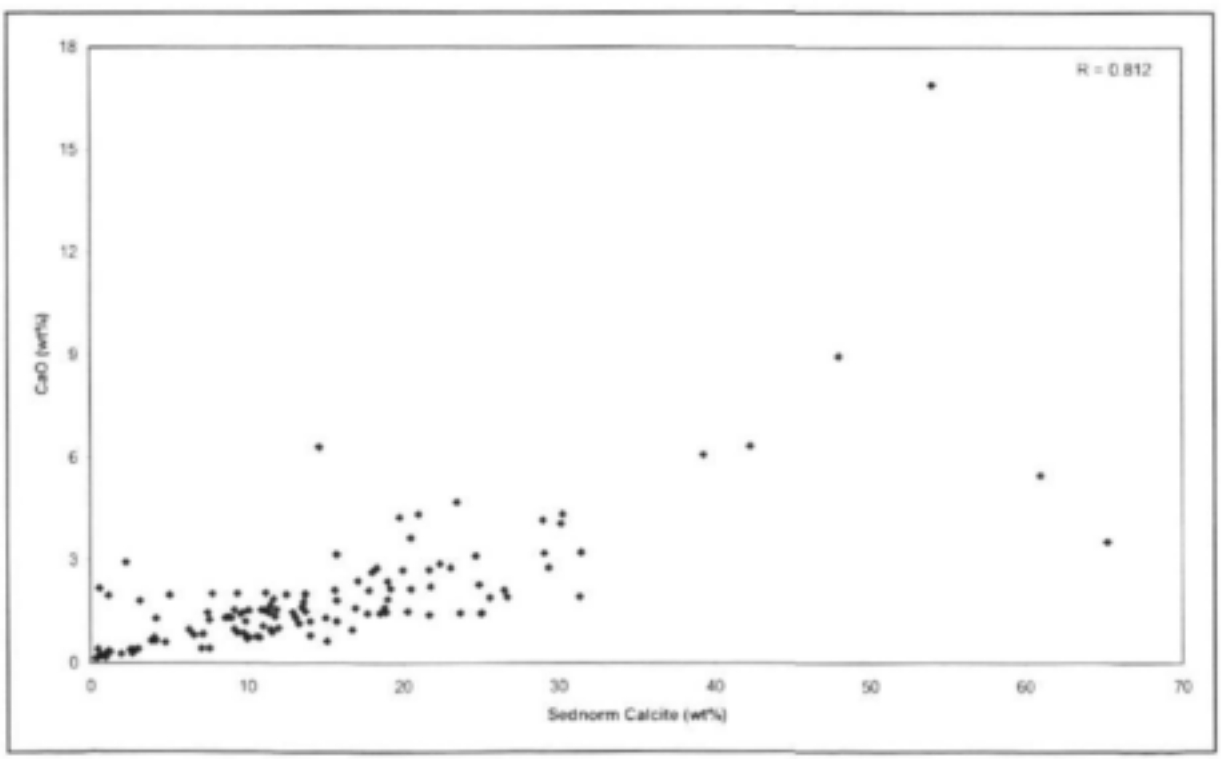

Figure 26. Relationship between normative Calcite and CaO percentages in coal samples

CaO is used to form calcite before any other Ca-bearing phase confirming the high correlation coefficient of r=0.812 as seen in Figure 26. However, dolomite does occur as the dominant carbonate is many coal and the correlation between magnesite and CaO (r=0.819) is slightly stronger than the one between calcite and CaO. Therefore, if enough MgO is present, CaO could be consumed by magnesite first. The excellent correlation between apatite and P_2O_5 in Figure 27 lies in the fact that it is the only phosphate phase allowed to consume all present phosphorus, and with the presence of sufficient CaO and lower P_2O_5, apatite could be formed until all P_2O_5 is used.

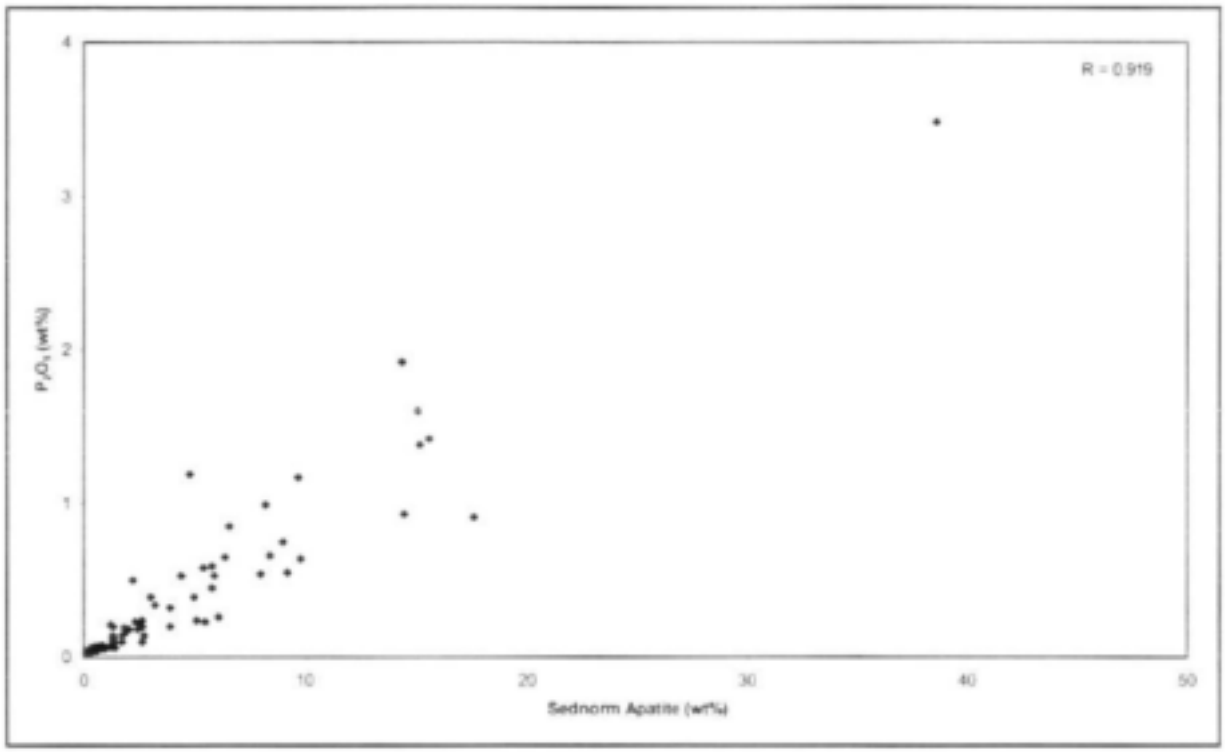

Figure 27. Relationship between normative Apatite and P_2O_5 percentages in coal samples

b. Sediments

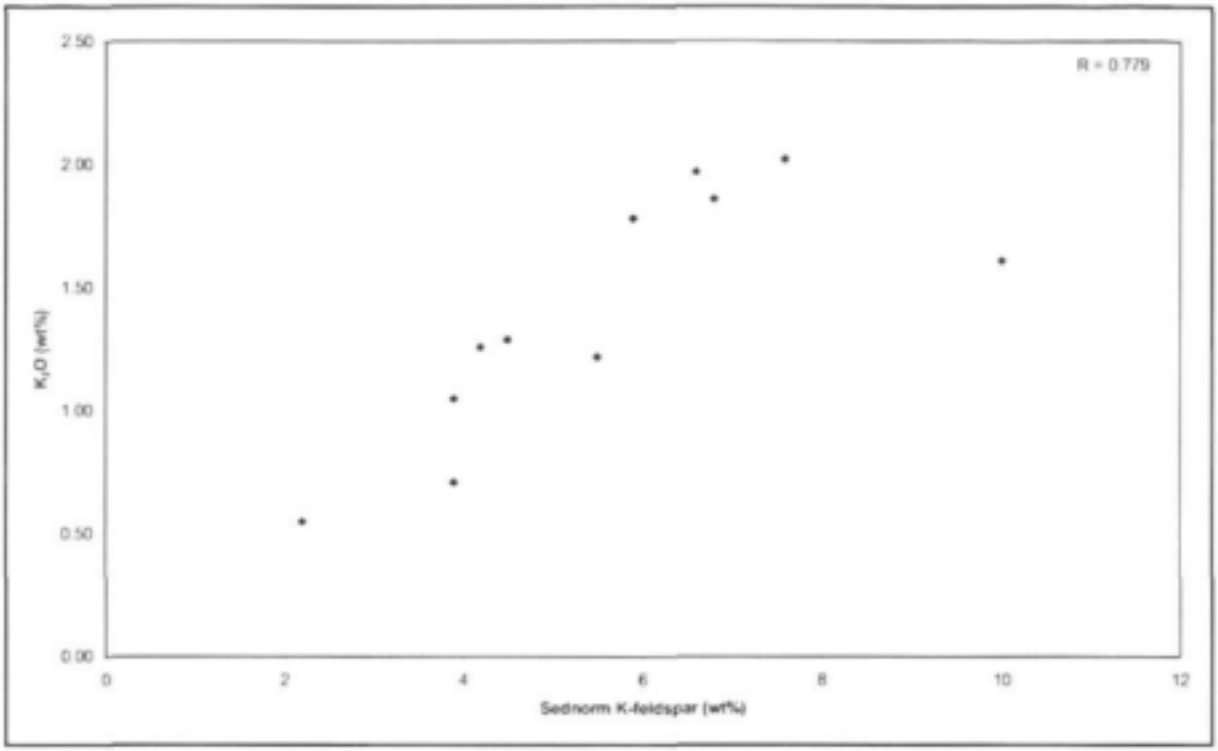

Figure 28. Relationship between normative K-feldspar and K_2O percentages in sediment samples

The correlation between feldspars and their compounds is best seen in the sediments where abundant K_2O and Na_2O is present. The correlation between K-feldspar and K_2O (as seen in Figure 3.30) and Na_2O is r=0.779 and r=0.769, respectively. A good correlation between K_2O and illite-smectite (r=0.831) is also observed in Figure 3.32. The correlation between Al_2O_3 and kaolinite is also more significant in the sediments (r=0.869) than in the coal as seen in Figure 3.31. This is probably because abundant Al_2O_3 is present in the sediments due to the fact that more alumino-silicate phases are present than in the coal, and kaolinite also occur as a dominant phase in the sediments.

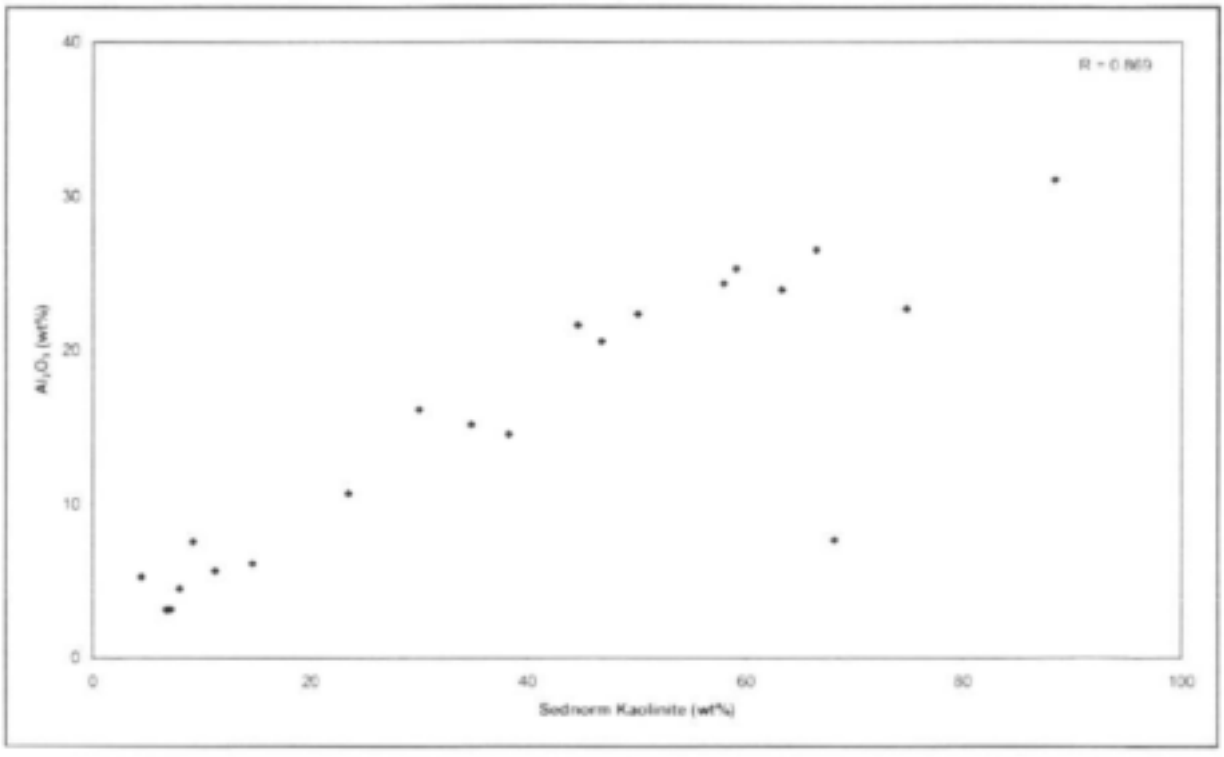

Figure 29. Relationship between normative Kaolinite and Al_2O_3 percentages in sediment samples

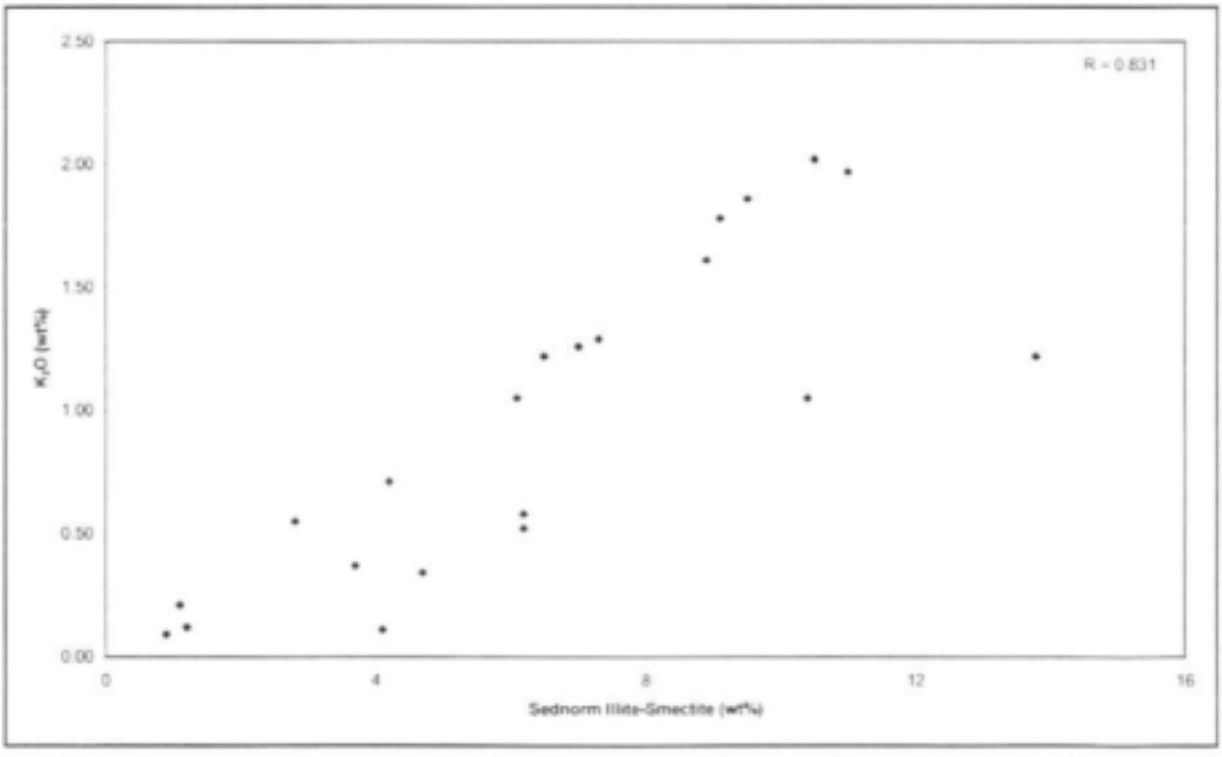

Figure 30. Relationship between normative Illite-Smectite and K_2O percentages in sediment samples

The mineralogical composition of coal and coal-bearing units are similar in some instances, although some significant differences are observed. The ability of this mineralogy to contribute to groundwater

character and the influence on ground water owing to a difference in mineralogy is the main objectives of this study, and these possible influences are discussed in the following chapters.

4 GEOCHEMICAL CHARACTERIZATION AND QUALITY OF COLLIERY WATERS

4.1 Quality of colliery waters

The chemical nature of water is influenced only by the entities with which it is in contact, i.e. water-rock interactions. Various mechanical factors and constraints in water movement play a significant role. The quality of water surrounding ore deposits might differ considerably to water where no such geological bodies are present. Depending on whether ore deposits are being mined, the manner in which they are mined and the rehabilitation procedures applied after mining has ceased, there are great differences in water quality regarding such scenarios.

The coalmines in the Mpumalanga Province are situated within the Olifants River and Vaal River Catchments. Rainwater in the region contains elevated sulphate concentrations, while a general rise in salt concentrations is observed in the Loskop Dam. Sulphate anions dominate waters of the Loskop Dam as well as the Witbank and Middelburg Dams. As mentioned in section 1, the weathered and unweathered Ecca aquifers are the most significant since the Pre-Karoo aquifers are at great depths and have a low-yielding character. The excellent quality of water in the weathered aquifer can be attributed to the many years of dynamic groundwater flow through the weathered sediments. Leachable salts have been washed from the system long ago and it is only the slow decomposition of clay particles, which presently releases some elements into the water. Water in the unweathered/fractured aquifer could possibly seep through the No. 2 coal Seam, causing higher salt loads there than in the waters of the weathered aquifer; nevertheless acceptable concentrations ranging between 1 and 400 mg/l are still obtained (Hodgson and Krantz, 1998).

With rapid industrial development in the province, several factors able to contribute to the deteriorating water quality were introduced. Power generation, municipal waste, sewage effluent, metallurgical and agricultural waste are some of the contributors to pollution, but the effects of mining activities seems to be the primary cause for concern regarding water quality, therefore its influence will be discussed in further detail. Water monitoring systems implemented over the last few decades display some significant results regarding the quality of both surface and underground water surrounding these mines, the key process giving reason for concern being acid mine drainage (AMD).

This study was aimed at correlating the water quality in a specific area with the mineralogical composition of the coal and its roof and floor lithologies in that area. However, this objective was unattainable for various reasons. In order to illustrate the mineral distribution across such an area, it is necessary to obtain spatial data from a structured, and more intensive sampling program. It is not always possible to sample even a smaller area, such as a mine, at regular intervals to gather enough information for setting up contour maps. So the task is more complicated when working with areas of this magnitude. Thus, samples collected from the mines included in this study were often kilometers apart.

There are some other constraints that could be unfavourable during procedures such as this. Accessing all lithologies underground in one area is not always viable, resulting in the need for borehole material. Although it is clear from the research done here that extensive planning and some modifications are needed to ensure that this specific objective is achieved, outstanding results were obtained from the exercise. A decision was made to limit the study to a mineralogical study with investigations in the acid-base potential of some samples. Most researchers choose to address the water quality predicament by finding the problem as well as a solution. However, the use of acid-base accounting allows researchers to approach the cause. Although it has been done previously in the region, this technique was applied here mainly to verify the potential of the coal and rocks in the coalfield to contribute to the geochemical character of water, and is laid out in section 5. Since no water samples have been analyzed, only a brief description of AMD, its influence on water quality and the factors controlling water quality are provided in the next sections of this section.

4.1.1 Sources of acid mine drainage (AMD)

Sulphuric acid is formed by reaction of water with iron sulphides, particularly the mineral pyrite, which is a common constituent in coal seams. It may be produced from drainage of mines from which sulphide ores are being extracted, from tailings produced in plants where the ores are processed and through groundwater emerging from abandoned mines charged with sulphuric acid and various salts of metals. Such chemical pollution also includes salts of zinc, lead, arsenic, copper and aluminium (Strahler and Strahler, 1973). The reactions of pyrite with oxygen and water generally found in literature (Grobbelaar, 2001; Azzie, 1999; Chelin, 2000) are quite simple and proceeds as follows:

Step one: The pyrite oxidizes upon contact with air and water

1) $2FeS_2 + 7\ O_2 + 2H_2O = 4SO_4^{2-} + 2Fe^{2+} + 4H^+$

Step two: Iron oxidizes to ferric iron

2) $4Fe^{2+} + 4O_2 + 4H^+ = 4Fe^{3+} + 2H_2O$

Step three: Precipitation occurs with ferric iron to ferric hydroxide

3) $Fe^{3+} + 3H_2O = Fe(OH)_3 + 3H^+$

Thus, the overall reaction can be written as:

$4FeS_2 + 15O_2 + 14H_2O = 8H_2SO_4 + 4Fe(OH)_3$

Once acid has been formed it will either remain and accumulate in the rock by filling pores, or be removed by water. Sufficient alkaline material is needed to neutralize AMD conditions depending on the extent of distribution of the acid. The most common acid consuming or neutralizing mineral is calcite ($CaCO_3$) and neutralization occurs via the reactions:

$$CaCO_3 + H^+ \rightarrow Ca^{2+} + HCO_3^-$$

or

$$CaCO_3 + 2H^+ \rightarrow Ca^{2+} + H_2CO_3$$

If acid generation continues long enough to exhaust the neutralizing ability, the pH will drop and create more favourable conditions for acid generation. The pH of natural waters, however, is controlled by reactions involving an acid-base system, such as the carbonic acid system (Azzie, 1999).

Chemical equilibrium models for the study of the carbonic acid system include both an open and a closed system. An open system assumes that the water is in equilibrium with the partial pressure of CO_2 in the atmosphere. This model is used when there is ample time for atmospheric carbon dioxide to saturate a solution. For example, this chemical model can be used to study the chemistry of shallow lakes, cooling towers and geological formations. In a closed system the acid-base reactions are much faster than gas dissolution equilibrium reactions. Natural systems tend to change relatively rapidly thus no equilibrium with the surrounding atmosphere is attained. The closed system is therefore is commonly used in most environmental engineering and environmental science applications. Equilibrium with the atmosphere is ignored in this case.

When $CO_{2\ (g)}$ is brought into contact with water it will dissolve forming carbonic acid (H_2CO_3) until an equilibrium state is reached. The carbonic acid will dissociate to hydrogen, bicarbonate (HCO_3^-) and carbonate (CO_3^{2-}) ions. In an open system the water will be in contact with a gas phase thus carbon dioxide will enter the solution and when the calcite dissolves it is referred to as "open system dissolution". If no gas phase is present, such as below the water table or tailings ponds below the surface, no carbon dioxide will be provided while the calcite dissolves. The solubility of calcite increases within an open system in comparison to a closed system. Dolomite could serve as a neutralizing agent for sulphuric acid, but it is less effective than calcite (Cruywagen, 2000).

Although very brief, this overview of AMD confirms that the generation and remediation of AMD is a cause for concern regarding most coalmines, as well as other mining sectors; especially since the effects are evident in the deterioration of aquatic and terrestrial life forms surrounding these areas.

4.1.2 The effects of AMD on colliery water quality

Research on AMD has gradually intensified since the problem becomes more apparent each year, and similar situations are encountered in coalmines elsewhere. The influence of coal mining methods on water quality is described comprehensively by Hodgson and Krantz (1998).

The dissolution of sodium, potassium and chloride-bearing minerals occur simultaneously with the oxidation of pyrite in the spoils of opencast mines. Accelerated pyrite oxidation occurs together with the precipitation of ferric hydroxide. The total sulphur gives little indication of the final pH of the spoil waters. Low sulphur content may still produce acid if insufficient neutralizing constituents are present, and when

neutralizing constituents are depleted water quality is sure to deteriorate. Water quality in shallow underground mines varies from acid to neutral to saline conditions (Hodgson and Krantz, 1998). In some cases water is not saturated with respect to sulphate due to periodic recharge, while other cases are observed where calcium sulphate dominates waters due to the carbonates in the coal. Low calcium and magnesium concentrations suggest that the base potential has been exhausted, and high metal concentrations are present due to a low pH (Hodgson and Krantz, 1998).

Water quantity in deep underground mines varies considerably depending on the mining method used, namely, bord-and-pillar, high extraction, stoping, longwall and shortwall mining. Water quality though could be explained in terms of bord-and-pillar and high extraction mining. Interstitial water in bord-and-pillar mines is dominated by sodium and chloride ions, and due to the small load, high concentrations of metals are not present. On the other hand, water in stagnant pools deteriorate due to the high acid generating potential of the coal Seam, which often increases once the base potential has been depleted. Natural alkalinity of water that flows into the mine or carbon dioxide from the atmosphere could suffice as a means to buffer acid. Water in high extraction mines is initially high in sodium, but later deteriorates due to pyrite oxidation and an increase in sulphate, calcium and magnesium takes place. Panel waters in such mines have high alkaline tendencies due to available carbonates (Hodgson and Krantz, 1998).

Waters from coalmines in other countries show the same character. Calcium sulphate type waters characterize abandoned opencast coalmines in Ohio, while magnesium concentrations are often similar to calcium concentrations, and elevated concentrations of sulphate, boron, fluoride and chloride are present (Haefner, 2002).

In a study examining sulphate transport and trends as an indicator of drainage from past and present coal mining in the Allegheny and Monongahela River Basins, USA, a comprehensive description of the effects of acid mine drainage is presented. The AMD effects on various rivers and streams in the basins are evident in the deaths of numerous aquatic plants and animals (Sams and Beer, 2000). Similarly, AMD water quality at an opencast coalmine in Indiana was characterized by high acidity, high concentrations of iron, manganese and sulphate, and lack of alkalinity. Remediation processes applied here included the placement of coal ash commonly used for its alkaline nature to improve AMD conditions (Martin *et al.*, 1990).

4.2 A model for the preliminary assessment of sources of pollution

From the time when monitoring water quality has become an integral part of operating a mine, more knowledge has been gathered concerning the causes, effects and solutions associated with water problems. It is necessary to understand unfavourable reactions that are associated with specific mine wastes and by-products, and how they affect the surrounding environment. Therefore, examining the potential of any source to contribute to pollution could be cost-effective and beneficial, as time and resources spent on remediation often amounts to vast quantities.

As seen from equations above, pyrite weathering eventually results in iron oxyhydroxide precipitation resulting in a greater net acid production. However, minewater often achieves equilibrium due to forward and reverse reactions occurring at a similar pace. Minerals such as carbonates and aluminosilicates also consume acidity and helps buffer pH. According to data presented by Banwart and Malmström (2001), calcite dissolves 3 orders-of-magnitude quicker than pyrite, which in turn dissolves nearly 3 order-of magnitude quicker than aluminosilicates as observed in Figure 31. If these minerals are present in similar quantities, calcite will produce sufficient alkalinity to neutralize the acidity produced by the pyrite until it is depleted (Figure 32).

Once calcite is depleted the acidity level will be determined by the weathering rates of pyrite and the silicates. Although the discharge might remain near-neutral throughout the lifetime of the calcite, the lifetime of pyrite corresponds to the contaminating lifetime of a site (Banwart and Malmström, 2001). On the other hand, this would only be partially true since the calcite depletion rate would be largely dependent on the pyrite oxidation rate due to the required neutralization. Secondly, once you have submergence with water the conditions will become progressively less oxic, thus the pyrite reaction rate decreases.

The mineral behaviour explained above formed the basis of a hydrochemical model for the preliminary assessment of minewater pollution proposed by Banwart and Malmström (2001). It was aimed at classifying a site in terms of the potential threat to the environment. The model estimates the contamination strength of the source, longevity and possible future changes in discharge quality. Firstly, the current mineral weathering rates are estimated by setting up an integrated mass-balance based on the water budget (including surface and groundwater flows), the associated water qualities and the yield from the present contaminant load (source strength). It is then possible to calculate the flow (mol s^{-1}) of a contaminant due to a process in a rock or ore deposit, by observing various water flows to and from the deposit and the contaminant concentration. This only applies for steady state water flow conditions i.e. once a mine has filled and decanting and seepage are balancing the inflow from recharge and groundwater influx.

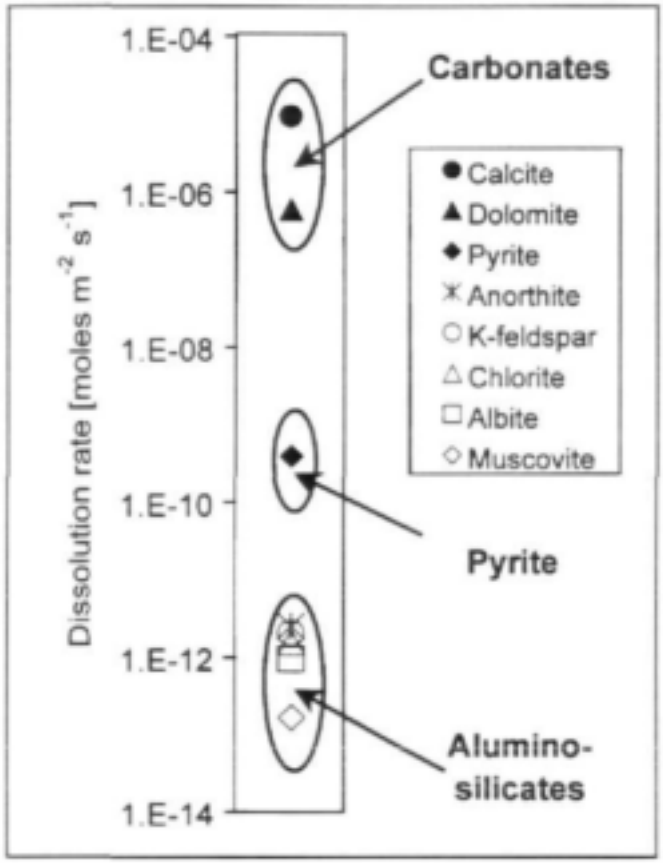

Figure 31. Surface area dissolution rates for source minerals far from solubility equilibrium at oxic conditions and pH 5 and 25°C (Banwart and Malmström, 2001)

Certain reaction products also provide evidence of specific weathering processes. The flow a reaction product is related to the rate of the weathering process, which is calculated in mol s^{-1}. Having obtained the weathering rate, an estimation of the duration of the weathering reaction is obtained by calculating the lifetime of the mineral in the deposit. The amount of the mineral is determined by aerial extent and depth of the source as well as on the composition of the rock and ore in it. This mineral content could be estimated using chemical analysis and thin sections. Now it is possible to predict the present acidity load, the neutralizing potential and the lifetime of further acid generating conditions (Banwart and Malmström, 2001).

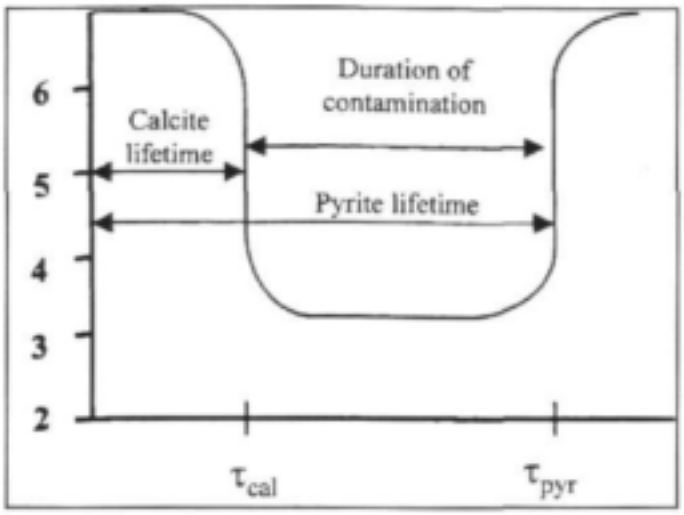

Figure 32. Relationship between trends in pH with the lifetime of minerals that produce and consume acidity (Banwart and Malmström, 2001)

Some results were obtained when the model was applied to a mine rock waste deposit located in the northern part of Sweden, a flooded abandoned coalmine with deep workings in northern England and a mine tailings deposit also situated in the northern part of Sweden. For the rock waste deposit it was predicted that the acid levels would be controlled by relative rates of sulphide and silicate mineral weathering since depletion of calcite prior to pyrite was expected. Acidic conditions would also exist after depletion of calcite in the abandoned coalmine. Although the lifetimes of both pyrite and calcite/dolomite in the tailings dumps were within the order of 100 years, the estimated lifetime of chalcopyrite was in the order of thousands of years, implying the need for long-term remediation (Banwart and Malmström, 2001).

5 ASSESSMENTS OF ACID GENERATION

The acid-base accounting (ABA) technique was used to assess the acid and neutralizing potential of samples analyzed in this study. The technique makes it possible to quantify the ability of a sample to produce acidic or alkaline seepage. A detailed explanation of the experimental procedure followed can be found in Hodgson and Krantz (1998), Cruywagen (2000) and Usher *et al.* (2001). The procedure applied to the samples in this study is briefly set out in Appendix 3 and includes the raw data.

5.1 ABA determinations for the Witbank and Highveld coalfields

Acid mine drainage results from the interactions of certain sulphide minerals with oxygen, water, and bacteria. Pyrite is recognized as the major source of acidic drainage. The acid potential (AP) is a measure of the potential of a sample to generate acidity according to the following reaction:

$$FeS_2 + 3.75O_2 + 3.5H_2O = Fe(OH)_3 + 2SO_4^{2-} + 4H^+$$

The amount of calcite required to neutralize a given amount of acid mine drainage depends on the behaviour of CO_2 during neutralization and on the pH reached. If the AMD is to be neutralized to pH 6.3 or above, then the following reaction may be written:

$$FeS_2 + 2CaCO_3 + 3.75O_2 + 1.5H_2O = Fe(OH)_3 + 2SO_4^{2-} + 2Ca^{2+} + 2CO_2$$

For each mole of pyrite that is oxidized, two moles of calcite are required for acid neutralization. On a mass ratio basis, for each gram of sulphur present, 3.125 g of calcite is required for acid neutralization. When expressed in parts per thousand of spoil, for each 10 ppt of sulphur present, 31.25 ppt of calcite is required for acid neutralization.

The stoichiometry in the previous equation is based on the exsolving of carbon dioxide gas out of the spoil system. In a closed system (as described in section 4), carbon dioxide is not exsolved, and additional acidity from carbonic acid is generated. Cravotta *et al.* (1990) proposed that up to four moles of calcite might be needed for acid neutralization as follows:

$$FeS_2 + 4CaCO_3 + 3.75O_2 + 3.5H_2O \square 2SO42^- + Fe(OH)_3 + 4Ca^{2+} + 4HCO_3^-$$

The stoichiometry of equation above shows that twice as much calcite would be required for acid neutralization. On a mass basis, for each 10 ppt of sulphur present, 62.5 tons of calcite is needed for acid neutralization in one thousand tons of spoil (Cravotta *et al.*, 1990).

Results obtained from the laboratory experimental procedure are used in calculating the AP, neutralizing potential (NP) and net neutralizing potential (NNP) as follows:

$$AP = \frac{SO_4\ (mg/L)/weight\ (g)}{1000} \times ml\ H_2O \text{ or } H_2O_2 = kg\ SO_4/t \text{ of sample}$$

$$AP\ (Open)\ (CaCO_3\ kg/t) = \frac{SO_4\ kg/t}{48} \times 50$$

$$NP\ (CaCO_3\ kg/t) = (N\ H_2SO_4 \times ml\ acid) - (N\ NaOH \times ml\ alkali)/weight\ (g) \times 50$$

Thus, the NNP is determined by subtracting the acid potential from the neutralizing potential.

$$NNP\ (Open) = NP - AP\ (Open)$$

In a closed system, AP (Closed) = AP (Open) x 2, and, NNP (Closed) = NP – AP (Closed) (Hodgson and Krantz, 1998).

There are various types of screening criteria used to interpret ABA results. According to Usher *et al.* (2001), an integration of Net Acid Generating Test (NAG) pH, Net Neutralizing Potential (NNP), Neutralizing Potential Ratio (NPR), and %S and NPR, could lead to a good classification of test results. The reader is referred to Cruywagen (2000) for a comprehensive description of the NAG procedure. The NAG pH obtained from this procedure can serve as a rough guideline as follows:

- If final pH = >5.5; the sample is non-acid generating,
- If final pH is between 3.5 and 5.5; the sample is low risk acid generating,
- If the final pH = <3.5; the sample is high risk acid generating.

When using the NNP as screening criteria, research has shown that there is a range from -20 to 20 kg/t $CaCO_3$ where a sample can become acidic or remain neutral. Thus, a sample with a NNP <20 is potentially acid generating and a sample with a NNP >20 might not generate acid (Usher *et al.*, 2001).

The NPR, or NP: AP, is the ratio between the acid and neutralizing potential. It ranges from <1:1 which suggests likely AMD generation to >4:1 suggesting no potential for AMD. By combining the NPR with the sulphide percentage, another set of rules can be derived as follows:

- Samples with less than 0.3% sulphide-S are regarded as having insufficient oxidizable sulphide-S to sustain acid generation.
- NPR ratios of >4:1 are considered to have enough neutralizing capability, while NPR ratios between 3:1 and 1:1 are inconclusive.
- NPR ratios of <1:1 with more than 0.3% sulphide-S are potentially acid generating (Usher *et al.*, 2001).

5.1.1 The Witbank coalfield

Data was available for 64 rock and coal samples in this coalfield. The raw data found in Appendix 3 is organized according to lithologies ranging from below the No. 1 Seam at the bottom of the dataset, to above the No. 5 Seam at the top. Although the dataset is limited, averages were used to illustrate the vertical distribution of acid and neutralizing potentials in the coalfield.

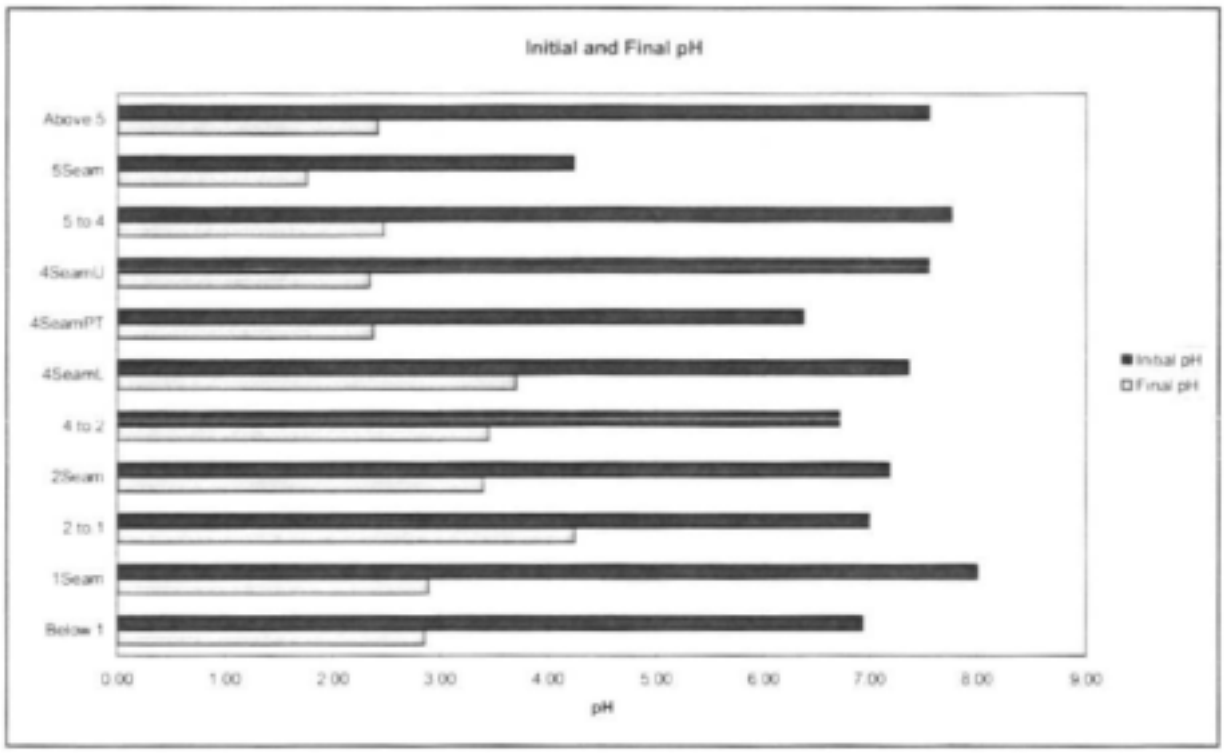

Figure 33. Initial and final pH's of the samples before and after complete pyrite oxidation and carbonate dissolution

From Figure 33 it is apparent that the natural or initial pH of both rock and coal samples are close to alkaline or at least to neutral conditions. With the exception of the No. 5 Seam all of the lithological units are expected to remain at these pH conditions if no oxidation takes place. A possible reason for the initial pH of the No. 5 Seam being much lower could be because it is situated closer to the water table. Any reactions that might have taken place could be due to groundwater movement through the Seam dissolving most of the carbonates. The final pH of all lithologies indicates that acidic conditions would dominate if complete sulphide oxidation was to occur. No. 5 Seam also has a lower final pH suggesting that total available carbonates could already be leached out leaving less sources of alkalinity to buffer the acid. It could also be that acid producing constituents were originally more abundant than acid consuming constituents.

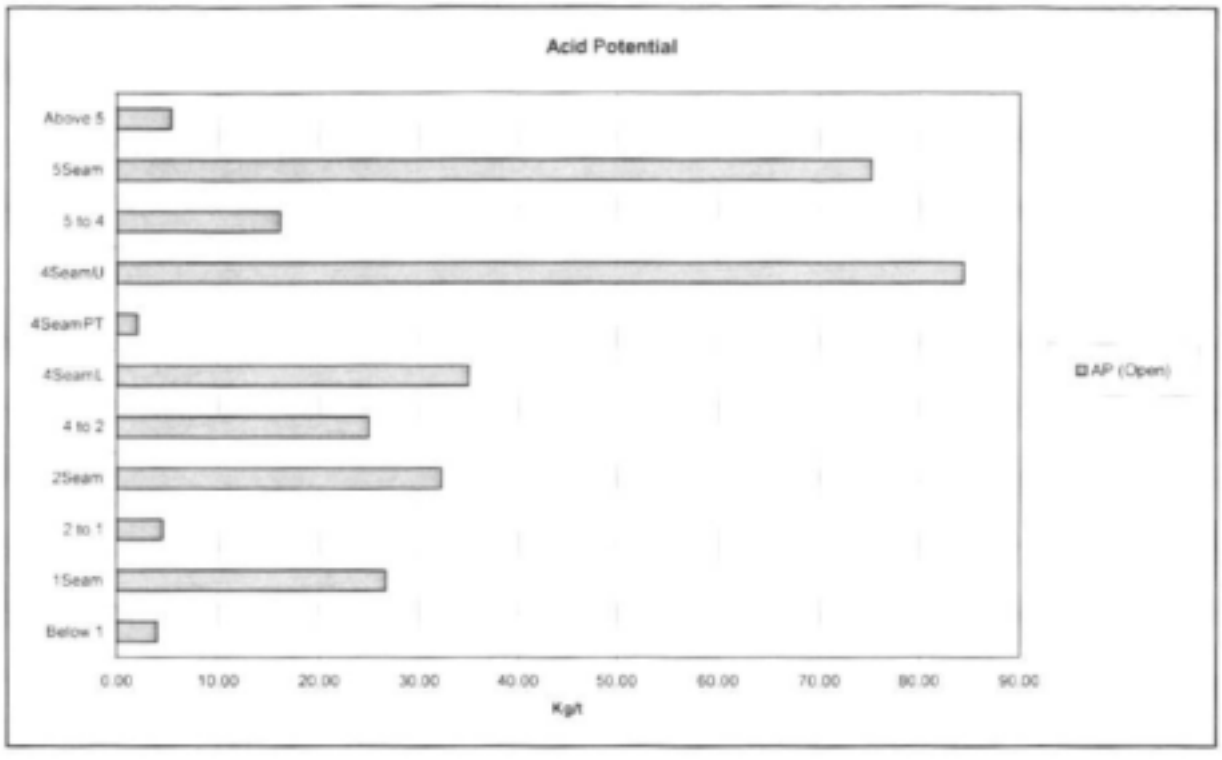

Figure 34. Acid potential (for an open system) for the Witbank coalfield

The AP in an open system is illustrated in Figure 34 above. Since the acid potential is determined primarily by the percentage of sulphur present it can be concluded that the rock units contain low concentrations acid producing minerals such as pyrite. This is evident in XRD interpretations, and is supported by XRF analyses and normative calculations as explained in section 3. Mineralogical investigations also proved that coal contained larger quantities of pyrite, thus the AP of the coal units are higher. The acid potential for No. 5 and No. 4 Upper seams both indicate that sulphides are very abundant in the seams.

However, the No. 5 Seam has a negative NP as seen in Figure 35, thus very few neutralizing constituents are present in this Seam. From interpretations in section 3, the Seam contained only minor quantities of calcite and dolomite, and very low CaO and MgO concentrations were obtained in XRF results, which is in good agreement with its NP. No. 4 Upper Seam on the other hand contains a larger NP and will thus have a stronger buffering ability. This is also confirmed by XRF results showing CaO concentrations averaging at 2.27 wt%.

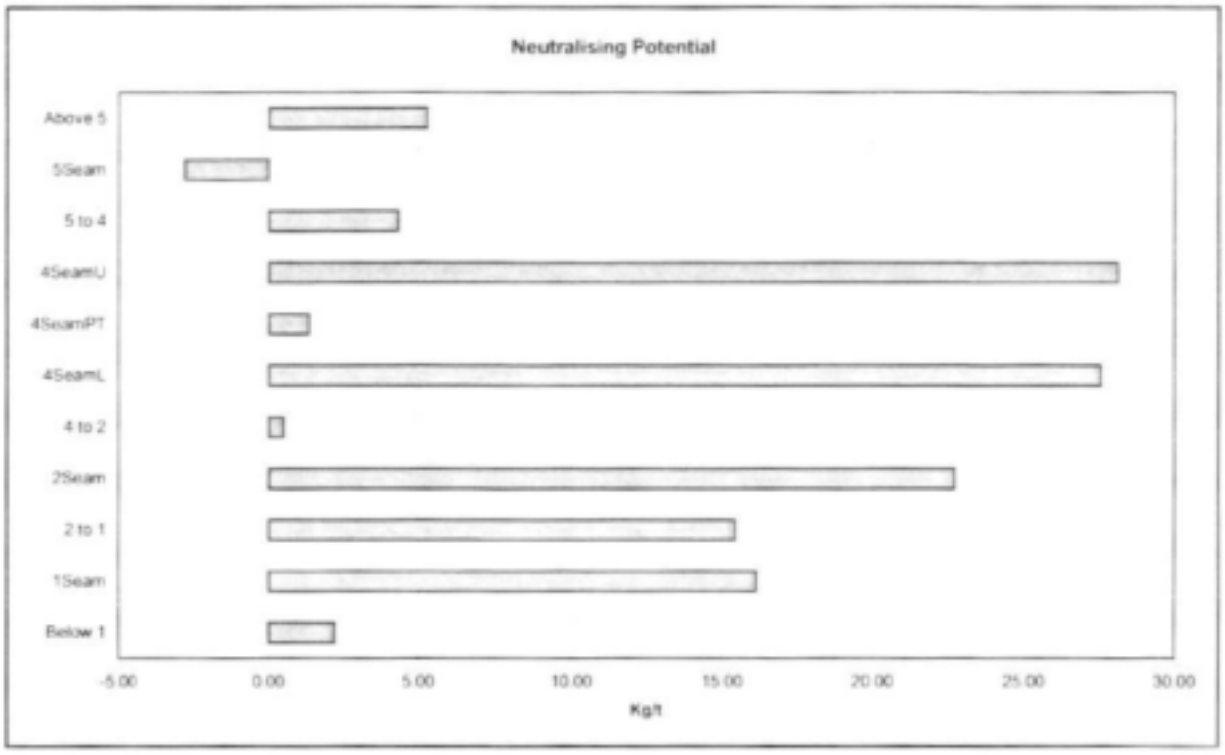

Figure 35. Neutralizing potential for the Witbank coalfield

Although neutralizing constituents are present in all the lithological units, Figure 36 clearly illustrates that the acid potential for both open and closed systems exceeds the neutralizing potential by excessive quantities. Only between No. 1 and No. 2 seams would sufficient alkalinity be provided to buffer acidity. CaO and MgO concentrations are not high enough in the roof rocks of the No.1 Seam and the floor rocks of No.2 Seam to clarify this neutralizing potential completely. The presence of feldspars and other aluminosilicates would contribute to the neutralizing potential even if it occurs at a slower rate (Banwart and Malmström, 2001). However, actual acid and neutralization release rates cannot be predicted with the technique, neither can the completeness of the reaction be assessed (Cruywagen, 2000). Thus, the pyrite reaction rate has to be very slow in order for the system to be brought back to neutral conditions by feldspars and aluminosilicates once the acidification has already occurred. Even though the neutralizing potential is low, pyrite seldom occurs in this unit; therefore little neutralizing potential is required.

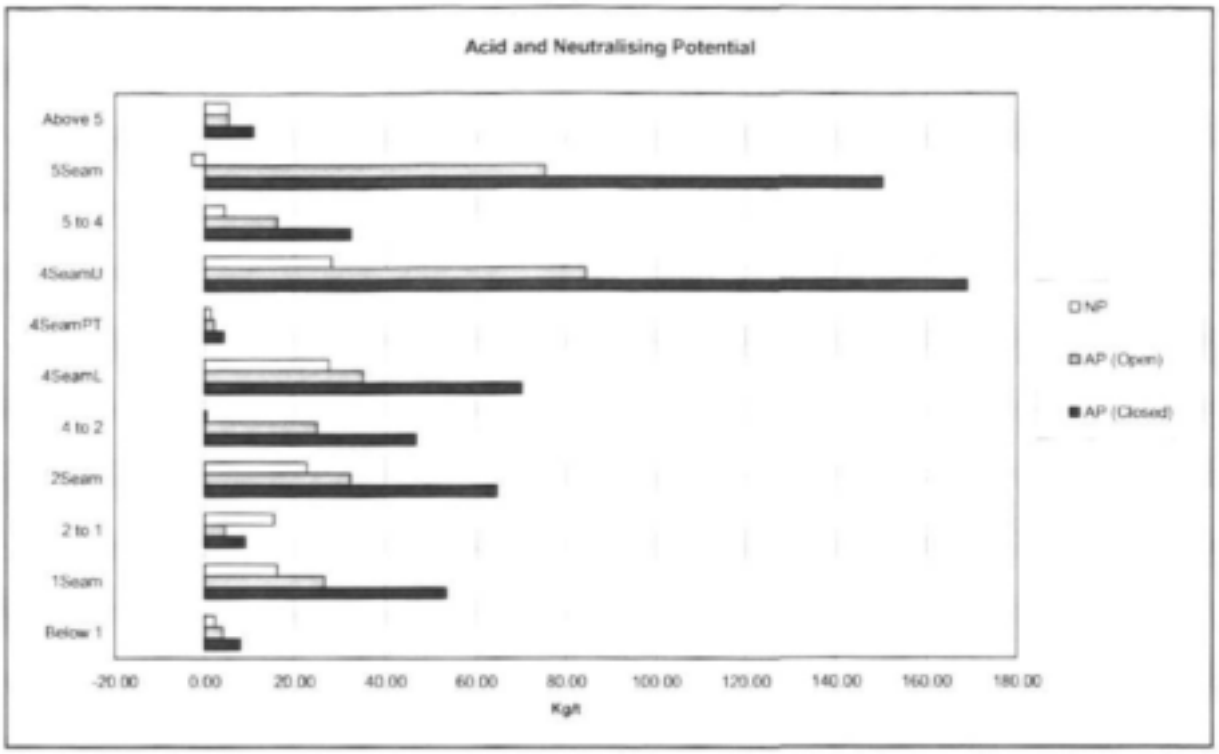

Figure 36. Acid potential (for an open and closed system) and neutralizing potential for the Witbank coalfield

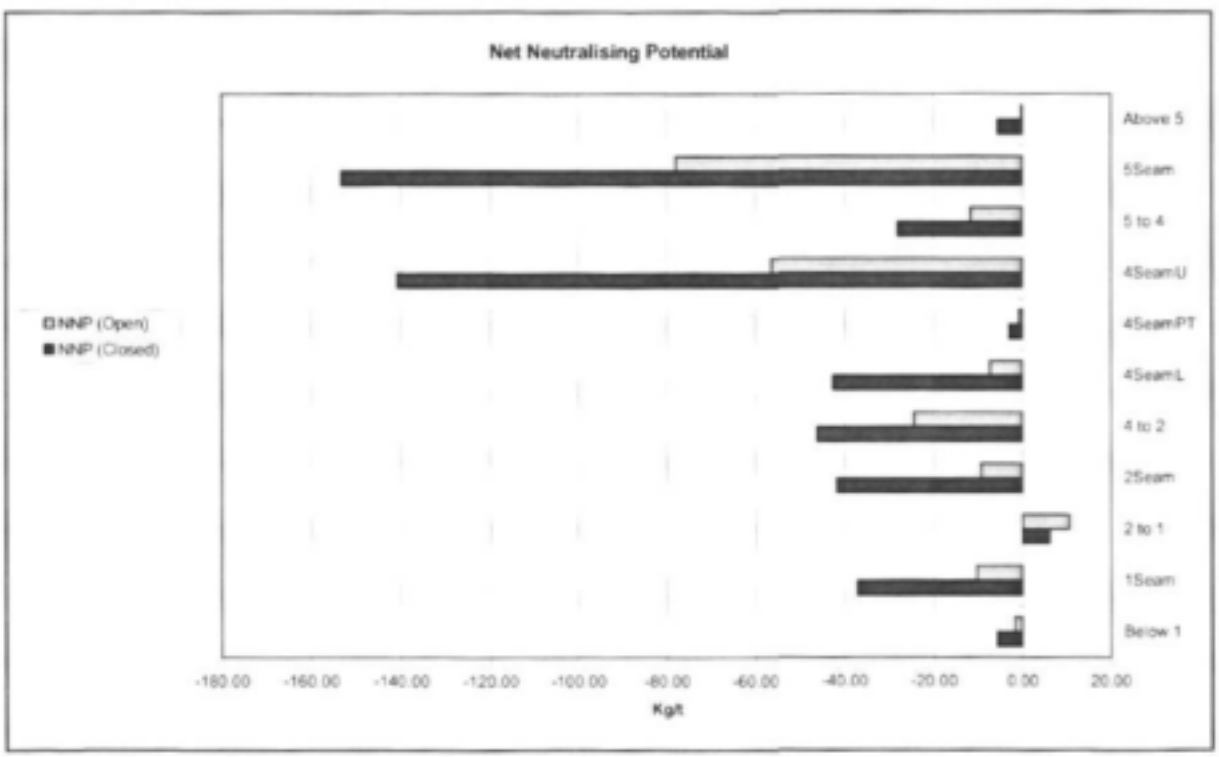

Figure 37. Net neutralizing potential for the Witbank coalfield

Acid-base accounting data on these coalfields has been generated by the Institute for Groundwater Studies at the UFS and are often presented as case studies in reports such as the Water Research Commission Reports. In many cases interpretations from results predict that water quality in and

surrounding the coalmines in the Witbank and Highveld coalfields will probably become acidic due to the environmental circumstances as well as rock and coal mineralogy. This investigation was a confirmation that lithological units will contribute greatly and negatively to the water quality in the area, unless remediation programs are implemented. A negative NNP is observed in Figure 37 for all lithological units except between the No.1 and No. 2 seams. The more negative the NNP becomes, the more $CaCO_3$ per ton of spoil will have to be added to neutralize the acidity.

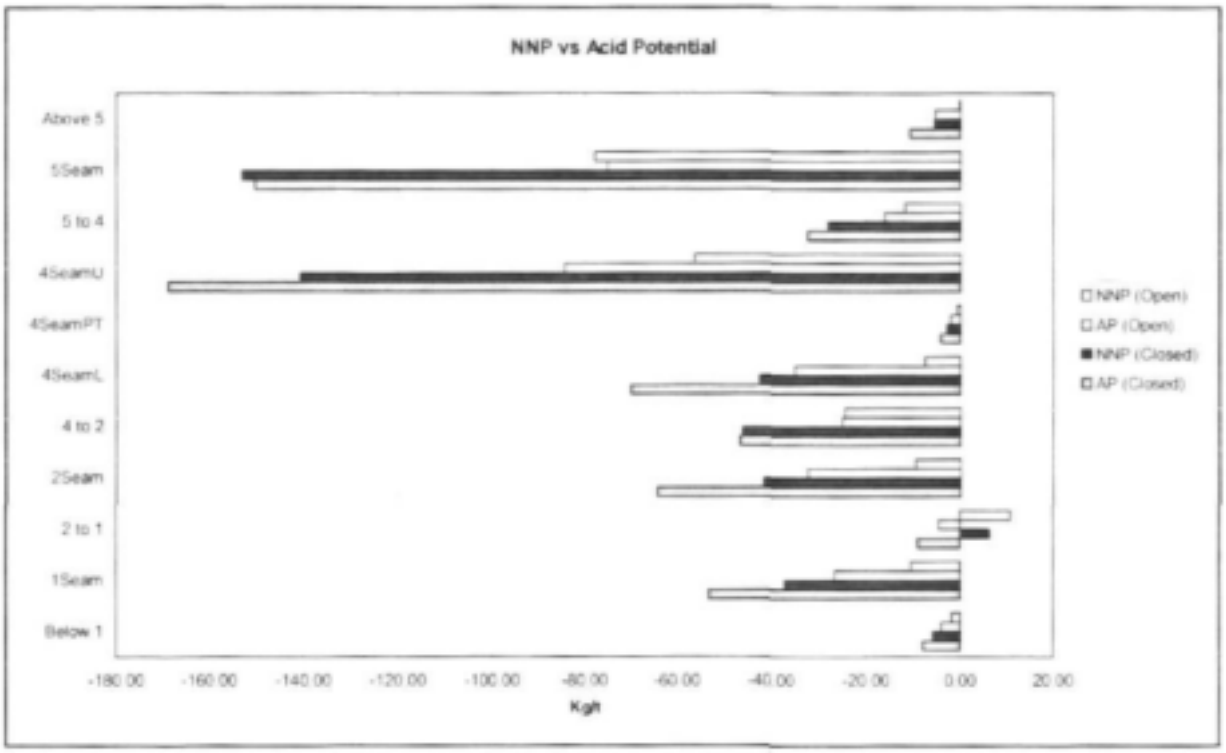

Figure 38. Acid potential (for an open and closed system) and net neutralizing potential (for an open and closed system) for the Witbank coalfield

The constant decrease in the AP, NP and NNP in depth is very obvious and possibly due to a lack of circulating groundwater, therefore a lack of leaching of reactive species in the lower units. Although sulphur increased or decreased in a specific direction horizontally in a Seam, no exact distribution was noted vertically for a borehole or for the dataset as a whole. Sulphur percentages were extremely variable and within ranges of 0.01 to as much as 20 wt% of a sample. A similar situation is observed for calcium. However, from the ABA results a trend in vertical distribution might exist. A multiple regression analysis performed on these samples showed that the sulphur percentage is 95% accountable for the NNP. Figure 38 illustrates this influence. The AP is plotted as a negative value in order for a comparison to be made. For most units the NNP is almost equivalent to or slightly less than the AP. A negative NNP indicates the inability of a sample to provide sufficient neutralizing constituents to buffer the acid produced, or stated otherwise, the acid produced was present in larger quantities than the alkalinity. In this study, the negative NNP corresponds well to the AP, thus the neutralizing potential was quite insufficient.

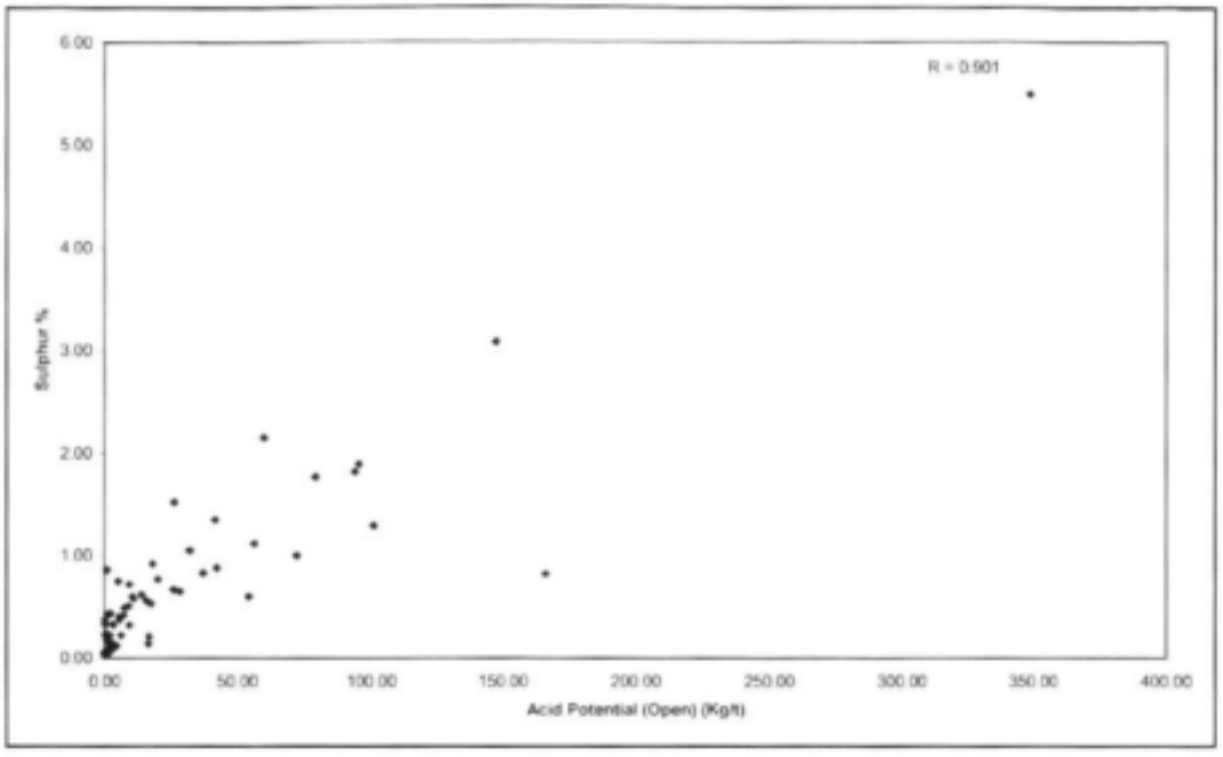

Figure 39. Acid potential (for an open system) and sulphur %

Good correlations between the AP and S %, and NP and CaO % can be seen in Figures 39 and 40 respectively. The sulphur obtained from XRF analyses is in good agreement with the AP (Open) as seen in Figure 39 ($r = 0.901$). Correlations for Fe_2O_3 and AP were insignificant, possibly due to the fact that most of the Fe_2O_3 was not present as pyritic Fe_2O_3 but as $FeCO_3$ or in montmorillonite, as concluded in section 3. Neither was there any noteworthy correlation between normative pyrite and AP.

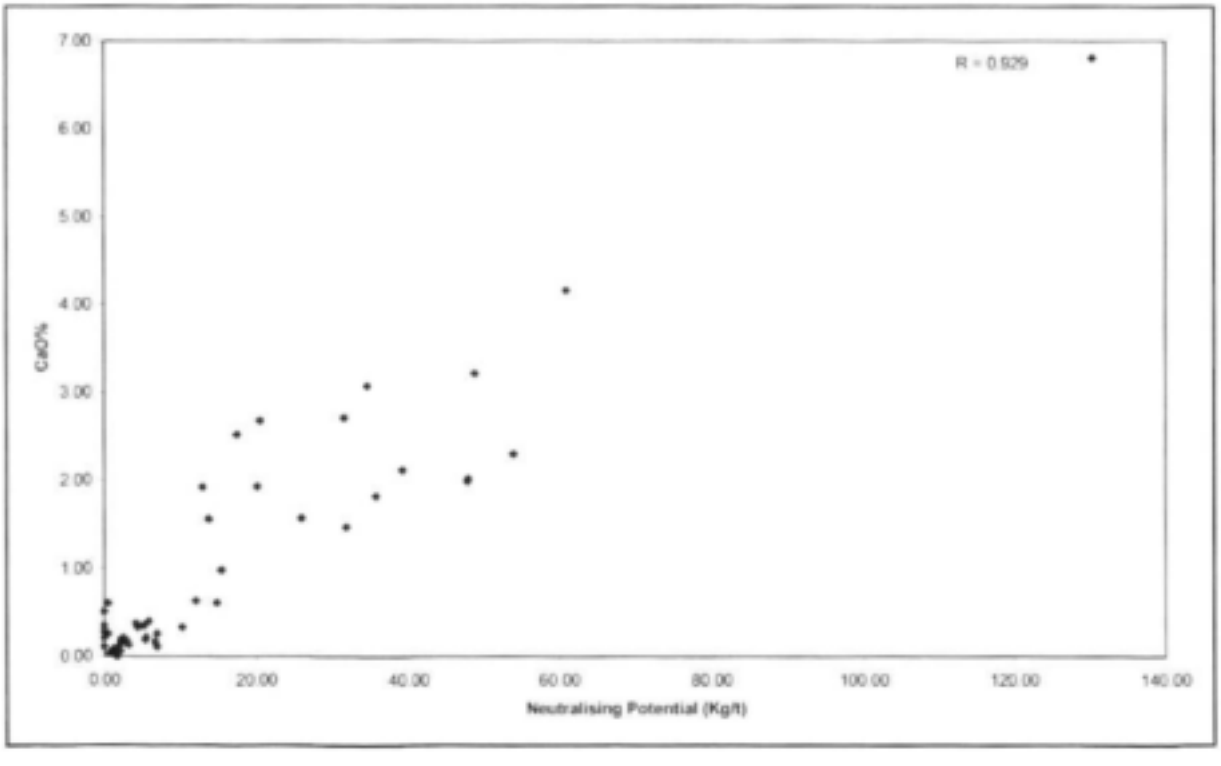

Figure 40. Neutralizing potential and CaO %

Although a significant correlation was obtained for the NP and CaO % (r = 0.929) (Figure 40) as well as the combined CaO and MgO % (r=0.906) and the NP. An insignificant correlation was observed between the NP and MgO (r=0.395), and between the NP and normative calcite (r=0.634) and dolomite (r=0.612).

Table 23. Average NPR (NP: AP) ratio and NNP for lithological units of the Witbank coalfield (open system)

Samples	NP:AP	NNP
Above 5	0.973	-0.15
5 Seam	-0.037	-77.97
5 to 4	0.268	-11.85
4 SeamU	0.333	-56.32
4 SeamPT	0.637	-0.78
4 SeamL	0.786	-7.50
4 to 2	0.020	-24.46
2 Seam	0.704	-9.55
2 to 1	3.355	10.84
1 Seam	0.606	-10.49
Below 1	0.553	-1.81

According to the screening criteria proposed by Usher *et al.* (2001), averages for NPR in Table 23 suggest that most lithological units are potentially acid generating. The unit the No. 1 and No. 2 coal seams are considered to be inconclusive. The average NNP values in Table 23, however, suggest that only No. 5 coal Seam, No. 4 Upper coal Seam, and between No. 4 and No. 2 coal seams are potentially acid generating. The other units could become either acidic or neutral.

In a case study presented by Usher *et al.* (2001) a comparable scenario for Optimum Opencast Colliery in the Witbank coalfield is observed. The lithological units were sampled in a similar manner to that in this study. An excess of AP over NP was present. The upper units had the lowest NP and AP. Since carbonates are more reactive than sulphides, neutralization potential leaching by circulating groundwater occurred in the upper units. A higher NP was also observed for the unit between No. 2 and No. 4 coal seams due to the lack of carbonate leaching with depth. For a detailed explanation of the techniques applied and test conducted on this colliery the reader is referred to Usher *et al.* (2001). The case study is in agreement with the findings in this study, which includes samples from other areas of the Witbank coalfield as well.

5.1.2 The Highveld coalfield

Limited acid-base accounting data was available for this coalfield, yet from the data for No. 4 and No. 5 seams tabulated in Appendix 3, it seems that the same situation could be expected as in the Witbank coalfield. The highest negative NNP values are also observed for the coal seams. Values range from approximately -156.14 to -25.66 kg/t.

Table 24. Average NPR (NP: AP) ratio and NNP for lithological units of the Highveld coalfield (open system)

Samples	NP:AP	NNP
Above 5	0.004	-110.68
5 Seam	-0.012	-156.14
5 to 4	0.005	-32.29
4 Seam	0.244	-38.31
Below 4	0.006	-25.66

The average NPR ratios and NNP as seen in Table 5-2 suggest that these samples have potential to generate acid.

By observations made from this data significant predictions can be made as to the influence mineralogy might have on the surrounding groundwater. The potential for these lithological units to contribute to the deterioration of groundwater is definitely evident. This method is, however, based on ideal situations where it is assumed that complete oxidation of sulphides and dissolution of carbonates will occur. The presence of these constituents does not necessarily guarantee their availability, which is often dependant on the minerals certain elements are contained, in as well as geochemical factors such as pH, Eh, temperature, etc. Secondly, the method does not take rates of weathering and oxidation into account. Thus, the prediction is more relevant when ideal conditions exist.

The sulphur analyzed at UFS represents total S. This would include the sulphide-S, sulphate-S and organic-S. The only sulphide detected by XRD interpretations during this study was pyrite. No sulphate phases were present in these interpretations, and it was not possible to determine the organic sulphur content with XRF techniques. The S concentration therefore accounts for the sulphide-S and the organic-S. In theory it is possible to calculate the AP from the analyzed S by multiplying the S value by 31.25 from the calculations explained in section 5.1. Assuming that all sulphide-S is available for oxidation, then the total S analyzed could be used to predict the AP for samples on which no acid-base determinations has been carried out. The correlation between the XRF S and the AP confirms that there is a good relationship between these components for the sample set as a whole.

Regarding the NP, the CaO analyzed at UFS includes Ca from all Ca-bearing phases such as montmorillonite, dolomite, fluorapatite, crandallite, and the major Ca-phase, calcite. The excellent correlation between the NP and CaO, and between the NP and combined CaO and MgO, confirms that these chemical components are largely responsible for NP values. It is then also possible to predict the

NP by using the CaO and MgO concentrations for samples for which no AP or NP data is available. The mineralogy therefore provides an alternative for determining acid and base potentials in the event that no ABA tests are available, and could be used to verify the accuracy of ABA analyses.

The application of ABA in this study offered a major contribution to understanding the complexities governing water-rock interactions. The time involved in such interactions often amounts to decades and even centuries. Nonetheless, interpretation of ABA data not only provides a preview of situations that might arise regarding groundwater quality in a certain area, but also offers ample time to decide on appropriate prevention or remediation programs.

6 CONCLUSIONS AND RECOMMENDATIONS

The conclusions of this investigation could be summarized as follow;

- Low-temperature ashing (LTA) and X-ray diffraction (XRD) carried out on selected samples accentuated the need and practicality of integrating other analytical techniques with XRD. XRD on LTA coal proved to be more accurate in identifying minerals that occur as rare constituents, i.e. < 5 modal percent, especially since the organic material in coal tends to obscure interpretations from raw coal XRD;
- There are numerous variables influencing the results from X-ray fluorescence (XRF) analyses on coal. Differences were observed, firstly, between whole coal and fusion disk XRF, and secondly, between whole coal results of mixed proportions of two samples. The calcination and fusion of coal samples introduces some difficulties concerning the loss of important constituents in coal, such as sulphur and possibly phosphorus. The conditions during preparation of XRF disks, such as temperature, need to be kept constant if similar results are to be obtained each time. A disadvantage of using whole coal briquettes refers to the "infinite thickness" issue. X-rays are often absorbed into coal briquettes resulting in lower count rates, while mass absorption is accounted for in fusion disks by the addition of La_2O_3 during preparation. The differences between whole coal results of mixed proportions of two samples could also be attributed mass absorption effects. Elements such as iron have a higher mass absorption resulting in lower count rates than is to be expected. The possibility of segregation of heavy minerals in samples during mixing and storage has been considered, and was minimized by correct sample handling and thorough mixing. The standard XRF technique is recognized as precise and reliable, but in this case whole coal analysis was more suitable.
- The mineral components in coal were expressed as a percentage of the inorganic constituents. Minerals detected in the XRD patterns were semi-quantitatively evaluated in terms of dominant (>40% of the mineral fraction), major (10-40%), minor (2-10%), accessory (1-2%) and rare (<1%) constituents. The inorganic fraction consisted primarily of dominant quartz and kaolinite, and sometimes even dominant pyrite, calcite and dolomite. The latter three phases were ubiquitous in the coal. The Ca-phosphate mineral, crandallite was detected in the western region of the Witbank and Highveld coalfields. Although only present in low concentrations, fluorapatite was detected throughout in the Witbank coal except in the extreme northeastern region. Fluorapatite was not detected in samples from the Highveld coal.
- Chemical analyses confirmed the mineralogical interpretations. The inorganic components make up approximately 8 to 35 wt% of a coal sample. SiO_2 concentrations varied between and 35 wt% of a sample, Al_2O_3 between 0.5 and 16 wt%, Fe_2O_3 between 0.03 and 10 wt%, and S between 0.15 and 8 wt%. Minor concentrations of CaO (0 to 8 wt%) and MgO (0 to 1 wt%) were present. P_2O_5 occurred in concentrations of 0 to 3.5 wt% and K_2O was in the order of 0 to 1.3 wt%. Na_2O values were the lowest varying between 0 and 0.45 wt%. The only difference in chemistry between Witbank and Highveld coal was a slight increase in Na_2O (0 to 0.51 wt%) in the

Highveld coal. The distribution of element oxides across the No. 2 coal Seam as noted in section 3.3 discuss particular trends, which probably exist in the other seams; however, this was not clearly discernible due to insufficient data for those seams.

- The different depositional environments that have been recognized by other workers in the coal-bearing strata of the Ecca Group are associated with characteristic physicochemical conditions. Such characteristic physicochemical conditions dictate the precipitation of typical mineral assemblages. Thus, based on theoretically considerations there should be a direct link between the depositional environment and the modal proportion of minerals and mineral assemblages. Coal and rock samples that were collected and analyzed in order to evaluate mineralogical variables as indicators of fluctuating palaeo-environments during the formation of the coal deposits. However, such a correlation could not be confirmed or denied using the existing database.
- The correlation between the XRF S and the AP confirms that there is a good relationship between these components for the sample set as a whole. ABA results for these samples show that the lithological units in the coalfields have the ability to contribute to deterioration in ground and surface water quality. Two types of screening criteria was used to determine whether acid or alkaline conditions will prevail once all acid consuming and acid producing minerals has been oxidized. From the NNP, or net neutralizing potential, it can be predicted that the No. 5 coal Seam, the No. 4 coal Seam and the unit between No. 2 and No. 4 coal seams will be predominantly acidic. The NNP of the other units vary between -20 kg/t and 20 kg/t, therefore these stratigraphic units could become either acidic or alkaline. The unit between No. 1 and No. 2 coal seams is the only unit possessing enough neutralizing potential to buffer the acid produced, but could still become acid since the NNP is less than 20 kg/t.
- The NPR or NP: AP ratios, for all stratigraphic units (except between No. 1 and No. 2 coal seams) are less than 1:1 suggesting that acid conditions will dominate. The NPR ratio between No. 1 and No. 2 coal seams is at least 3:1 implying that enough buffering capacity is available to counteract the acid. The AP and NP are largely dependant on the presence of pyrite and calcite, respectively. Good correlations were obtained between the NP and CaO% and the AP and S%; therefore it is possible to use the mineralogy to predict these factors. It should also be remembered that these predictions do not take time and weathering rates into consideration, thus such conditions will only be attained once ideal situations are reached.
- Trends in the regional distribution of minerals in the No. 2 seam were studied. Variations in regional mineral distribution corresponded with the variation in water quality. Regional maps showing the distribution or trends in mineralogy and an overall interpretive map of acid generating potential based solely on mineralogy, was compiled.

A significant amount of useful mineralogical information has been compiled during the course of this study. However, the interpretation of the available data has not yet been optimized. We recommend that the interpretation of available information should be completed and that additional information should be gathered wherever required.

7 REFERENCES

Azzie, B. A. (1999). *The geochemistry and quality of water from selected collieries on the South African Highveld.* M.Sc thesis (unpubl.), University of Cape Town, South Africa, 181 pp.

Azzie, B. A. (2002). *Coal mine waters in South Africa: Their geochemistry quality and classification.* Ph.D thesis (unpubl.), University of Cape Town, South Africa, 480pp.

Banwart, S. A. and Malmström, M. E. (2001). Hydrochemical modelling for preliminary assessment of minewater pollution. *Journal of Geochemical Exploration,* **74**, 73-97.

Bates, R. L. and Jackson, J. A. (eds.) (1980). *Glossary of Geology Second Edition.* American Geological Institute, 751pp.

Bouška, V. (1981). *Geochemistry of coal.* Elsevier Scientific Publishing Company, Netherlands, 284pp.

Bühmann, C. and Bühmann, D. (1988). *Sedimentary petrology of coal-bearing Ecca sediments.* Final Project Report (unpubl.), University of Natal, South Africa, 27pp.

Cadle, A. B., Cairncross, B., Christie, A. D. M. and Roberts, D. L. (1990). The Permo-Triassic coal-bearing deposits of the Karoo Basin, southern Africa. Economic Geology Research Unit, University of the Witwatersrand, Johannesburg, 218, 38pp.

Cairncross, B. (2001). An overview of the Permian (Karoo) coal deposits of southern Africa. *Journal of African Earth Sciences,* **33**, 529-562.

Catuneanu, O., Hancox, P. J. and Rubidge, B. S. (1998). Reciprocal flexural behaviour and contrasting stratigraphies: a new basin development model for the Karoo retroarc foreland system, South Africa. *Basin Research,* **10**, 417-439.

Chelin, M. J. (2000). *Water in the coal mining industry – An assessment of water management issues facing the coal mining industry of the Witbank and Middelburg Dam catchments.* M.Sc thesis (unpubl.), University of Pretoria, South Africa, 138 pp.

Cravotta, C. A., Brady, K. B., Smith, M. W. and Beam, R. L. (1990). Effectiveness of Alkaline Addition at Surface Mines in Preventing or Abating Acid Mine Drainage: Part 1, Geochemical Considerations. *In*: Proceedings of the 1990 Mining and Reclamation Conference and Exhibition, West Virginia University, **1**, 221-226.

Cruywagen, L. (2000). *Static geochemical methods in determining acid mine drainage.* M.Sc thesis (unpubl.), University of the Free State, South Africa, 93 pp.

Ebbing, D. D. (1993). *General Chemistry, 4th Edition.* Houghton Mifflin Company, p. 664-665.

Falcon, R. M. S. (1986). A brief review of the origin, formation, and distribution of coal in southern Africa, 1879-1898. *In*: Anhaeusser, C. R., and Maske, S. (Eds.), *Mineral Deposits of Southern Africa,* I. Geol. Soc. S. Afr., 1020 pp.

Fourie, J. (2003). Analyses of the lithofacies, mineralogy and geochemistry, and the prediction of the mine drainage quality of a future opencast mine in the northeastern Witbank coalfield. Honours project (unpubl.), University of the Free State, South Africa, 86 pp.

Franson, M. A. H., Greenberg, A. E., Trussell, R. R. and Clesceri, L. S. (Eds.) (1985). *Standard methods for the examination of water and wastewater, 16th Edition.* American Public Health Association, American Water Works Association, Water Pollution Control Federation, 1268pp.

Gaigher, J. L. (1980). *The mineral matter in some South African coal.* M.Sc thesis (unpubl.), University of Pretoria, South Africa, 60 pp.

Gluskoter, H. J. (1965). Electronic low-temperature ashing of bituminous coal. *Fuel*, **44**, 285-291.

Grobbelaar, R. (2001). *The long-term impact of intermine flow from collieries in the Mpumalanga coalfields.* M.Sc thesis (unpubl.), University of the Free State, South Africa, 136 pp.

Haefner, R. J. (2002). Water quality and geochemical modelling of water at an abandoned coalmine reclaimed with coal combustion by-products. *United States Geological Survey*, Water-Resources Investigations Report 02-4216, 33 pp.

Hodgson, F. D. I and Krantz, R. M. (1998). Groundwater quality deterioration in the Olifants River Catchments above the Loskop Dam with specialised investigations in the Witbank Dam Sub-Catchment. Report to the Water Research Commission by the Institute for Groundwater Studies, University of the Orange Free State, WRC Report No. 291/1/98, 272pp.

JCPDS International Centre for Diffraction Data. (1980a). Mineral Powder Diffraction File Data Book. JCPDS International Centre for Diffraction Data, U.S.A, 1168pp.

JCPDS International Centre for Diffraction Data. (1980b). Mineral Powder Diffraction File Search Manual. JCPDS International Centre for Diffraction Data, U.S.A, 484pp.

Jordaan, J. (1986). Highveld coalfield, 1985-1994. *In*: Anhaeusser, C. R., and Maske, S. (Eds), *Mineral Deposits of Southern Africa*, I. Geol. Soc. S. Afr., 1020 pp.

Khan, M. A., Ahmad, I., Jan, M. T. and Karim, I. (2002). Mineral matter identification in some Pakistani coal. *Fuel Processing Technology*, **75**, 1-8.

Kruger, S. J. (1981). *'n Mineralogiese ondersoek van die asfraksie van steenkool van die Springbokvlakte-Steenkoolveld.* M.Sc thesis (unpubl.), Rand Afrikaans University, South Africa, 172 pp.

Kunze, G. W. and Dixon, J. B. (1986). Pre-treatment for Mineralogical Analysis. *In*: Klute, A. (Ed), *Methods of Soil Analysis Part 1: Physical and Mineralogical Methods 2nd edition*, Soil Science Society of America, Inc., Wisconsin, USA 91-100.

Mackowsky, M.-Th. (1968). Mineral matter in coal. *In*: Murchison, D. G., and Westoll, T. S. (Eds), *Coal and Coal-bearing Strata*, Robert Cunningham and Sons Ltd., 309-321.

Martin, J. D., Duwelius, R. F. and Crawford, C. G. (1990). Effects of surface coal mining and reclamation on the geohydrology of six small watersheds in west-central Indiana. *United States Geological Survey*, Water-Supply Paper 2368, 71pp.

McCarthy, M. D. B., Newton, R. J. and Bottrell, S. H. (1998). Oxygen isotopic compositions of sulphate from coal: Implications for primary sulphate sources and secondary weathering processes. *Fuel*, **77**, 677-682.

Nicholls, G. D. (1968). The Geochemistry of Coal-bearing Strata *In*: Murchison, D. G., and Westoll, T. S. (Eds), *Coal and Coal-bearing Strata*, Robert Cunningham and Sons Ltd., 269-307.

Norrish, K. and Hutton, J. T. (1969). An accurate X-ray spectrographic method for the analysis of a wide range of geological samples. *Geochim. Cosmochim. Acta*, **33**, 431-453.

Nriagu, J. O. and Moore, P. B. (Eds.) (1984). *Phosphate minerals.* Springer-Verlag, Berlin, 442pp.

O'Shay, T., Hossner, L. R. and Dixon, J. B. (1990). A modified hydrogen peroxide method for determination of potential acidity in pyritic overburden. *Journal of Environmental Quality*, **19**, 778-782.

Rao, P. D. and Walsh, D. E. (1999). Influence of coal deposition on phosphorous accumulation in a high latitude, northern Alaska coal Seam. *International Journal of Coal Geology*, **38**, 261-284.

Reeder, R. J. (Ed.) (1983). Carbonates: Mineralogy and Chemistry *In: Reviews in Mineralogy*, **11**. Miner. Soc. Amer., 394pp.

Ribbe, P. H. (Ed.) (1974). Sulphide mineralogy *In: Reviews in Mineralogy*, **1**. Miner. Soc. Amer., 284pp.

Rietveld, H. M. (1969). A profile refinement method for nuclear and magnetic structures. *Journal of Applied Crystallography*, **2**, 65-71.

Sams, J. I. and Beer, K. M. (2000). Effects of coalmine drainage on stream water quality in the Allegheny and Monongahela River Basins – Sulphate transport and trends. *United States Geological Survey*, Water-Resources Investigations Report 99-4208, 23 pp.

Snyman, C. P. (1998). Coal. *In:* The Mineral Resources of South Africa (M. G. C. Wilson and C. R. Anhaeusser, eds.): Handbook, Council for Geoscience, **16**, 136-205.

Smith, D. A. M. and Whittaker, R. R. L. G. (1986a). The coalfields of southern Africa: An introduction, 1875-1878. *In:* Anhaeusser, C. R., and Maske, S. (Eds), *Mineral Deposits of Southern Africa*, I. Geol. Soc. S. Afr., 1020 pp.

Smith, D. A. M. and Whittaker, R. R. L. G. (1986b). The Springs-Witbank coalfield, 1969-1984. *In:* Anhaeusser, C. R., and Maske, S. (Eds), *Mineral Deposits of Southern Africa*, I. Geol. Soc. S. Afr., 1020 pp.

Smith, R. M. H., Eriksson, P. G. and Botha, W. J. (1993). A review of the stratigraphy and sedimentary environments of the Karoo-aged basins of Southern Africa. *Journal of African Earth Sciences*, **16**. No. 1/2, 143-169.

Spiker, E. C., Pierce, B. S., Bates, A. L. and Stanton, R. W. (1994). Isotopic evidence for the source of sulphur in the Upper Freeport coal bed (west-central Pennsylvania, USA). *Chemical Geology*, **114**, 115-130.

Strahler, A. N. and Strahler, A. H. (1973). *Environmental Geoscience: Interaction between natural systems and man*. John Wiley & Sons, Inc., 511pp.

Stratten, T. (1986). Environmental and stratigraphic setting of the Karoo Basin and its mineral deposits, 1863-1873. *In:* Anhaeusser, C. R., and Maske, S. (Eds), *Mineral Deposits of Southern Africa*, I. Geol. Soc. S. Afr., 1020 pp.

Styan, W. B and Bustin, R. M. (1984). Sedimentology of the Fraser River delta peat deposits: a modern range analogue for some deltaic coal. *In:* Rahmani, R. A., and Flores, R. M. (Eds), *Sedimentology of Coal and Coal-bearing Sequences*, Spec. Publs int. Ass. Sediment., **7**, 241-271.

Thomas, R. J., von Veh, M. W. and McCourt, S. (1993). The tectonic evolution of southern Africa: an overview. *Journal of African Earth Sciences*, **16**. No. 1/2, 5-24.

Usher, B. H., Cruywagen, L. de Necker, E. and Hodgson, F. D. I (2001). On-site and laboratory investigations spoil in opencast collieries and the development of acid-base accounting procedures. Report to the Water Research Commission by the Institute for Groundwater Studies, University of the Orange Free State, WRC Report, 262pp.

Van der Spuy, D. and Willis, J. P. (1991). The occurrence of aragonite in carbonate lenses in coal from the Witbank area. *South African Journal of Geology*, **94**(2/3), 178-180.

Van Vuuren, C. J. and Cole, D. I. (1979). The stratigraphy and depositional environments of the Ecca Group in the northern part of the Karoo Basin. *In:* A. M. Anderson and W. J. van Biljon (Editors.), Some sedimentary basins and associated ore deposits of South Africa. *Geol. Soc. S. Afr. Spec. Publ.* **6**, 103-111.
Vassilev, S. V. and Vassileva, C. G. (1996). Occurrence, abundance and origin of minerals in coal and coal ashes. *Fuel Processing Technology*, **48**, 85-106.

Vaughan, D. J. and Craig, J. R. (1978). *Mineral chemistry of metal sulphides*. Cambridge University Press, London, 493pp.

Wainerdi, R. E. and Uken, E. A. (eds.) (1971). *Modern methods of geochemical analysis.* Plenum Press, New York, 397pp.

Ward, C. R. (1974). Isolation of mineral matter from Australian bituminous coal using hydrogen peroxide. *Fuel*, **53**, 220-221. (Letters to the Editor).

Ward, C. R. (Ed.) (1984). *Coal geology and coal technology.* Blackwell Scientific Publications, Australia, 345 pp.

Ward, C. R. (1986). Review of mineral matter in coal. *Australian Coal Geology*, **6**, 87-110.

Ward, C. R. and Gurba, L. W. (1998). Occurrence and distribution of organic sulphur in macerals of Australian coal using electron microprobe. *Organic Geochemistry*, **28**, 635-647.

Ward, C. R. (1999). Mineral characterisation for combustion – The contribution from the geological sciences. *In*: Gupta, R., Wall, T. F. and Baxter, L. A. (Eds.), *The Impact of Mineral Impurities in Solid Fuel Combustion*, Kluwer Academic/ Plenum Publishers, New York, 23-32.

Ward, C. R., Taylor, J. C. and Cohen, D. R. (1999). Quantitative mineralogy of sandstones by X-ray diffractometry and normative analysis. *Journal of Sedimentary Research*, **69** (5), 1050-1062.

Ward, C. R., Spears, D. A., Booth, C. A., Staton, I. And Gurba, L. W. (1999). Mineral matter and trace elements in coal of the Gunnedah Basin, New South Wales. Australia, *International Journal of Coal Geology*, **40**, 281-308.

Ward, C. R., Taylor, J. C., Matulis, C. E. and Dale, L. S. (2001a). Quantification of mineral matter in the Argonne Premium Coals using interactive Rietveld-based X-ray diffraction. *International Journal of Coal Geology*, **46**, 67-82.

Ward, C. R., Bocking, M. and Ruan, C. (2001b). Mineralogical analysis of coal as an aid to Seam correlation in the Gloucester Basin, New South Wales, Australia. *International Journal of Coal Geology*, **47**, 31-49.

Ward, C. R. (2002). Analysis and significance of mineral matter in coal seams. *International Journal of Coal Geology*, **50**, 135-168.

Williamson, I. A. (1967). *Coal mining geology.* Oxford University Press, London, 266pp.

8. APPENDIX 1: ANALYTICAL TECHNIQUES, SAMPLE LOCALITIES & SAMPLE DESCRIPTIONS

CONTAINED ON THE ATTACHED CD ROM

9 APPENDIX 2: ANALYTICAL RESULTS

CONTAINED ON THE ATTACHED CD ROM

10 APPENDIX 3: BOREHOLE LOGS AND DESCRIPTIONS

CONTAINED ON THE ATTACHED CD ROM

Other related WRC reports available:

On-site and laboratory investigations of spoil in open-cast collieries and the development of acid-base accounting procedures

Usher BH; Cruywagen L-M; de Necker E; Hodgson FDI

Current predictions suggest that most South African collieries will at some stage in future decant acid water. This will have a serious impact on aquatic life in streams and other water users. Results from the many methods that are used internationally to predict the production of acid mine drainage, do not agree. This project expanded on its aim to investigate the various acid-base accounting (ABA) procedures (which are used as a first-order classification procedure for predicting whether mine decant water will turn acidic) to include a range of complementary predictive techniques and evaluate them under field conditions. The result was the description of a suite of acid-drainage prediction tools, applicable to South African open-cast coal-mine conditions and the coining of a new acronym, ABATE (derived from Acid-Base Accounting, Techniques and Evaluation), to describe this approach, that in addition to static ABA techniques, include long-term kinetic testing and geochemical modelling. Through a workshop held to involve the leading consultants and regulating authorities, consensus was obtained concerning the tests to include in the ABATE system and their standardisation.

Report Number: 1055/1/03 **ISBN: 1 77005 053 1**

TO ORDER: Contact **Publications** - Telephone No: 012 330 0340
Fax Number: 012 331 2565
E-mail: publications@wrc.org.za

1770054405

Water Research Commission
Private Bag X03, Gezina, 0031, South Africa
Tel: +27 12 330 0340, Fax: +27 12 331 2565
Web: http://www.wrc.org.za